"Electrophysiological Studies On The Caudal Photoreceptor Of The Crayfish, Pacifasticus leniusculus".

RHODA ELLIS

Thesis submitted for the degree of Master of Philosophy of the University of St. Andrews

July 2004

School of Biology
Bute Building
University of St. Andrews
St. Andrews
Fife
KY16 9TS

ABSTRACT

- The caudal photoreceptors (CPRs) are bilaterally-paired neurons located in the terminal ganglion of the crayfish ventral nerve cord. Each CPR has an axon which runs the length of the animal on the contralateral side of the nerve cord. When activated, they induce behaviors such as backwards walking. The CPRs are also mechanosensory integrating interneurons.
- The photic response was recorded intracellularly in the presence of the voltage-gated Na^+ channel blocker, tetrodotoxin (TTX), to reveal the shape of the underlying generator potential.
- The generator potential has an initial transient peak, followed by a sustained plateau. There is a small "off" response. This waveform reflects the shape of the spike frequency response in the intact preparation.
- Application of the neuromodulator serotonin changes the spike frequency response of the CPR. It induces spontaneous firing by altering the properties of synaptic inputs to the CPR but does not significantly alter the generator potential of the photic response.
- Lithium reduced the photic response and caffeine increased it, confirming the involvement of IP_3 and Ca^{2+} as second messengers in the transduction cascade. Staurosporine had no effect, suggesting the absence of a phosphorylation step.
- The generator potential was reduced in amplitude by bathing the preparation in 20% sodium saline in the presence of TTX, indicating that it is sodium-dependent.
- No evidence was found for a membrane conductance change during the photic response.
- Application of tetraethyl ammonium ions (TEA) enhanced the magnitude of the generator potential depolarization, suggesting that voltage-gated K^+ channels normally limit and sculpt the shape of the potential. TEA also induced "flickering" of the generator potential which means that it might directly affect the transduction mechanism.

278 Words

DECLARATIONS

(i) I, Rhoda Ellis, hereby certify that this thesis, which is approximately 26,510 words in length, has been written by me, that it is the record of work carried out by me and that it has not been submitted in any previous application for a higher degree.

31st Jan 2005

(ii) I was admitted as a research student in October, 1999 and as a candidate for the degree of MPhil. in March, 2004; the higher study for which this is a record was carried out in the University of St Andrews between 1999 and 2004.

31st Jan 2005.

(iii) I hereby certify that the candidate has fulfilled the conditions of the Resolution and Regulations appropriate for the degree of MPhil. in the University of St Andrews and that the candidate is qualified to submit this thesis in application for that degree.

31st Jan 05

COPYRIGHT DECLARATION

A Unrestricted

In submitting this thesis to the University of St Andrews I understand that I am giving permission for it to be made available for use in accordance with the regulations of the University Library for the time being in force, subject to any copyright vested in the work not being affected thereby. I also understand that the title and abstract will be published, and that a copy of the work may be made and supplied to any *bona fide* library or research worker.

date signature of candidate

ACKNOWLEDGEMENTS

I would like to thank the Maitland Ramsey Bequest for funding this research and Dr. William Heitler for his supervision and encouragement.

I would also like to thank my parents, Duncan, and all my friends who have been constant their support and understanding.

ABBREVIATIONS

CAMP	3'5'-cyclic monophosphate
cGMP	Cylic guanosine mono-phosphate
CPR	Caudal photoreceptor
DAG	diacylglycerol
EPSP	Excitatory Post-Synaptic Potential
EOP	Extra-ocular photoreceptors
GDP	guanosine di-phosphate
5'-GMP	guanosine mono-phosphate
GTP	guanosine tri-phosphate
IP_3	Inositol triphosphate
IPSP	Inhibitory Post-Synaptic Potential
KDa	kilo Dalton
LG	Lateral Giant Fibre
mV	Millivolt
PDE	Phosphodiesterase
PI	phosphatidylinositide
PIP2	phosphatidylinositol bisphosphate
PI-PLC	phosphatidylinositol phospholipase C
PLC	phospholipase-C
R	Rhodopsin
R*	Activared rhodopsin
SRC	Subrhabdomeric cisternae
TEA	Tetraethyl ammonium
TTX	Tetrodotoxin

CONTENTS

LIST OF TABLES AND FIGURES

CHAPTER 1: INTRODUCTION

1.1 General Introduction

The ability to detect light is invaluable to an animal that wishes to interact with the world around it. A range of light detecting apparatus exists from the simplest pigmented eye spot of single celled *Euglena*, which when illuminated causes the animal to move into the light, to the complex machinery of the human eye, capable of image formation and able to distinguish words on a page.

Although it had previously been suggested that the eye had evolved independently forty times in the animal kingdom, Dawkins (1996) claims this to be an underestimate and that the actual figure could be as high as sixty. Both these hypotheses were drawn from morphological studies; since then genetic investigations have shown a conservation of the genes that control eye development from fly to mammal. Halder, *et al.* (1995) found that the mouse gene *small eye*, which is the homologue to the *Drosophila* gene *eyeless*, could be introduced into *Drosophila* embryos where it induced ectopic compound eyes on the leg of the fruit fly.. Dawkins (1996) does not deny that the genes responsible for the development of eyes have been conserved across the phyla. He accepts that there may have been a common ancestor that had rudimentary light sensitive patches on its surface; able only to distinguish the difference between night and day and from this the sophisticated eyes we know today evolved. In addition to the 'true' eyes many animals have evolved additional photoreceptors. This study examines one particular type of photoreceptor, the extra-ocular photoreceptor in the tail of the crayfish, known as the crayfish caudal photoreceptor (CPR). However, before discussing the CPR it would be prudent to summarize and compare what is know about two of the more common visual photoreceptors from the vertebrates and invertebrates: the rod of the mammalian eye and the retinular cell of the ommatidium of the crustacean compound eye.

1.1.1 The Vertebrate Visual Systems

The image of an object in the external world enters the mammalian eye through the pupil, the size of which is controlled by the aperture of the iris, and is focused by a single lens. The shape of the lens is adjusted, *i.e.*, elongated or relaxed, by a set of muscles within the eye with the image being inverted as it passes through the lens, and it is this inverted image that finally projects onto the retina at the back of the eye. The retina is composed of two classes of highly

specialized photoreceptors, rods and cones, which extract information about the hue and intensity of light.

Rods are elongated in shape, and are much more sensitive to light than cones, and because of this it is their function to mediate night vision. Cones, on the other hand, show their functional importance in the sensitivity to different wavelengths of light. They can be sub-divided into three types, named after their peak waveform sensitivity, *i.e.*, red, green, and blue. These three types of photoreceptors form the basis for colour vision in most of the great apes. Both rods and cones share the same transduction cascade.

1.1.2 The Transduction Cascade in the Mammalian Rod Photoreceptor

The rod (illustrated in Figure I.i, panel A) is divided into two segments, the inner segment containing the cell body, nucleus and synaptic terminal, and the outer segment containing the photoreceptive ultrastructure, *i.e.*, the discs. Molecular aspects of the transduction pathway of vertebrate photoreceptors have been reviewed by Hurley (1987) are described in brief (Figure I.i, panel B).

In the absence of light the membrane potential of the outer segment of the rod is held at -40mV by a 'dark current' carried largely by the inflow of Na^+ through cGMP-gated ion channels within the membrane. When light is absorbed by, and activates the photo-pigment rhodopsin, a transduction cascade is initiated the end result of which is the closure of Na^+ channels. The consequent loss of dark current causes a negative shift in membrane potential to -70mV.

The photo-pigment, which is a conjugate of a protein, opsin, and the vitamin-A aldehyde retinal (a light-absorbing chromophore), is located on the disc membrane of the outer segment. When activated by light rhodopsin undergoes a change in the three-dimensional structure to produce metarhodopsin (R*). It is this activated form of rhodopsin which stimulates the GDP-GTP exchange reaction (Godchaux and Zimmerman, 1979) on the G-protein, transducin, and it is this GTP portion of transducin that activates the enzyme cGMP phosphodiesterase (PDE) which catalyzes the breakdown of cGMP to 5'-GMP. The PDE activation cycle would continue indefinitely until R* is inactivated. It has been suggested by Liebman and Pugh (1982) that an ATP-dependent quenching of PDE activation, partly as a consequence of rhodopsin phosphorylation, occurs within seconds of rhodopsin

Figure I.i

Vertebrate Phototransduction

Panel (A) The transduction pathway of the vertebrate rod, based on the diagram presented by Yarfitz and Hurley (1994).

Panel (B) The structure and ion channels of the vertebrate rod based on the diagram presented by Kandel, Schwartz and Jessell (1991).

(A)

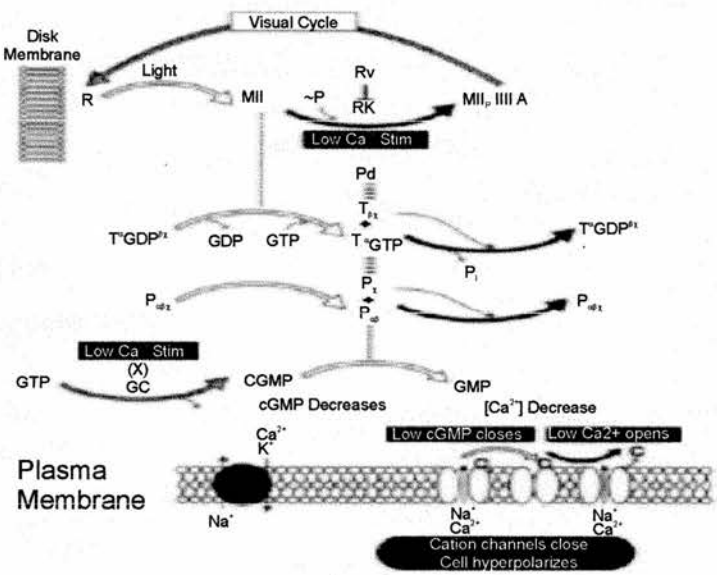
Visual Cycle
Disk Membrane
Light
R
MII
Rv
~P
RK
MII, IIII A
Low Ca Stim
Pd
GDP
GTP
P
Low Ca Stim
(X)
GC
CGMP
GMP
cGMP Decreases
[Ca2+] Decrease
Low cGMP closes
Low Ca2+ opens
Plasma Membrane
Na+
Cation channels close
Cell hyperpolarizes

(B)

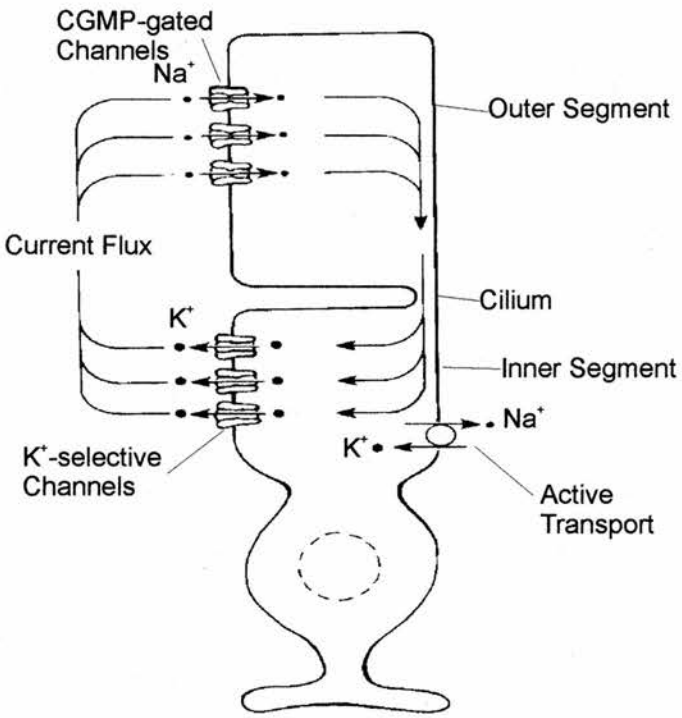
CGMP-gated Channels
Na+
Outer Segment
Current Flux
Cilium
K+
Inner Segment
Na+
K+
K+-selective Channels
Active Transport

photolysis. Phosphorylated R* is a much less efficient activator of transducin than the unphosphorylated form. Additionally, arrestin (a 48-kDa protein present in photoreceptor outer segments, may compete with transducin for binding sites phosphorylated R*, thereby further reducing the efficiency of PDE activation (Wilden, *et al.*, 1986). Reducing the concentration of cGMP in the outer segment of the rod reduces the number of Na^+ channels that are held open, thereby reducing the dark current, and thus causing a light-induced hyperpolarization of the cell.

1.1.3 The Invertebrate Compound Eye

In the invertebrate world the requirements of a visual system are somewhat different given the habitat in which most of the animals live. A great number of them, in particular the crustaceans, are aquatic thereby bringing their own pressures and limitations on the structure of the eyes.

There are several types of invertebrate eyes:

1. Stemmata – single lens eyes, usually found in larvae that can only extract limited information about size, shape and movement.
2. Ocelli – single lens eyes, found in both larvae and adults in some species, *e.g.*, the woodlouse. In general these eyes are incapable of forming images, although some spiders (e.g. the Jumping Spiders) have specialized high-resolution ocelli (Land and Nilsson, 2002).
3. Compound eyes – which is the type most frequently found in insects and crustaceans. (It is this type of invertebrate eye that will be used as the comparison with the vertebrate rod cell.)

As the name suggests, compound eyes are made up of many compartments known as ommatidia, arranged in order to form a convex structure. There are two main types of compound eyes: apposition and superposition. The first, apposition compound eyes, are most commonly found in the diurnal insects such as the fly, where there is a requirement for high visual acuity. Each ommatidium is comprised of a hexagonal tube, with a lens of transparent cuticle at the external face, or cornea, from which a cone of transparent 'jelly', the crystalline cone, projects backwards. At the base of this structure is the retinula, the site of photoreception. Eight retinal cells, each having a specialized portion, project into the centre of the structure to form the rhabdom, the main photoreceptive region in the ommatidium. The

membrane of the rhabdom contains a photosensitive pigment similar to rhodopsin, the first step in the transduction cascade. In the apposition compound eye each lens forms a tiny (inverted) image at the tip of each rhabdom; these tiny images are then combined so that the insect "sees" only one clear image. In order to produce such a good image this type of eye requires there to be a lot of ambient light, which is why most of the aquatic crustaceans, that inhabit environments with restricted light levels, have developed the second type, superposition compound eyes instead. The crucial anatomical difference between the two types of eye is the *clear zone*, across which rays of light are focused on to a single retina on which the image forms rather than one that is broken up into discrete ommatidial units as seen in the apposition eye. However, in order to attain a greater capture of light high acuity has been sacrificed.

The crayfish has developed a particularly specialized form of superposition eye, the reflecting superposition eye (illustrated in Figure I.ii panel (B)) which uses mirrors rather than lenses to focus light (Vogt (1975) as quoted by Land and Fernald, 1992; Land and Nilsson, 2002). This means that a pencil of light passing through each mirror box is pre-focused, reaching the receptors as a fine beam, thereby improving image resolution but giving a narrower field of view. The opaque nature of the mirrors means that no light enters from neighbouring facets. This 'mirror-box' design only works with the right-angle corners of the square cone and not hexagonal cone.

1.1.4 Transduction in the Compound Eye

The photoreceptors of the compound eye contain a pigment from the rhodopsin family. When a photon of light of an appropriate wavelength is captured by 'rhodopsin' (R), the metarhodopsin state is reached. Metarhodposin is far more stable in its arthropod form and is not bleached (broken down) as it is in vertebrates. This photoactivated rhodopsin activates Gq-type G-protein in the crayfish photoreceptor (Terakita, *et al.*, 1993). This Gq protein was localized to the rhabdomeric membranes, where rhodopsin is known to be located. Visual Gq must be a transducer in invertebrate rhabdomeric photoreceptors.

There is a recognised link between Gq and the down steam components inositol triphosphate (IP_3) and calcium, but the exact nature of this link is as yet unknown. Brown *et al.* (1992) injected IP_3 into the ventral photoreceptors of *Limulus*, and proving its involvement in the

Figure I.ii

Invertebrate Phototransduction

Panel (A) Transduction pathway of the vertebrate visual photoreceptor based on the diagram presented by Yarfitz and Hurley (1994).

Panel (B) Structure of the ommatidia in the crayfish super position compound eye based on a diagram presented by Vogt (1980).

(A)

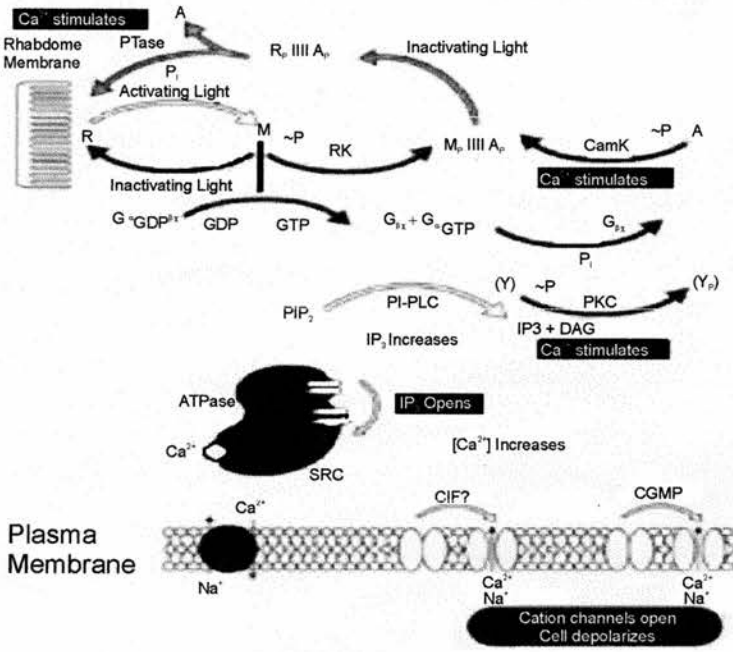
Ca++ stimulates
A
Rhabdome Membrane
PTase
Inactivating Light
Activating Light
R
M
~P
RK
CamK
Inactivating Light
GDP
GTP
PIP2
PI-PLC
IP3 Increases
(Y)
PKC
IP3 + DAG
Ca++ stimulates
ATPase
IP3 Opens
Ca2+
SRC
[Ca2+] Increases
Plasma Membrane
Ca2+
Na+
CIF?
CGMP
Cation channels open
Cell depolarizes

(B)

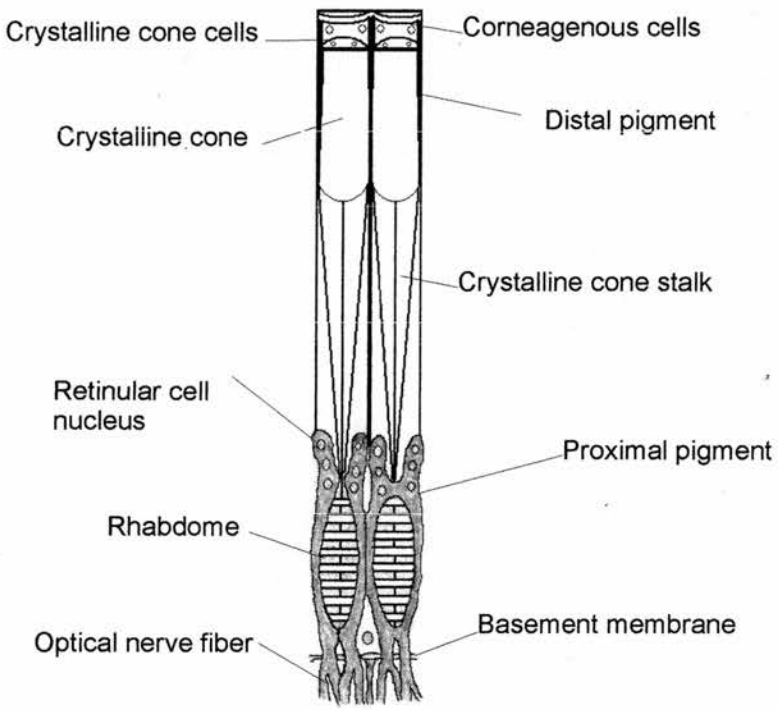
Crystalline cone cells
Corneagenous cells
Distal pigment
Crystalline cone
Crystalline cone stalk
Retinular cell nucleus
Proximal pigment
Rhabdome
Basement membrane
Optical nerve fiber

transduction cascade by its ability to release calcium from subrhabdomeric cisternae (SRC) and elicit an electrical response resembling photoexcitation. Calcium is thought to cause the opening of cation channels in the membrane, in contrast to the closing of ion channels in the vertebrate system, and results in the depolarization of the photoreceptor.

Table 1.1 highlights some of the main differences between vertebrate and invertebrate visual systems.

Table 1.1 The Main Differences Between Vertebrate And Invertebrate Visual Systems

	Invertebrate	**Vertebrate**
Ultrastructure	Microvilli	Ciliary
Membrane shift	Depolarization	Hyperpolarization
Permeability change	Opening of Na^+ channels	Closing of Na^+ channels
Resting potential	-70mV	-40mV
Dark current	No	Yes

1.1.5 Extra-ocular Photoreception in Vertebrate and Invertebrate Animals

Many animals have evolved additional photoreceptors, extra-ocular (or extra-retinal) photoreceptors to compliment their 'true' eyes (reviewed by Millott, 1968; Wolken and Mogus, 1979). The main function of these extra-ocular photoreceptors is the entrainment of circadian rhythms. They detect ambient light levels for the synchronization of internal "biological clocks" with local time, for it is important that animals perceive the passing hours and changing of the seasons in order to regulate their physiology, setting daily patterns of hormones for growth and reproduction by this information.

However, it can be difficult to define these extra-ocular photoreceptors (EOP). For what may be considered an eye in one animal may only be an EOP in another. This is especially so for the lower invertebrates, many of which never need to form an image and rely on their eyes to provide only very basic information as to light levels or direction of light.

Table 1.2 Vertebrate Extra-retinal Photoreceptors

Animal	Location	Type of EOP	Behavioural Function	Reference
Atlantic salmon *Salmo salar*	Pineal complex	Neural	Not stated	Philip *et. al.*, (2000)
Dogfish Shark *Scyliorhinus caniculus* L.	Epiphysis cerebri	Neural		Hamasaki and Streck (1971)
Duck*Ana platyrhinchos*	Pineal organ	Neural	Testicular function	Hisano *et. al.*, (1972)
Eel *Anguilla anguilla*	Third ventricle Diencephalon	Neural	Nocturnal motor activity	Van Veen, *et al.* (1976)
Frog *Rana pipiens*	Frontal organ	Neural	Not stated	Eldred and Nolte (1978)
Frog *Rana Temporaria* and *Rana catesbeiana*	Pineal complex Frontal organ and epiphysis cerebri	Neural	Not stated	Hartwig and Baumann (1974)
Iguanid Lizard *Sceloporus olivaceus*	Unknown – not Pineal organ or Parietal eye	Presumed to be Neural	Circadian Rhythms	Underwood and Menaker 1970
Mouse	Inner retina	Neural	Circadian rhythms	Freedman *et al.* (1999) Lucas *et. al.* (1999); Provencio *et. al.* (2002)
Neon Tetra *Paracheriodon innesi*	Iridocytes	Dermal	Not stated	Lythgoe *et. al.*, (1984)
Neonatal Rats	Harderian Gland	Neural	Circadian rhythms, maintenance of Pineal serotonin levels	Wetterberg *et. al.*, (1970)
Newly hated Pigeon *Columba livia*	Skin	Dermal	Initiation of feeding pattern	Harth and Heaton (1973)
Puffer fish *Fugu rubripes*	Brain	Neural	Not stated	Philip *et. al.*, (2000)
Rainbow Trout *Salmo irideus*	Pineal organ	Neural	Circadian Rhythms	Dodt (1963)
Tiger Salamander *Ambystoma tigrinum*	Pineal organ	Neural	Compass orientation via celestial cues	Taylor, (1972)

Table 1.3 Invertebrate Extra-ocular Photoreceptors.

Animal	Location	Type of EOP	Behavioural Function	Reference
Alfalfa weevil *Hypera postica*	Head	Presumably neural	Host plant recognition	Meyer (1977)
Aplysia	Uncertain	Neural	Circadian rhythm	Block *et. al.*, (1974)
Bivalve Mollusc *Lima scabra*		Dermal		Mpitsos, (1973)
Butterfly	Genetalia			Arikawa *et. al.* (1981)
Crayfish	Terminal ganglion	Neural	Backwards walking behaviour	Prosser, (1934)
Crayfish	Cerebral Ganglion	Neural	Circadian rhythm	Sandeman *et. al.*, (1990)
Diadematid Sea Urchin *Centrostephanus longispinus*	Chromatophores in the Epilthelium	Dermal	Colour Changing	Gras and Weber, (1983)
Fruit fly *Drosophila melanogaster*	Posterior margin of compound eye			Hofbauer and Buchner, (1989) Yasuyama and Meinhertzhagen (1999)
Lamellibranch mollusc	Siphon	Neural	Siphon retraction	Kennedy (1960)
Locust *Locusta migratoria*	Brain	Neural		Lundqvist *et. al.*, (1996)
Moth *Manduca sexta*			Entrainment of Circadian Rhythms	Truman, (1974)
Sea Anemone *Calamactis praelongus*	Muscle Tissue			Marks, (1976)
Sea Anemone *Metriduim senile*	Muscle Tissue			North, (1957)
Worm *Nereid polychaetes*		Neural/dermal?	Slow tail withdrawal; backward-pointing parapodial reflex	Gwilliam (1969)

There are three types of extra-ocular photoreceptors have been described: dermal, diffuse and neural, which are found throughout both the invertebrates and vertebrates. Tables 1.2 and 1.3 list a selection of extra-ocular photoreceptors that have been studied. Vertebrate extra-ocular photoreceptors can be found in a number of neural locations, which are thought to develop from the embryonic forebrain (Philip, *et al.*, 2000). The most significant of these being the inter-cranial pineal organ or pineal body (epiphysis cerebri), which contains photoreceptors in all non-mammalian vertebrates. Other locations include the inter-cranial parapineal organ found in many bony fish and lampreys, the extracranial third eye variously called the frontal organ (frogs) or the parietal eye or parietal body (lizards), as well as photoreceptors found in deeper regions of the brain. Studies of the ultrastructure of such locations have revealed that they contain well organized photoreceptors which resemble visual photoreceptors (Eakin and Westfall, 1960; Wurtman, *et al.*, 1968).

Foster originally claimed that "mammals are unique among vertebrates in that they appear to have lost extra-retinal photoreceptors, using their eyes for both image detection and the regulation of temporal physiology" (cit. loc.: Foster and Soni (1998)). However, there is now evidence of an expansive net of photoreceptive ganglion cells within the inner retina, separate from the structure of rods and cones (Freedman, *et al.*, 1999; Lucas, *et al.*, 1999; Provencio, *et al.*, 2002) which could be considered to be EOPs, in the same way those found at posterior margin of compound eye in *Drosophilia* (Hofbauer and Buchner, 1989; Yasuyama and Meinertzhagen, 1999) are classed as extra-ocular photoreceptors.

1.2 The Crayfish Caudal Photoreceptor

The crayfish has two types of extra-retinal photoreceptors, in addition to its compound eyes. One is situated in the cerebral ganglion (Sandeman, *et al.*, 1990) and the other, the caudal photoreceptor (CPR), in the terminal ganglion of the ventral nerve cord (Prosser, 1934). Kennedy (1963) discovered that the CPR is, in fact, a pair of neurons whose dendritic branching and cell body are encompassed within the terminal ganglion, but whose axons run in parallel (Kennedy, 1963; Galeano, 1976), one in each hemi-connective, rostrally to the brain (Kennedy, 1963; Wilkens and Larimer, 1972) terminating in the vicinity of the antennal and para-olfactory lobes (Simon and Edwards, 1990). This pair of neurons are completely isolated from one another, there being no evidence for any electrical coupling or synaptic activity between them (Kennedy, 1963).

Stimulation of the CPR with a fine beam of light narrowed down the site of photoreception to the dendritic branches; the cell body and the neurite leading to it showed no evidence for photoreceptive properties or light response, nor did the axon (Wilkens and Larimer, 1972). This was backed up by an investigation into the ultrastructure of the cell using colloidal gold filling which found the dendritic processes to contain, and be surrounded by, densely-packed membrane layers similar to the microvillar structures seen in other invertebrate photo-sensory cells (Kruszewska, 1991). The CPR is unusual among photoreceptors in that it produces a change in membrane potential and action potentials, as opposed to most other photoreceptors where there is only a change in the membrane potential. This made the initial detection of the photic unit in the crayfish ventral nerve cord by Prosser (1934) by extracellular recording significantly easier. Many physiological characteristics have been described such as its long latency between the onset of the stimuli and the onset of the response (Kennedy, 1958a; Galeano, 1976), and the temperature sensitivity of this response which slows down when cooled (Kivivuori, 1982; Belanger, 1988).

The CPR, however, differs from other photoreceptive cells in that it appears to have evolved photosensitity as a secondary property. In addition to its photic response it also functions as a simple mechanosensory intergrating interneuron (Flood and Wilkens, 1978; Galeano and Beliveau, 1973; Wilkens and Marzelli, 1979). Water movements on one side of the tail fan stimulate the CPR on that ipsilateral side eliciting an excitation while producing a concurrent inhibition in the contralateral CPR (Simon and Edwards, 1990). Its gross anatomy resembles that of numerous other ascending interneurons, with this function but which do not show any photosensitivity. (Kennedy, 1963b,c; Wilkens and Larimer, 1972; Flood and Wilkens, 1978;).

1.2.1 Function of the Crayfish Caudal Photoreceptor

The crayfish is partially nocturnal animal, often remaining concealed within burrows during daylight hours when it would otherwise be more vulnerable to predation. Animals whose compound eyes have been removed still show a preference for darkness, which is subsequently lost when the CPR are destroyed (Simon and Edwards, 1990). This photo-negative activity is thought to be the most significant behaviour that the CPR is involved in. It has been shown that illumination of the tail-fan can trigger backwards walking in the intact animal (Welsh 1934; Edwards 1984; Simon and Edwards, 1990), and repetitive abdominal

flexion and leg movements when the animal is restrained (Larimer and Kennedy, 1969; Kovac, 1974a; 1974b; Edwards, 1984; Moore and Larimer, 1987).

This could be thought of as a retreat response rather than an escape response given the time-frame over which the CPR would affect such behaviour. However, light can be a very powerful stimulus in the escape behaviours of many invertebrates. The scallop, for instance, inhabits the sandy sea-bed, where, despite its cryptic appearance, it is exposed and susceptible to being preyed upon. When a shadow is cast by something passing over-head, inhibition of the light response from its eyes triggers a defensive action - the animal clamps shut. In the crayfish, which spends the majority of its time burrowed away, illumination of the CPR may have the reverse effect. The long latency between stimulus of the CPR and its response (Kennedy, 1958a) means that it is unlikely that the CPR is directly mediating an escape response itself, but it may be contributing to the effectiveness of the giant-fibre mediated escape response. Illumination lowers the CPR's threshold for tactile stimulation (Kennedy and Preston, 1960), thus making it more sensitive to water movements when the animal is out of the safety of its burrow.

1.2.2 Does the Caudal Photoreceptor Play a Role in the Entrainment of Circadian Rhythms?

In general extra-ocular photoreceptors have been implicated in the entrainment of circadian rhythms (Wolken and Mogus, 1979) but the majority of studies on the CPR have shown its main behavioural significance to lie in the initiation of backwards walking (Welsh 1934; Edwards 1984; Simon and Edwards, 1990) and lowering the threshold for tactile stimulation (Kennedy and Preston, 1960). Chappel (1960) claimed that the CPR can regulate diurnal activity cycles in crayfish whose eye stalks have been ablated. Page and Larimer (1976) reaffirmed the CPR's ability to entrain electroretinalgram amplitude although they stated that the CPR was not necessary for entrainment, and animals whose CPR has been severed could still entrain circadian rhythms presumably with their eyes. Two further papers (Fuentes-Pardo and Inclan-Rubio, 1987; Inclan-Rubio and Fuentes-Pardo, 1987) also support the CPR's involvement in circadian rhythms. However all of these studies can be countered or at least held up to doubt in light of a study by Sandeman *et al.* (1990) that the crayfish possess another class of EOP in the cerebral ganglion. The evidence for this second class of EOP being involved in the entrainment of circadian rhythms is far stranger and it seems to have no other possible function. It is therefore; possible that when Chappel (1960) removed the eye

stalks of crayfish it was their cerebral EOPs rather than the CPR that were maintaining the animal's biological clock. However this is not to say that the CPR has no effect on circadian rhythms for it may still be able to influence the animal in the absence of the eyes and cerebral EOPs, although one could question why the crayfish would evolve two anatomically distinct classes of EOP to perform the same task. There is strong evidence that the function of the cerebral EOP is to synchronize the animal's internal rhythms; therefore it becomes more likely that the CPR exists to perform some other function.

1.3 The Aims Of This Thesis

The aims of this thesis are to expand what is known about the photic response of the crayfish caudal photoreceptor. The methods employed in this study are outlined in Chapter 2, and each subsequent chapter deals with a different aspect of the CPR's function.

In Chapter 3 the method of template recognition is examined by comparing the extracellular and intracellular recordings made simultaneously from the CPR. This technique is then employed to build a frequency curve of the action potentials over the course of the photic response which was then compared to the exposed generator potential in the presence of tetrodotoxin (TTX), in order to verify the hypothesis that the depolarization of the generator potential dictates the frequency of the action potentials elicited.

The involvement of serotonin in crayfish antagonistic behaviour has been well described, as has its role in modulating the lateral giant fibre escape system. In this study the photic response of the CPR was tested for any modulatory effects that may occur from increase levels of serotonin. For this the CPR was examined both in its role as a primary photoreceptor and as a mechano-sensory integrating interneuron.

The transduction pathway of the crayfish caudal photoreceptor is not very well understood. Kruszewska (1991) and Kruszewska and Larimer (1993) provided evidence that this transduction pathway is meditated by IP_3/Ca^{2+} second messengers suggesting that the pathway may resemble that of the invertebrate visual photoreceptors. During the course of this study several reagents were applied to the preparation to identify any changes in the photic response that could reveal any other steps of the cascade.

The transduction cascade of sensory cells will usually result in the opening or closing of an ion channel in order to convey information, and it is assumed that the same is occurring in the CPR. However, it is unknown whether the ionic conductance responsible for the generator potential is an increase or a decrease. The depolarization of invertebrate visual photoreceptors has been shown to be produced by an opening of Na^+ channels, and if the CPR was transducing light in the same manner as the visual photoreceptors then it would follow that the photic response would also result from an influx in Na^+.

Previous studies by Kruszewska (1991) and Wilkens (1988) mention incidental observations that a reduction in sodium concentration has a negative effect on the photic response of the CPR. This concept is pursued further in this study by reducing the sodium concentration of the saline in preparations whose voltage-dependent channels have already been blocked by TTX. This is then combined with an examination of conductance changes over the course of the photic response via small square pulses of injected current, and experiments into the possible role of K^+ in the photic response.

In the final chapter the new information gained about the CPR will be put together with the existing knowledge in order to produce an overall model of how the CPR works.

CHAPTER 2: GENERAL MATERIALS AND METHODS

2.1 Animals: Maintenance and Dissection

Mature *Pacifasticus leniusculus* of both sex and approximately 10-15cm in length from rostrum to telson were obtained from a commercial supplier (Riversdale Farm, Dorset). The crayfish were maintained in a tank approximately 1.5m^2, 15cm deep with aerated, filtered fresh water, containing plastic tubes serving as substitute burrows. Plastic netting was placed over the top of the tank to prevent the crayfish from escaping.

Animals were isolated in smaller tanks for two week prior to experimentation in order to reduce any influence of social hierarchy. When crayfish fight the winner gets a dominant status and its serotonin level increase, whilst the loser becomes subordinate and its serotonin level decreases (Edwards and Kravitz, 1997; Yeh, *et al.*, 1996; Yeh, *et al.*, 1997). Therefore, by taking them out of these social situations, it is likely that all experimental animals will have similar social status and intrinsic serotonin levels (Yeh, *et al.*, 1996; Yeh, *et al.*, 1997).

Prior to dissection the animals were chilled in ice for 20 min to make them docile. Animals were sacrificed by making an incision on the ventral side between the 3rd and 4th pairs of walking legs, and then cutting right round and through the animal (anatomy illustrated in Figure II.i). The anterior nervous system was destroyed by cutting up the ventral surface of the anterior half through the brain. For all experiments, the abdominal portion of the ventral nerve cord was excised as follows: the dorsal exoskeleton of the abdominal section was removed by cutting along the sides of the animal to reveal the large flexor muscle blocks below. The animal was pinned out with dress-makers pins through the tail fan and legs in a dish filled with physiological saline, pH 7.4 with the following composition (mmol/L): 207.5 NaCl; 5.4 KCl; 13.5 $CaCl_2.2H_2O$; 2.6 $MgCl_2.6H_2O$; 10 HEPES.

All subsequent dissection was performed under a binocular microscope (Wang Biomedical) using a magnification of x40. A midline incision was made between the bilateral flexor muscle blocks in order to separate them. The individual muscle blocks were then carefully raised and dissected away exposing the ventral nerve-cord.

The nerve roots were exposed, and the nerve cord excised using small scissors to obtain as much of the nervous system as possible. The main abdominal artery, which runs ventrally

Figure II.i

General Anatomy of the Crayfish *Pasifasticus leniusculus*

Rostral

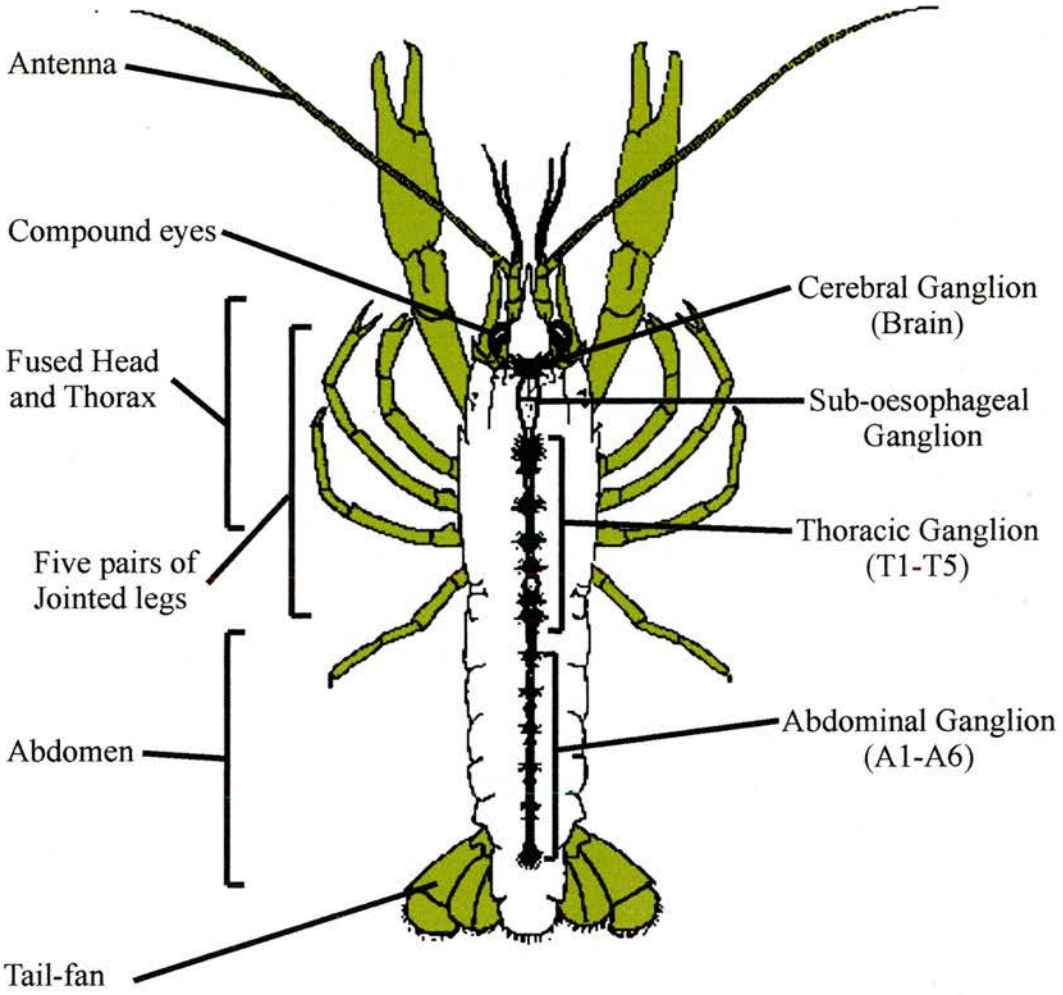

Caudal

along the length of the nerve cord, was then teased away in order to make recording from the connective more effective.

For intracellular recordings and experiments requiring the permeation of pharmacological agents, the nerve sheath covering the dorsal surface of the terminal ganglion, A6 was removed. This was achieved by carefully tearing a small hole in the sheath using forceps and then cutting a square out of the sheath using scissors.

There are two caudal photoreceptors (CPR), each with an axon in one hemi-connective. When recording extracellularly from the intact connective the action potentials from these two neurons have a similar size and shape, and it is easy to confuse which action potential belongs to which neuron. Therefore, in order to facilitate accurate analysis, one of the cells was eliminated. This was achieved by hemi-sectioning the connective on the right hand side between abdominal ganglia A4 and A5, thus removing the anterior projection of signal from that CPR, so that only the left CPR could be recorded from further along connective.

2.2 Electrophysiology

2.2.1 Experimental Chamber

For electrophysiological studies the nerve cord was placed in a rectangular transparent, Perspex chamber (15cm by 3cm by 4cm) see Figure II.ii. The chamber consists of three compartments. The main compartment on the upper surface of the chamber is shallow and lined with Sylgard. The preparation was pinned out dorsal side uppermost in this compartment, using minute metal pins through the nerve roots. The other two compartments are located at either end of the main compartment and are connected by a tube running underneath.

The chamber was perfused with oxygenated, circulating physiological saline with a total bath volume of 4ml. Pure oxygen (BOC) was supplied through a narrow plastic tube placed at the bottom of compartment A. This established circulation of saline driven by the rising oxygen bubbles.

The addition of high concentration pharmacological agents (max volume 200µl, at 20 times the final concentration) into compartment B ensured that the agent passed through the circulation system, and was at the desired final concentration before reaching the preparation,

Figure II.ii

The Experimental Chamber

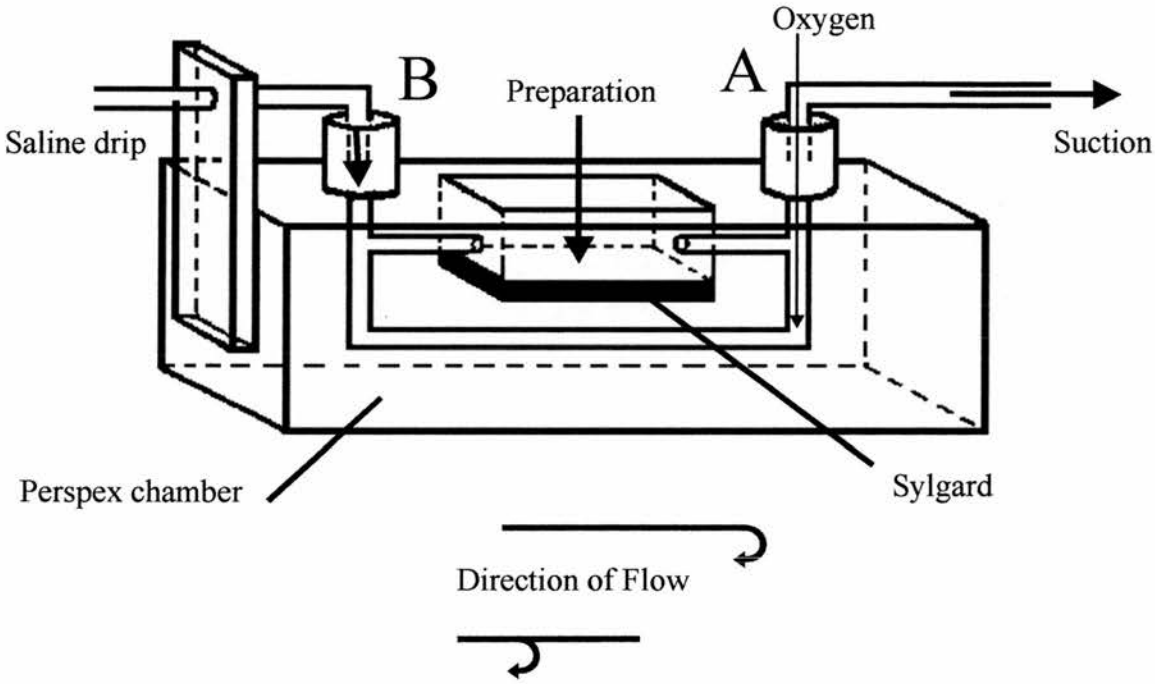
Oxygen
A
B
Preparation
Saline drip
Suction
Perspex chamber
Sylgard
Direction of Flow

and minimising mechanically-induced artefacts. A dye was used to test uniform mixing and to make sure there were no obvious null spots in which high concentrations could collect.

During a wash approximately 30-40 ml of fresh saline was 'dropped' into compartment B from a reservoir positioned higher than the chamber. The flow of saline was controlled by use of a small roller clamp, at approximately 30 drops per minute. The level of saline was kept constant by surface suction applied to compartment A, ensuring a constant bath volume.

The preparation was orientated such that the anterior end of the nerve cord was positioned close to the compartment into which pure oxygen was bubbled, and the posterior end towards the compartment where saline was added. This arrangement ensures that there is minimal disruption to the tissue in the region of the terminal ganglion, where impalement of the CPR with microelectrode was performed.

Electrophysiological recordings were made within a Faraday cage, the top, back and sides of which were covered in carbon-filled black-out material. The front of the cage needed to remain accessible so was fitted with a removable curtain of the same material. The cage was supported on the solid frame of an anti-vibration table (Iso-station VH3048-Opt: Newport, CA USA), with the experimental chamber and electrode micro-manipulators placed on the floating surface.

2.2.2 Illumination

During dissection, and experimental set-up, the preparation was exposed to ambient and focussed light causing the photoreceptor to undergo an uncontrolled light response. It was, therefore, necessary to stabilize the photic response prior to experimentation by leaving it in complete darkness within the cage for 15-20 minutes, once the extracellular electrodes had been attached.

The stimulating light source was emitted from a halogen lamp (Lumina: Chiu Technical Corporation). The light was focused on to the preparation via a fibre optic cable resulting in an intense beam of light. Timing of illumination was controlled via a data acquisition computer program, through which the extracellular and intracellular traces were recorded. Passage of light from the lamp housing to the fibre-optic cable was regulated by a shutter

mechanism operated by a magnetic solenoid-relay, opening and closing under the direction of the time constraints entered into the program.

The standard light regime was to record background activity of the preparation in the dark for 5 seconds prior to a 4 second light pulse. Recordings continued for up to 60 seconds in order to capture the complete response. This sequence was repeated at 3 minutes intervals for the duration of the experiment, during which time the preparation was not exposed to any other light source that could stimulate the CPR. However, the preparation could be examined under a red light because the photoreceptor has no physiological response to red light (Bruno and Kennedy, 1962). Therefore this lighting could be used when adding pharmacological agents or washing the preparation.

2.2.3 Extracellular Recording

Two bipolar hooks electrodes were used to record the extracellular activity of the CPR in the connective in response to light. One was placed underneath the connective between the last thoracic ganglion T5 and the first abdominal A1, and the other between ganglia A3 and A4 (see Figure II.iii). The electrodes were insulated with a Vaseline and paraffin oil mix. This was applied in the absence of saline to ensure good contact with the electrodes then the saline was replaced. The output of the electrodes was amplified, and filtered (high cut and low cut 200Hz–2KHz Model 1700: A-M systems Differential AC amplifier) and displayed on a digital oscilloscope (20ms/Sec ocilloscope DSO 1604: Gould).

2.2.4 Extracellular Stimulation

In those experiments designed to investigate the mechano-sensory integrating interneuronal aspect of the CPR, a suction electrode was used to stimulate nerve roots of the terminal ganglion (A6). The suction electrode was held in a micromanipulator and was attached to the nerve root of interest. The tip of the suction electrode was positioned over the severed end of the nerve root. A 5ml syringe was used to generate gentle back pressure which sucked the nerve root into the tip of the electrode. The suction electrode was connected to the an isolated stimulator.

2.2.5 Intracellular Recording

2.2.5.1 Electrodes

Microelectrodes were drawn from 7cm long pieces of 1mm filamented thick wall glass tubes

Figure II.iii

Electrode Arrangement on the Abdominal Section of the Crayfish Ventral Nerve Cord

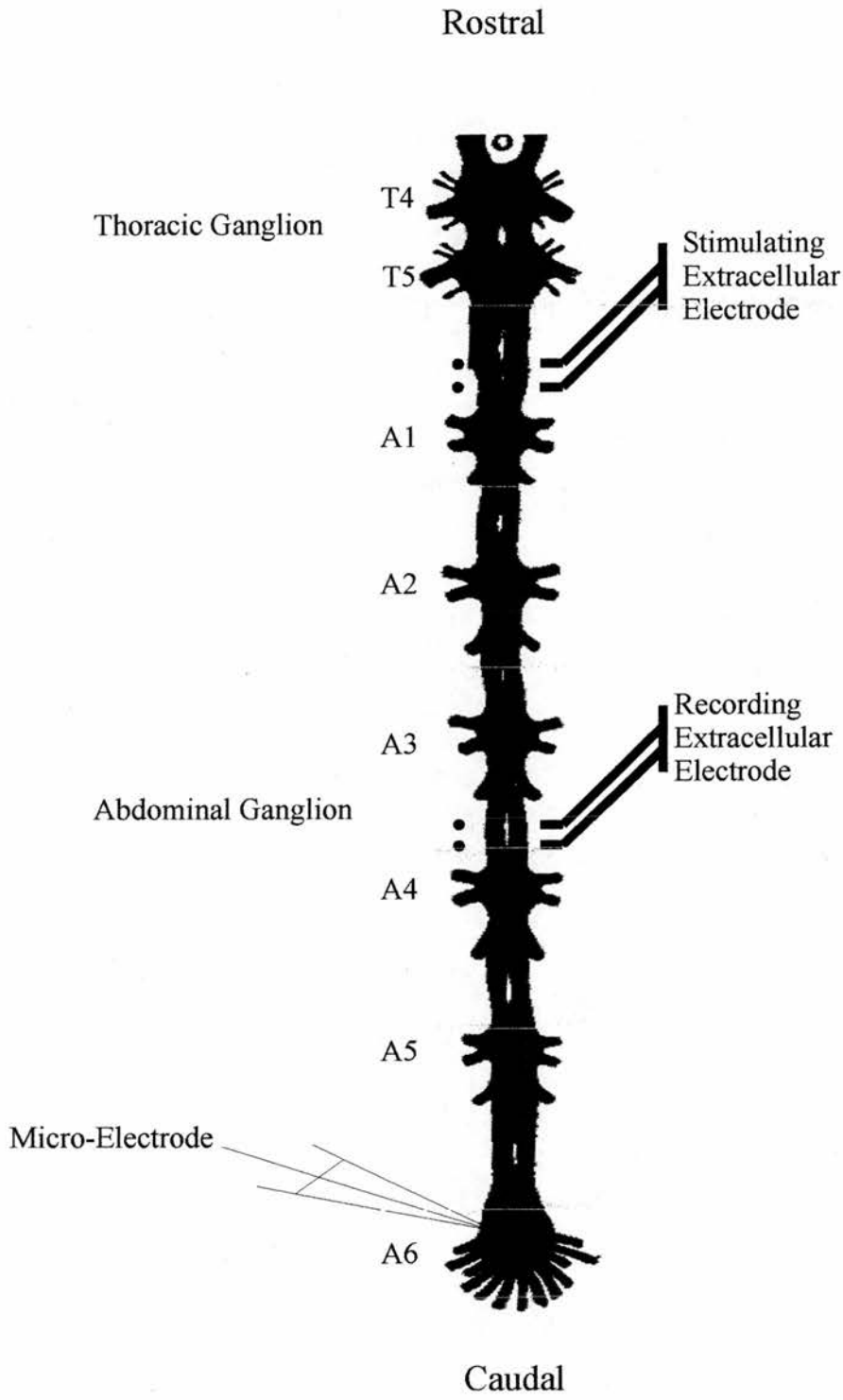
Rostral
Thoracic Ganglion
T4
T5
Stimulating
Extracellular
Electrode
A1
A2
A3
Recording
Extracellular
Electrode
Abdominal Ganglion
A4
A5
Micro-Electrode
A6
Caudal

(GC100TF-15: Clark Electromedical Instruments, Pangbourne England). Briefly, both ends of the glass tube were clamped and the tube heated in the middle while the two ends are pulled apart by an electrode puller (P-97 Sutter Instruments Co.).

Electrodes were filled with an electrolyte solution of either 3M potassium acetate for standard electrodes or 1M lithium chloride for Lucifer Yellow staining. The electrode resistance was measured by passing 1 nanoamp of positive or negative current through the electrode. The resistance of standard 3M potassium acetate was ideally between 20 and 50 MΩ. The Lucifer Yellow electrodes were made using the same program on the electrode puller, but had a higher resistance, 50 - 80 MΩ, because they were filled with dye.

A silver/silver chloride wire was inserted to approximately halfway along the body of the electrode, the other end of which was soldered to a shielded cable. The electrode was mounted on a micro-manipulator. The intracellular signal was DC amplified (Axo-Clamp 2B, Axon Instruments Corp.) and displayed on the digital oscilloscope.

2.2.6 Preparation Earth

For most experiments a standard chlorinated silver/silver chloride earth wire was used, but for those involving a change in the ionic composition of the saline an agar bridge was used in order to eliminate any possible artefacts from the electrochemical interactions between the saline and the earth wire.

The agar bridge was constructed from a plastic Gilson pipettor tip (200µl) filled with agar (Sigma Chemical Co. Ltd.) and saturated with potassium chloride with a chlorided silver wire embedded in the gel. This wire was grounded through the intracellular amplifier. The appropriate type of earth wire was placed in the main compartment of the experimental chamber.

2.2.7 Impalement

None of the anatomical features of the CPR can be seen under the dissecting microscope when looking at the desheathed terminal ganglion, as the cell is situated approximately in the middle of the ganglion. The electrode was lowered to the surface of the terminal ganglion in the left-hand anterior region where the main neuropile branching of the cell occurs.

Impalement of the CPR with the intracellular microelectrode was attempted in the dark, because it was found to be easier to penetrate the silent CPR. As the electrode was moved through the tissue it was "tapped" into neurones using mechanical vibration. Impalement of a neurone was indicated by a sudden negative shift in membrane potential of between -60mV and -70mV. In order to determine whether that the cell penetrated was the CPR, a test light pulse was given. If the cell penetrated was not the CPR then the traces on the oscilloscope from the extracellular electrodes would show a light response, but that from the intracellular electrode would not. If the CPR had been successfully penetrated, there would be a positive shift in the membrane potential, *i.e.*, a depolarization, and a 1:1 match between spike activity in the extracellular and intracellular traces.

2.3 Neuron Identification

Due to the obvious electrophysiological response of the CPR to light it was not deemed necessary to confirm the identity of this neurone anatomically following all experiments. However, anatomical studies were undertaken in order to establish whether the CPR in *Pacifasticus leniusculus* was structurally similar to those in other species.

This was achieved using microelectrodes containing Lucifer Yellow. The electrode was filled at the tip with 5% Lucifer Yellow in lithium chloride, by capillary attraction. Then the electrode was backfilled with 1M Lithium chloride. Negative current pulses 0.5 seconds long were passed through the electrode at 1 second intervals, depositing dye within the cell. Currents of between 1 and 5 nA were used for as long as the electrode could remain in the cell, usually for up to an hour.

Preparations were dehydrated in an Ethanol series 70%, 85%, 90%, 95%, 100%, 100% and cleared in methylsalicilate. They were mounted on concave slides, and photographed. Drawings were made using camera lucida.

2.4 Data Capture

Intracellular and extracellular recordings were digitized with 16-bit AD, at 20 KHz. Data was downloaded straight on to computer via EGAA and CPR data acquisition. These recordings were then analysed with in Dataview© (Dr. W. J. Heitler). Storage of data was on hard disk and CD ROM.

CHAPTER 3: NATURAL PROPERTIES OF THE CAUDAL PHOTORECEPTOR IN THE CRAYFISH, *Pastifasticus leniusculus*

3.1 Introduction

The light response of the crayfish caudal photoreceptor (CPR) was reported independently by Prosser (1934) and Welsh (1934); however the first detailed description of the properties of the CPR came from Kennedy (1958a), followed by a subsequent study by Kennedy and Preston (1960). They showed that the CPR has a relatively long latency from the onset of a light stimulus to the onset of the light response, which has been attributed to a multistage biochemical cascade later investigated by Kruszewska (1991). The result of the biochemical cascade being a depolarizing generator potential followed by action potentials once the depolarization has reached threshold.

The crayfish CPR is unusual in that it is one of the few photoreceptors to produce action potentials as part of its photic response. Most photoreceptors, especially the visual, have no need to produce action potentials because they are conveying signals over a much shorter distance. However, the CPR conveys information the length of the animal from the site of photoreception in the very last ganglion of the ventral nerve cord all the way to the cerebral ganglion. Given that the CPR must convey information over such a long distance it could be assumed that many of the subtleties found in other photo-transduction systems would be lost. In lower light levels the rod does not hyperpolarize to the same degree as it would in intense light levels. This response to light is passed on to the next level of neurons in the retina through graded chemical synaptic transmission.

Alternatively, the CPR uses the frequency of tonic action potentials as a means of transmitting a graded response. Intense light levels evoking a higher frequency of action potentials than lower light levels. Galeano and Chow (1971) were the first to display the frequency of action potentials over time. They showed that the frequency of action potentials produced by the CPR is also dependent on other factors such as pre-exposure of the tissue preparation to light and the duration of any light stimulus.

In the present study simultaneous recordings were made intracellularly from the dendrites of the CPR in the terminal ganglion and extracellularly from the axon in the inter-ganglionic connective some distance away. This meant that firstly, the CPR could be used as a model to

evaluate the template recognition component of the Dataview© program as an analytical tool. Using threshold recognition analysis of the intracellular recording each action potential in the intracellular recording was matched one to one with those identified by the template recognition, allowing for verification that the template recognition analysis works. The accuracy and limitation of this tool and what makes a good template were also explored. Secondly, these techniques, along with the removal of action potentials from the photic response with TTX, were used to investigate in detail the relationship between the amplitude of the generator potential and the frequency of the action potentials which emanate from the CPR. Then, finally, exposure of the CPR to repetitive light stimuli was used to establish a protocol for the proposed further experimentation of this study.

3.2 Additional Material and Methods

Tetradotoxin (TTX) was added from aliquots to reach a final bath concentration of [7.5 x 10^{-10}M] in some preparations in order to block voltage dependent Na^+ channels thus eliminating the firing of action potentials.

3.3 The Caudal Photoreceptor Of *Pacifasticus leniusculus*

3.3.1 Anatomy

In *Pacifasticus leniusculus*, the neuropile branching of the left CPR is mainly on the left-hand side of the terminal ganglion; with the main branches being in the anterior half of the ganglion (see the photograph in Figure III.i and camera lucida drawing in Figure III.ii). The dendritic branching occurs about halfway down through the ganglion. There is a large projection over to the right hand side of the ganglion which descends within the ganglion and results in the cell body.

There are no obvious anatomical features, at the level of the light microscope, to indicate that the CPR is a 'primary' photoreceptor. Structurally this cell has the appearance of many other integrating interneurons in the terminal ganglion, and it is its physiological properties which lead to its classification as an extra-ocular photoreceptor.

Figure III.i

Photograph of the Caudal Photoreceptor

Photograph of the left hand crayfish caudal photoreceptor within the terminal ganglion stained with Lucifer Yellow.

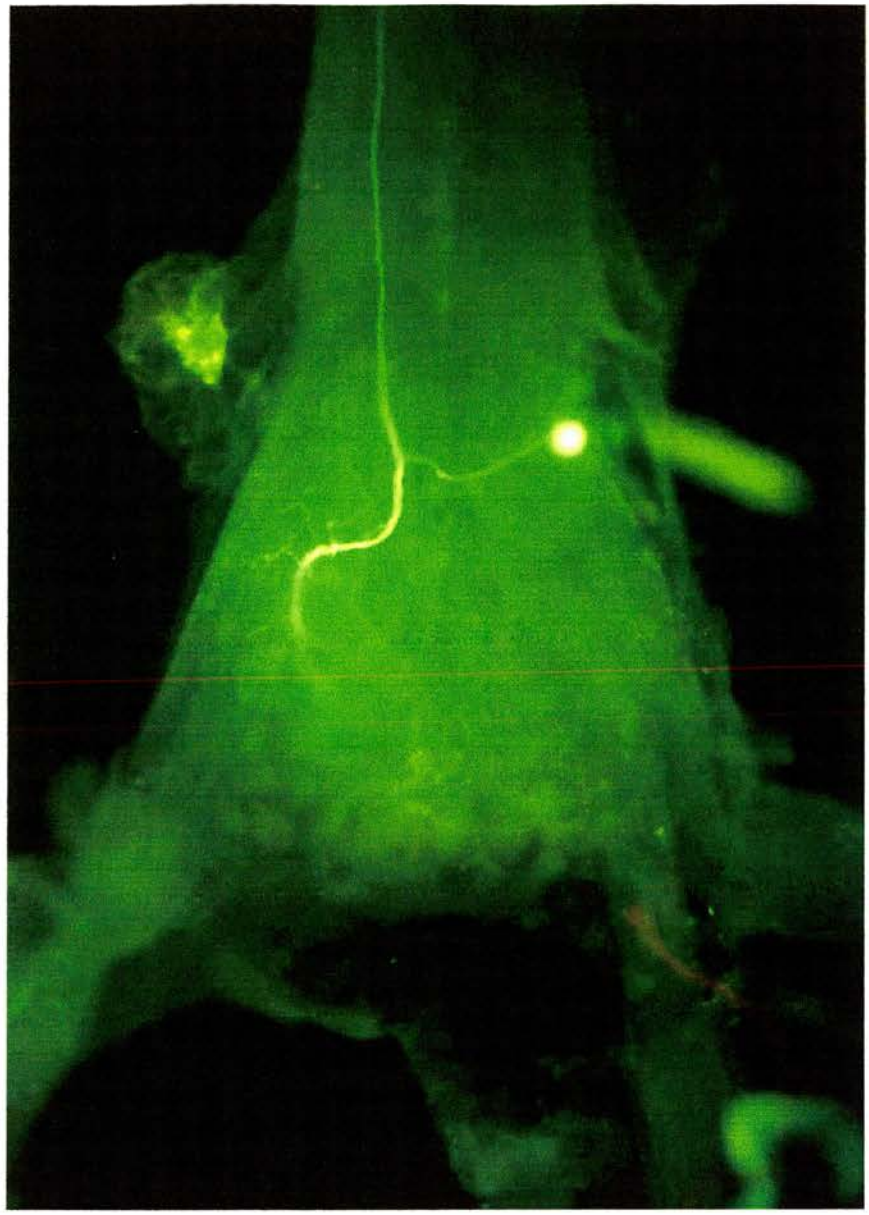

100µM

Figure III.ii

Camera Lucida Drawing of the Caudal Photoreceptor

Camera lucida drawing of the left hand crayfish caudal photoreceptor within the terminal ganglion stained with Lucifer Yellow.

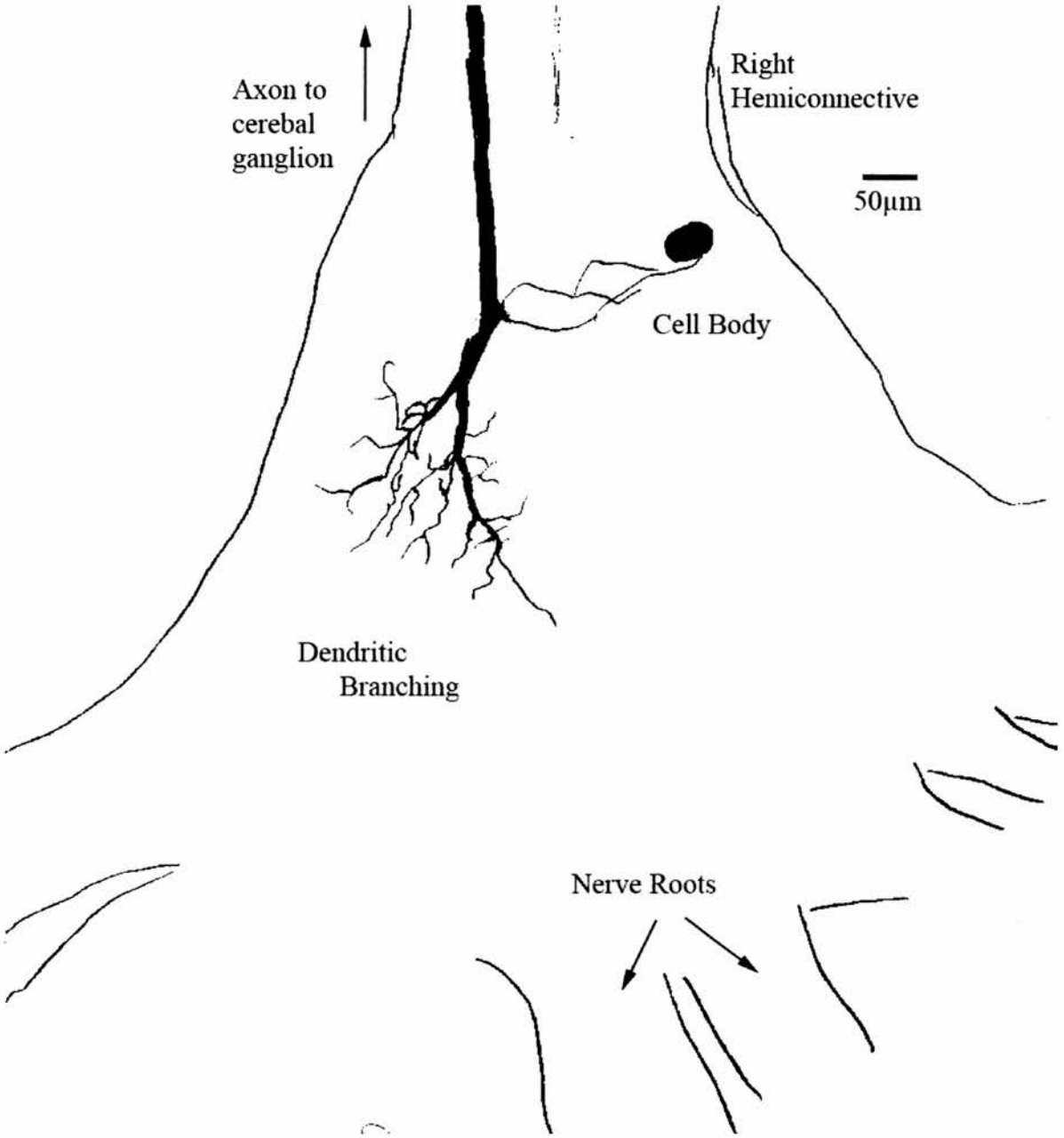
Axon to
cerebal
ganglion
Right
Hemiconnective
50µm
Cell Body
Dendritic
Branching
Nerve Roots

3.3.2 Physiology

The resting potential of the CPR in the dark is -77.9 (s.d.=11.2, n=14, single measurements taken from separate preparations). Frequently the membrane potential was initially more positive following impalement of the CPR with the micro-electrode, but stabilized after maintaining the tissue preparation in the dark for 10-15 minutes. This observation was interpreted as indicating that the cell recovering from damage incurred during impalement.

3.3.2.1 The light response of the caudal photoreceptor

Figure III.iii shows a typical intracellular recording of the CPR in response to a four second pulse of light. When the cell was exposed to the light there was a mean delay of 658ms, (s.d.=210, n=14), followed by a peak depolarization (mean = 13.0mV, s.d. = 5.6mV, n = 14, measured from the dark potential to the base of the spikes). This peak decline, after a brief period, to a plateau potential (mean = 8.9mV, s.d. = 3.5mV, n = 14) which was sustained, until the light pulse ceased. When the preparation returned to the dark there was a slight depolarization (known as the "off-response"), followed by a slow return of the membrane potential to its baseline levels. The depolarization in the presence of light is referred to as the **generator potential.** Superimposed on the generator potential, action potentials (mean amplitude 19.5mV, s.d. = 8.3, n = 14) signalled to other neurons in the anterior of the VNC that light have been detected. The frequency of these action potentials appears to mimic the generator potential suggesting that the level of depolarization of the generator potential dictates the frequency with which action potentials fire. (This is discussed further in section 3.5).

3.4 Analysis of Caudal Photoreceptor Action Potential

3.4.1 Extracellular Caudal Photoreceptor Recording and Template Recognition

The inter-ganglionic connectives between the abdominal ganglia carry the axons of hundreds of neurons; some conveying information from one ganglion to the next, others travelling the full length of the animal's nervous system. Recording from such a connective can detect a mass of action potentials of different shapes and sizes. However, it is possible to make sense of this complexity if one accepts that a single neuron will produce the same shape and size of action potential relative to the recording electrodes. Therefore, given a constant position of the recording electrodes between recordings within a preparation, then the size and shape of the action potentials from that particular neuron should also remain constant.

Figure III.iii

Intracellular Recording of the Caudal Photoreceptor

The photic response of the crayfish caudal photoreceptor in response to a four second light stimulus recorded with an intracellular microelectrode.

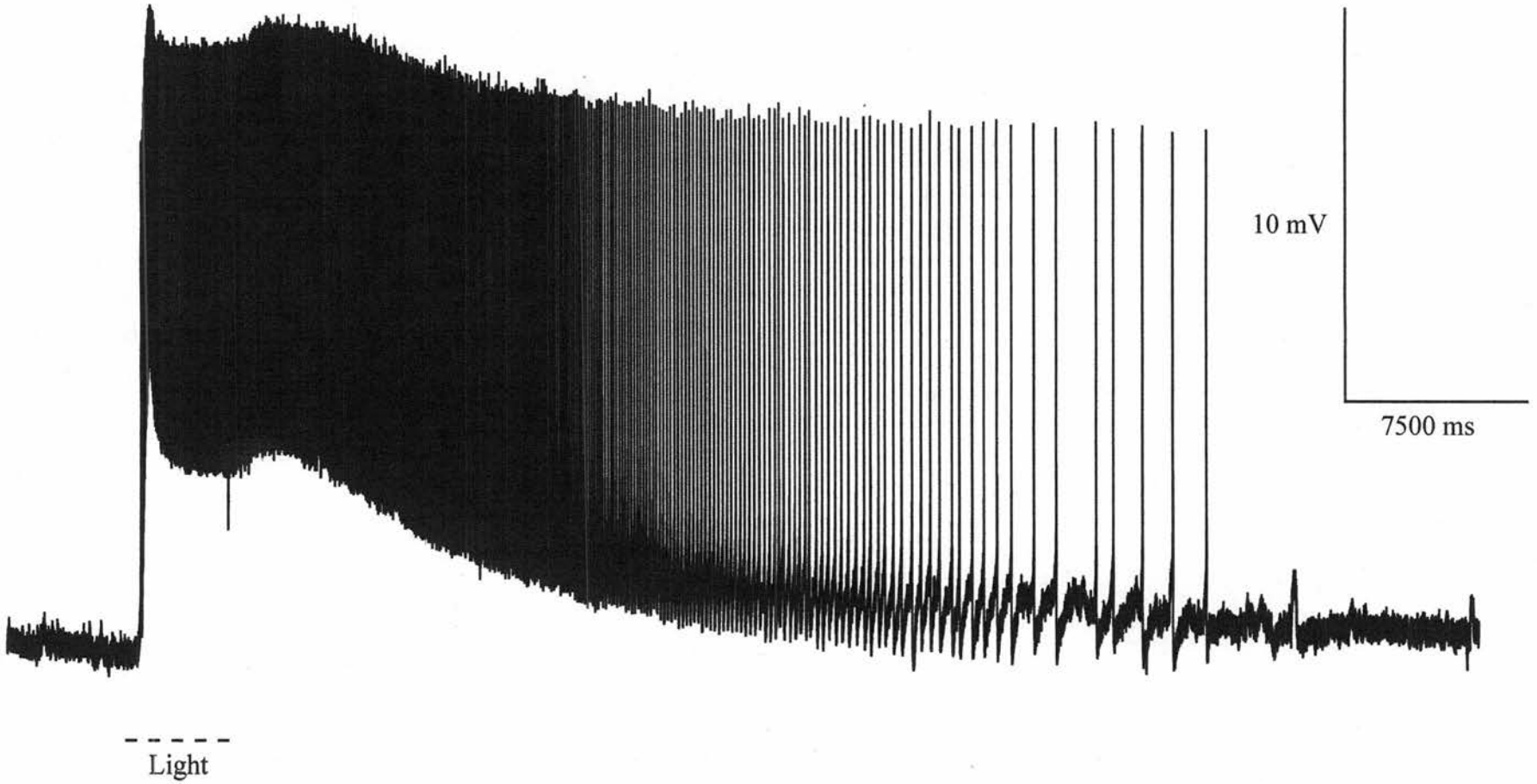
10 mV
7500 ms
Light

Template recognition analysis can be used to discern which action potentials come from a specific neuron.

However, to make use of this technique it is necessary to identify an initial action potential as a template. The CPR has a distinctive firing pattern in response to light, and it is usually possible to identify at least one impulse as designating from the CPR, with a high degree of probability. Figure III.iv (panel A) shows an example of an extracellular recording where the CPR response is extremely obvious. However often there is significantly more background activity which disguises the action potentials of the CPR, making selection of an initial template more difficult.

The extracellular recording shown in Figure III.iv is expanded, and a single action potential taken as a template is indicated in panel (B). Templates can be made from either a single action potential or from an average of several. Once a template has been defined, computer software compares the template with each successive section of the overall record. If the waveform of the raw data in the record matches the template within a well-defined accuracy criterion, that section of the raw data is marked as an "event" which indicates the occurrence of a recognized action potential at that time. From this series of events a frequency curve may be generated (panel C).

3.4.2 Intracellular Recording and Threshold Recognition

In order to confirm that the template recognition correctly detected all of the action potentials from the neuron, a one-to-one comparison may be made with action potentials from an intracellular recording taken from the dendritic region of the cell, using threshold recognition. This is a much simpler analytical tool that detects positive deflections from a horizontal cursor that can be arbitrarily set, see Figure III.v panel (A). Each deflection is an event and from these events a frequency curve can again be generated (panel (B)). This was compared with an extracellular recording taken simultaneously from the inter-ganglionic connective shown in panel (C) and the frequency curve plotted from data extracted from the extracellular recording by template recognition, panel (D).

3.4.3 Comparison of Spike Recognition Methods

The intracellular recording method reveals the exact pattern of CPR action potentials unambiguously, and visual inspection of events detected by the threshold method can confirm

Figure III.iv

Template Recognition Analysis of an Extracellular Recording of the Photic Response of the Caudal Photoreceptor

Panel (A): extracellular recording of the photic response.

Panel (B): a single action potential from the caudal photoreceptor used as the template to which others are matched.

Panel (C): the action potential frequency distribution curve derived from the template recognition analysis of the extracellular recording in panel (A).

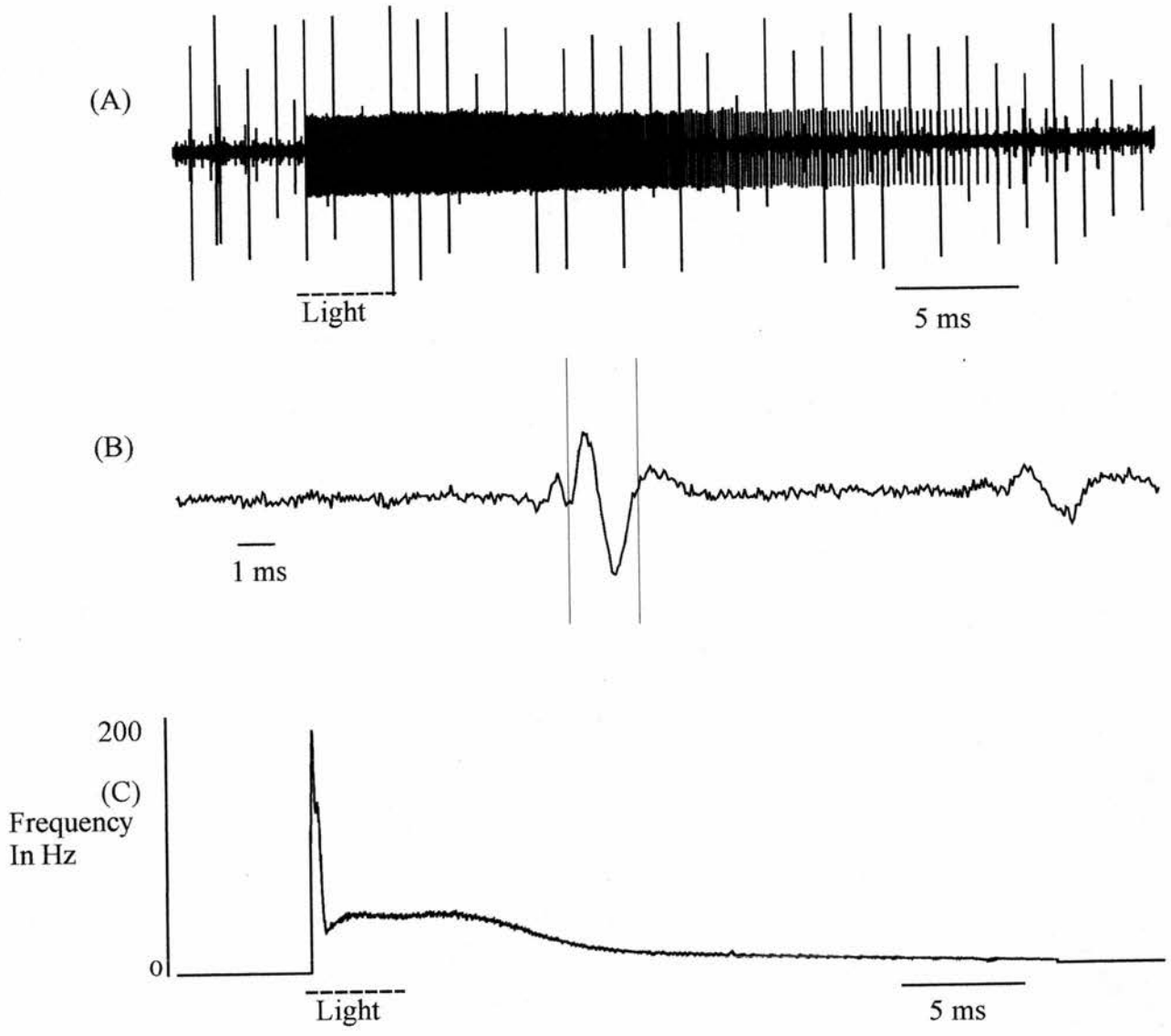
(A)
Light
5 ms
(B)
1 ms
200
(C)
Frequency
In Hz
0
Light
5 ms

Figure III.v

Comparison of Threshold Recognition and Template Recognition of Action Potentials

Panel (A): intracellular recording of the photic response showing the horizontal cursor used in threshold recognition.

Panel (B): action potential frequency distribution curve derived from threshold recognition analysis of the intracellular recording in panel (A).

Panel (C): extracellular recording of the photic response made simultaneously with the intracellular recording in panel (A).

Panel (D): action potential frequency distribution curve derived from template recognition analysis of the extracellular recording in panel (C).

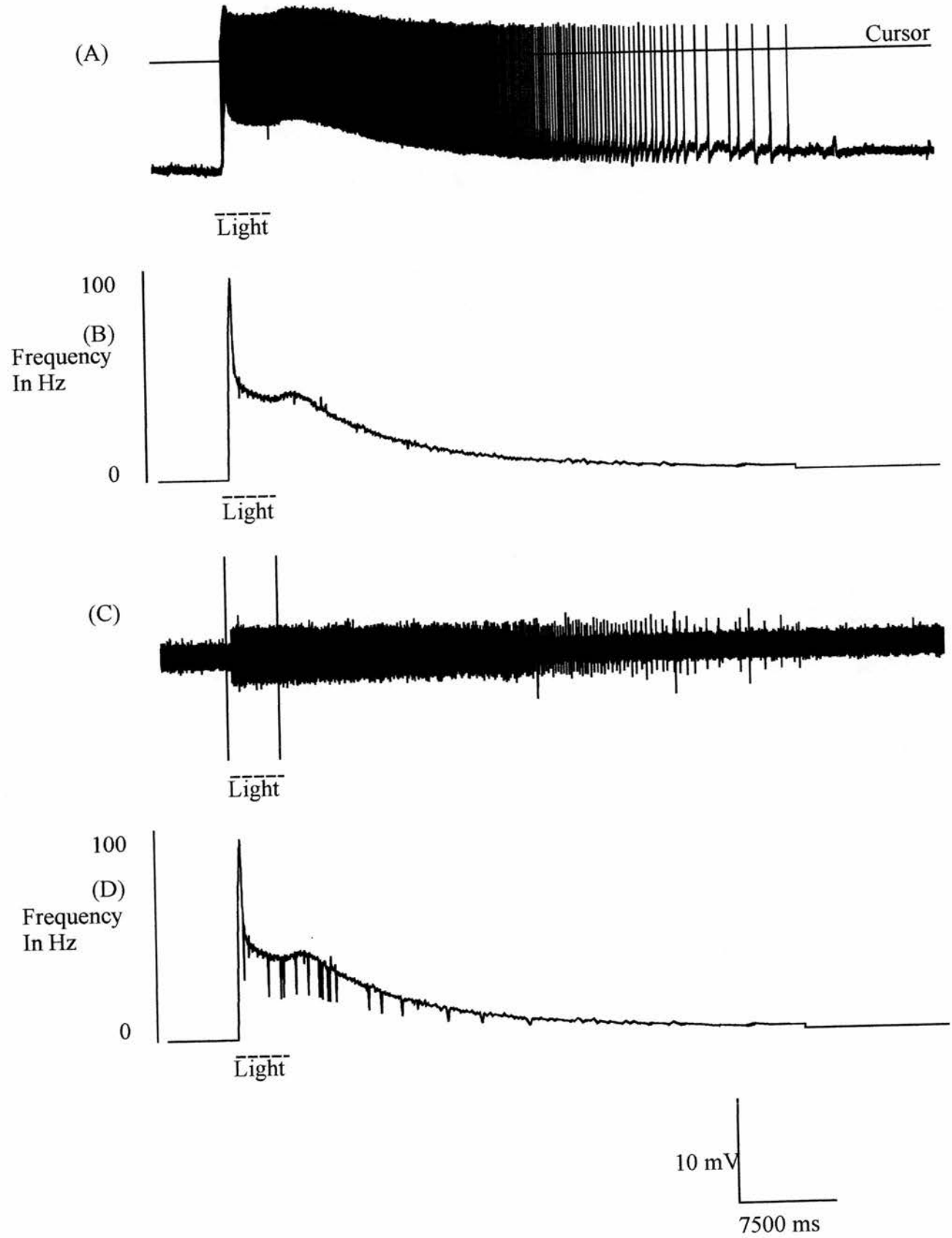
(A)
Cursor
Light
100
(B)
Frequency
In Hz
0
Light
(C)
Light
100
(D)
Frequency
In Hz
0
Light
10 mV
7500 ms

an exact match between event and action potentials. However, intracellular recording of the CPR is technically much more difficult than extracellular recording, and therefore much analysis relies on the latter technique. It is therefore necessary to explore the accuracy of the template technique against the "gold standard" of intracellular recording.

For the most part, frequency curves generated by the two analytical tools are broadly similar as shown in Figure III.v. However, there are a few disparities in the curve generated by extracellular template recognition where there are sudden changes in frequency (Figure III.v panel (D) indicated by arrows).

Frequency is determined by the time between one action potential and the next. When the time between two action potentials is short, as it is at the initial peak, *i.e.*, when the inter-spike time is in the order of 6 ms, then the frequency is high (140Hz), whereas, when the time is longer, *i.e.*, 19ms then the frequency is low as in the plateau phase of the response (58Hz).

In Figure III.v (panel B), where frequency curve has been generated from intracellular recording, the curve is almost smooth. This indicated that there are no sudden changes in CPR action potential frequency, and that therefore the irregularities in the frequency plot generated by template recognition are due to errors in recognition.

Figure III.vi shows the repertoire of errors that may occur using template recognition. Panel (A) depicts an action potential from a neuron other than the CPR that has been falsely identified by the template. This false positive will appear as a high frequency deviation on any frequency curve because the inter-spike time between events is shortened by being placed between two true CPR action potentials. False negatives, on the other hand, appear as a low frequency deviation on the frequency curve because of the expanded inter-action potential time due to non-recognition of an action potential from the CPR. Panel (B) shows an example of an action potential from another neuron superimposed with that from the CPR, thus disrupting the configuration of the action potential on the extracellular recording and making it unrecognizable when compared with the template. There may also be occasions when an action potential is not recognised although it is clearly similar to the other CPR action potential (panel C). In this case the recognition criterion has been set slightly too narrowly, and a genuine CPR action potential falls just outside the recognition window.

Figure III.vi

Errors in Template Recognition

Panel (A): False positive. An action potential from a non-CPR neuron (arrow) is mis-recognized as matching the template for the CPR action potential. This would represent itself as a high frequency outlier from the frequency curve of the photic response.

Panel (B): False negative. An action potential from the CPR has temporally collided with an action potential from another non-CPR neuron, thus distorting the shape of the extracellular recording making it unrecognizable to the template (arrow). This would represent itself as a low frequency outlier from the frequency curve of the photic response.

Panel (C): False negative. An action potential from the CPR (arrow) has failed to be recognized by the template, however from the frequency of the surrounding this action potential it is possible to predict that it is in fact from the CPR. This missed action potential would represent itself as a low frequency outlier from the frequency curve of the photic response.

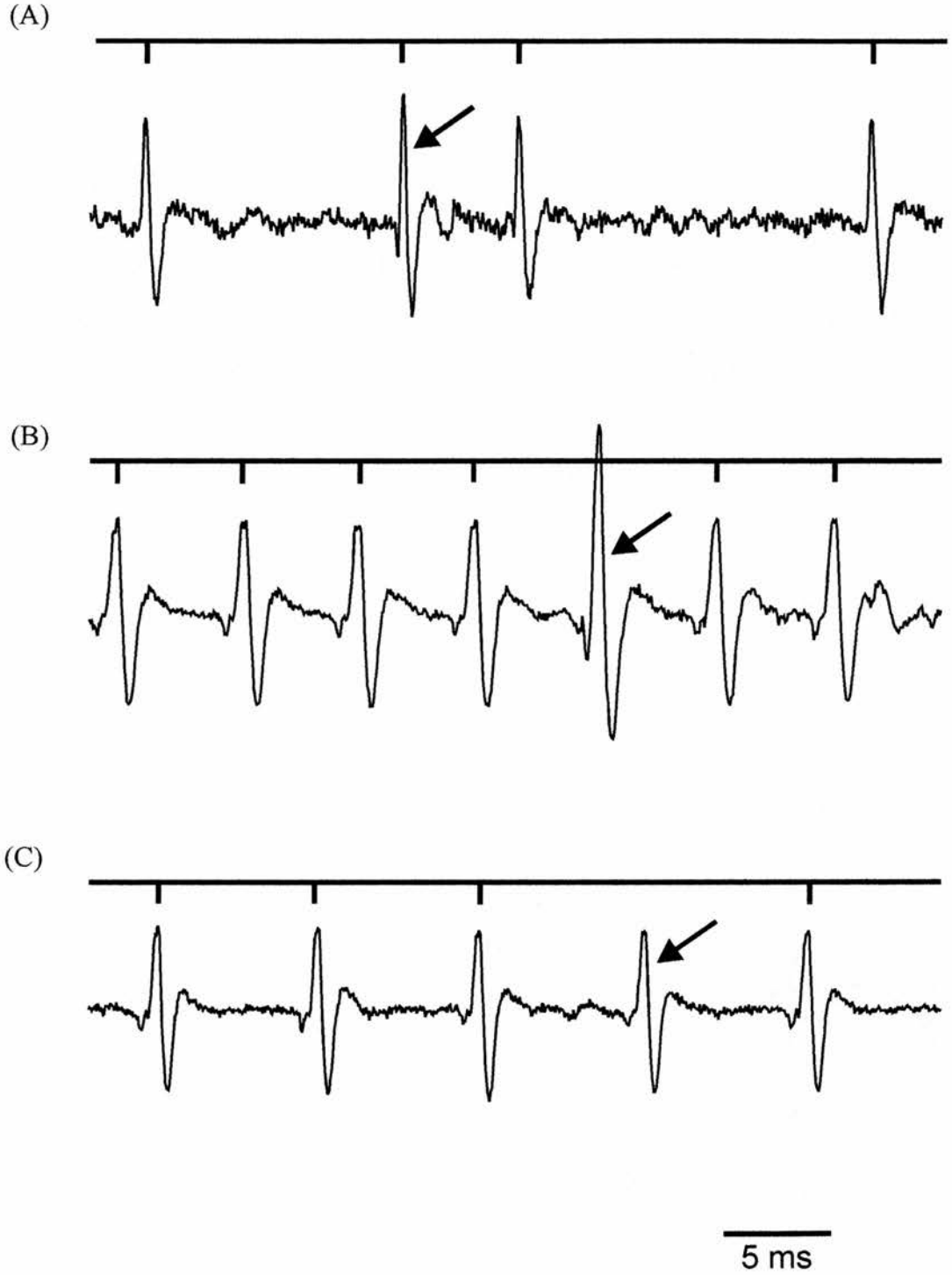
(A)
(B)
(C)
5 ms

3.4.4 Percentage Accuracy

Changing the percentage accuracy alters how close a match an action potential has to be before identified by the template recognition analysis. There is a fine balance between expanding the percentage accuracy sufficiently to identify all of the action potentials from the CPR and making it so large that the template recognizes too many action potentials from other neurons. Figure III.vii shows a graph of the number of action potentials that were identified as matching the template when the percentage of allowed error was varied. When the allowed error was very small very few action potentials were identified. Once the allowed error was set at 7 or 8% then the number considerably increased. It is know from intracellular recordings that there are in fact 655 action potentials in this photic response, and this value is reached when the allowed error is set to 18%. Any more than that and action potentials from other neurons are misidentified as matching the template.

3.5 The Relationship Between Generator Potential And Action Potential Frequency

Intracellular recording reveal the membrane potential of the CPR during the response to light, but it is difficult to discern the generator potentials directly because of the occurrence of action potentials once the potential depolarizes above threshold. These action potentials can be elucidated by applying TTX, which blocks voltage-dependent sodium channels.

Figure III.viii shows an example of an intracellular recording (panel A) from which a action potential frequency curve has been generated (panel B). The action potentials were eliminated by bathing the preparation in TTX, thus revealing the underlying membrane potential (panel C). The resulting plot may be compared directly with the frequency curve from the action potentials. The overall shape of the curves shown in panel B and in panel C appears to be the similar. Both have an initial peak, followed by a plateau. There is a slight rise when the light stimulus ceases, an "off-response"; followed by a slow decline with the membrane voltage returning to baseline levels. Deflections in both curves occur at the same temporal point. When the generator potential becomes depolarized there is an increase in spike frequency and when the generator potential hyperpolarises there is a decrease in the spike frequency. There is, however, a significant difference in that the peak is much larger in the frequency trace (panel B) than would be expected from the change in the generator potential (panel C). Another discrepancy between the two graphs is the size and shape of the off-response. The plateau approaching the off-response in the generator potential (panel C) depolarizes slightly, and the off-response is much bigger than in the action potential

Figure III.vii

Percentage Accuracy Graph

The number of action potentials identified as matching the template varies according to the percentage accuracy of the template recognition analysis.

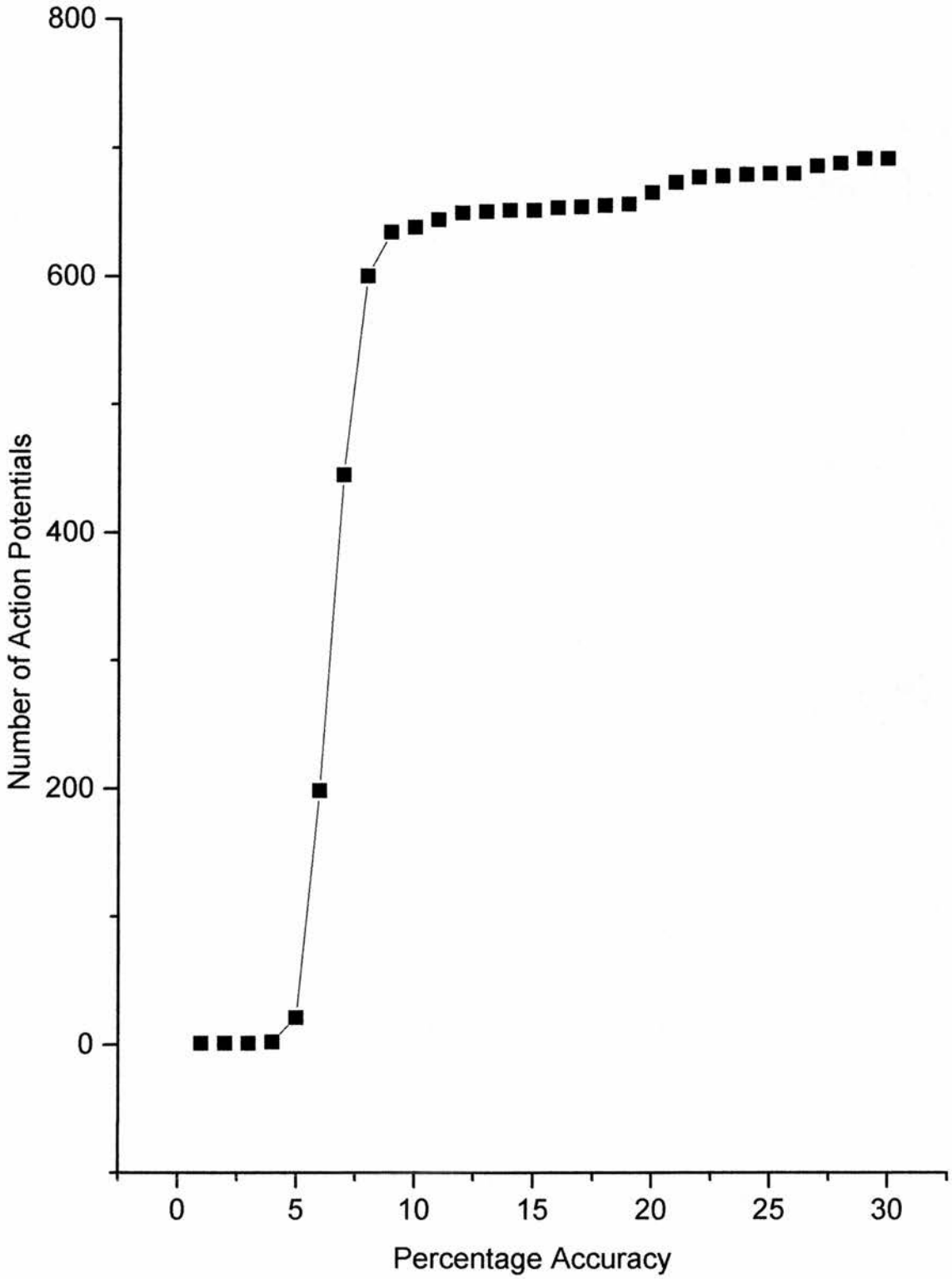
800
600
400
200
0
Number of Action Potentials
0
5
10
15
20
25
30
Percentage Accuracy

Figure III.viii

Relationship between Generator Potential and Spike Frequency

All of the data in this figure comes from a single preparation.

Panel (A): an intracellular recording of the photic response.

Panel (B): action potential frequency distribution curve from template recognition on the extracellular recording.

Panel (C): an intracellular recording of the photic response in the presence of TTX.

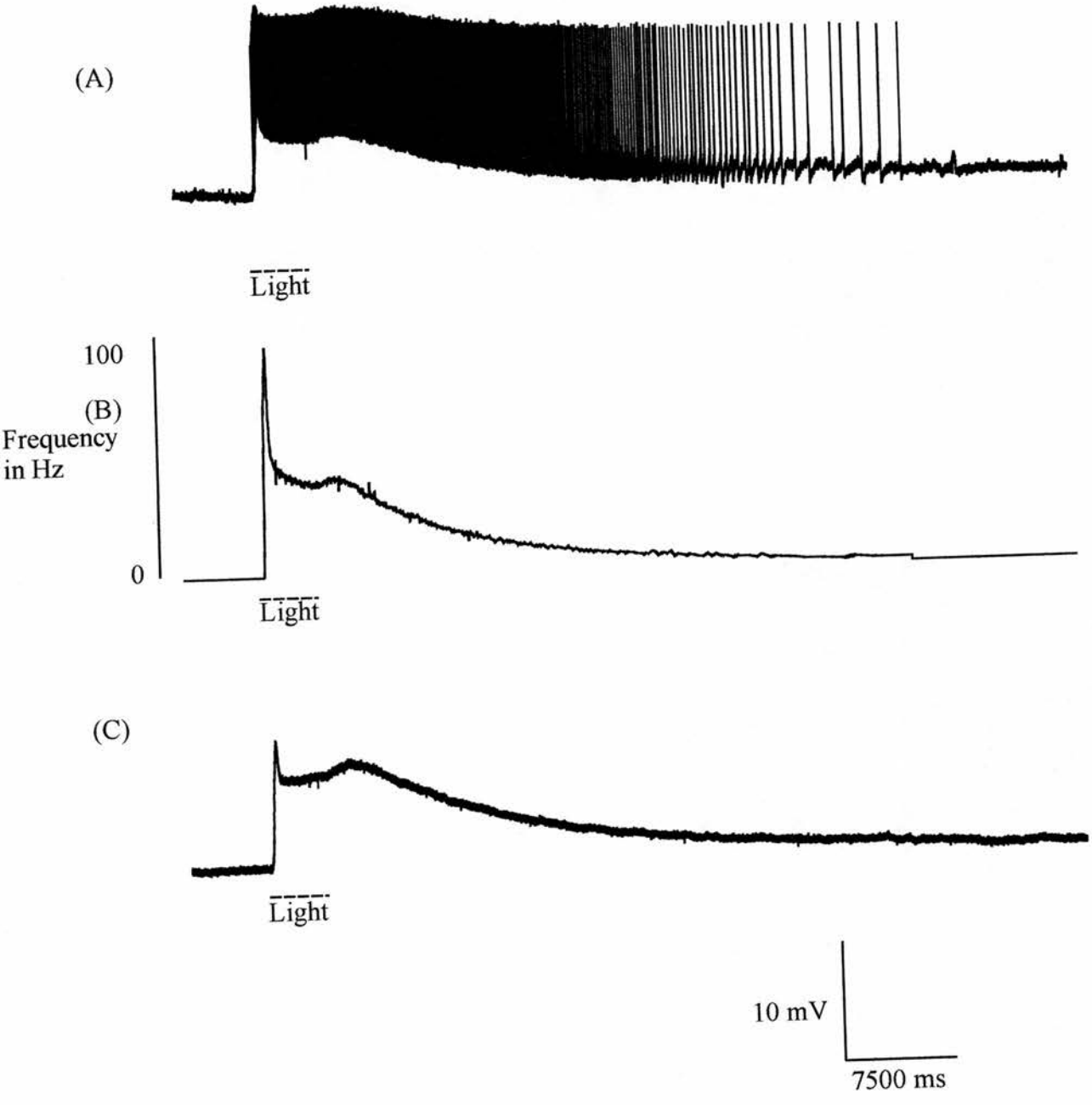
(A)
Light
100
(B)
Frequency
in Hz
0
Light
(C)
Light
10 mV
7500 ms

frequency graph, where the plateau has a slight decline, and a smaller off-response.

3.6 Artificial Current Injection And The Photic Response

The frequency curve of the photic response is characterized by a initial high-frequency response followed by a plateau phase. Similarly the generator potential is characterized by a transient large depolarization followed by a plateau. The question arises as to whether the initial frequency transient is entirely caused by the generator potential or whether standard cellular properties such as spike frequency adaptation also contribute to this transient. To investigate this increasingly large current pulses were injected into the CPR, and a comparison was made between these artificially-induced and the light induced action potential frequency. The action potential frequency of a standard photic response to a four second light stimulus is indicated in Figure III.ix. It shows the typical initial peak followed by a decline to a plateau. The increased current pulses injected in this series of experiments confirmed that an increase in current/membrane potential shift does increase the frequency of spikes induced. Pulses of 1.0 and 1.5 nanoamps were used and are indicated by red and blue in Figure III.ix. In all of the current injections (n=4), irrespective of the amount of current passed, there was an initial peak which only lasts for 3-4 action potentials. This was followed by an overall decline in the spike frequency over the duration of the current pulse. This suggests that spike frequency adaptation does play some role in sculpting the shape of the spike frequency photic response, but that the underlying generator potential plays the major role.

3.7 Repetitive Light Stimulation

In order to have a baseline with which to compare the results from other experiments it was necessary to monitor the response of the CPR to repetitive light stimulation. This was achieved by recording both extracellularly and intracellularly. A standard light regime, *i.e.*, starting the recording 5 seconds prior to the light stimulus as a baseline, followed by a light pulse for 4 seconds, and darkness for another 3 minutes until the next light stimulation, was used. This light regime was decided upon because the interval of 3 minute is sufficient for the cell to recover and, hence, to give a consistent light response on the next stimulation, but short enough to acquire a number of light responses within the realistic time frame of a pharmacological experiment.

3.7.1 Extracellular Recording of Repetitive Stimulation Over 3 Hours

Although this experiment was performed five times the results presented here are from a

Figure III.ix

Adaptation to Injected Current Pulses in Relation to the Frequency Distribution of the Photic Response

The black line is the frequency of action potentials elicited by a light stimulus of four seconds.

The red line is the frequency of action potentials elicited by a 1.0 nanoamp square pulse of current injected into the CPR.

The blue line is the frequency of action potentials elicited by a 1.5 nanoamp square pulse of current injected into the CPR.

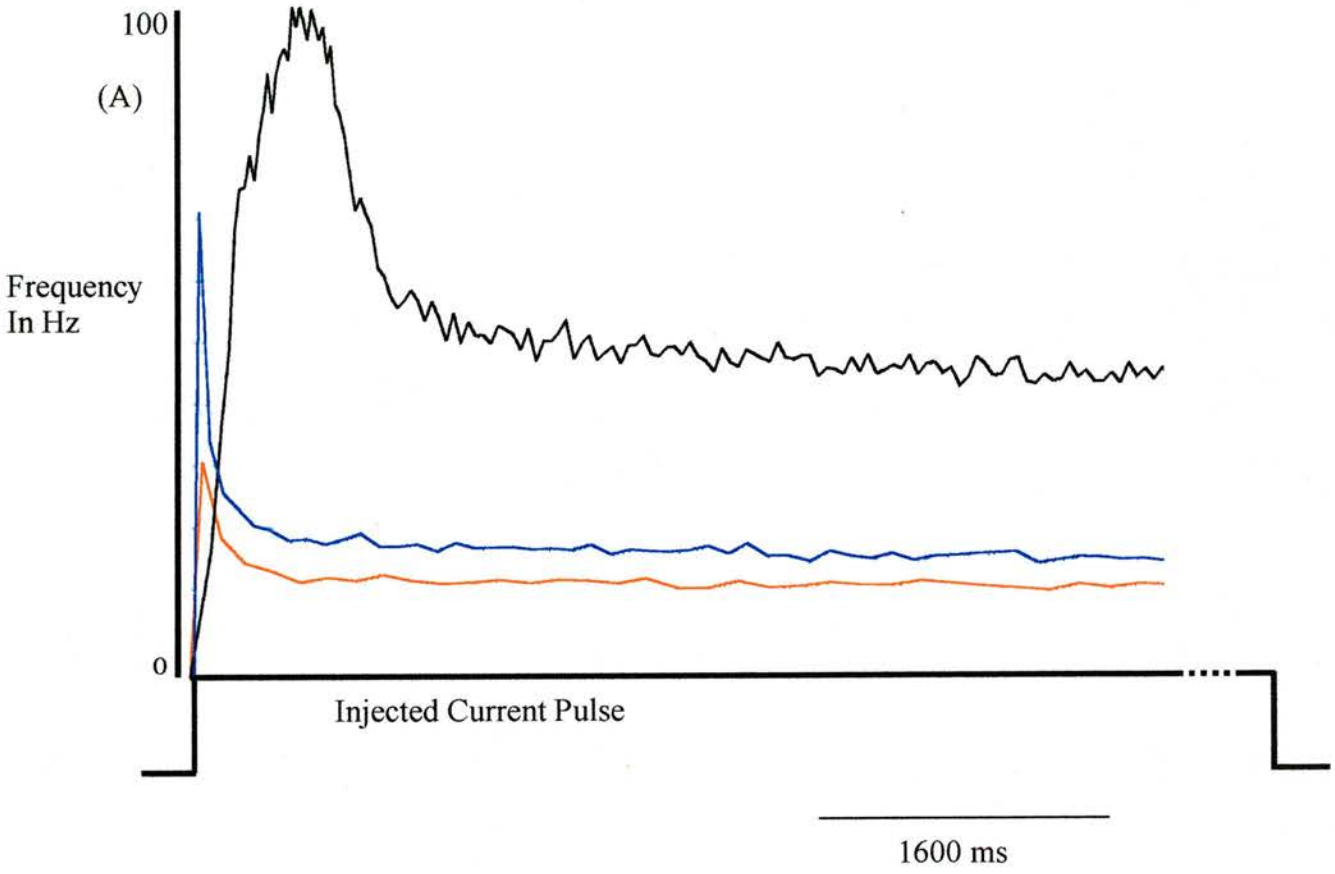
100
(A)
Frequency
In Hz
0
Injected Current Pulse
1600 ms

single experiment in order to facilitate comparison.

The number of action potentials elicited in each photic response remains fairly constant over three hours after an initial decline, while the duration of that response slowly declines over time (Figure III.x). The latency of the photic response is in the order of 500ms; however as can be seen in graph (A) of Figure III.xi there is initially a much longer latency between the light onset and the first spike of the light response when the cell has been maintained in darkness for a long period of time prior to experimentation. This increased latency time accounts for the outlying first data point on graph (A). After the first spike there is a steady, but slight, increase in latency over 3 hours of repetitive stimulation at 3 minute intervals. There is a similar delay in the time at which the initial peak in spike frequency occurs in the first data point, followed by a steady delay with time (B). Initially the frequency of the peak is much greater, and then there is a decline in the peak frequency which levels out at approximately 150Hz (C). The plateau frequency does not change much over the 3 hour duration of the experiment.

3.7.2 Intracellular Recording of Repetitive Stimulation Over 3 Hours

A complementary series experiments were performed in the presence of TTX to ensure that the extracellular measurements recorded accurately reflect the cellular events, and to identify whether there were any changes in the generator potential of the cell that cannot be observed by other means. This was repeated four times however the data shown here is from one single experiment.

The graphs in Figure III.xii show the variation in the generator potential of the photic response to repeated stimulation. The graph in panel (A) shows a pronounced but the gradual negative shift in the recorded value of the membrane potential which may be attributed to the non-biological phenomenon of drift caused by changes in the resistance of the electrode rather than the membrane potential of the CPR becoming more negative. The size of the peak (panel B) and the height of the plateau (panel C) vary very little over time, whereas there is slightly more variation in the area under the curve of the generator potential which appears to increase over time. The generator potential has a time-varying voltage waveform and it is unclear at what point a single voltage measurement could best characterize the photic response. Therefore, the time integral (*i.e.* area under the curve) of the membrane potential was

Figure III.x

Repetitive Light Stimulation of the Caudal Photoreceptor - Measurements Taken From Extracellular Recordings

Panel (A): graph of the number of action potentials per photic response when the preparation was subjected to a four second light stimulus every three minutes.

Panel (B): graph to show the duration of the photic response from the first spike to the last spike when the preparation was subjected to a four second light stimulus every three minutes.

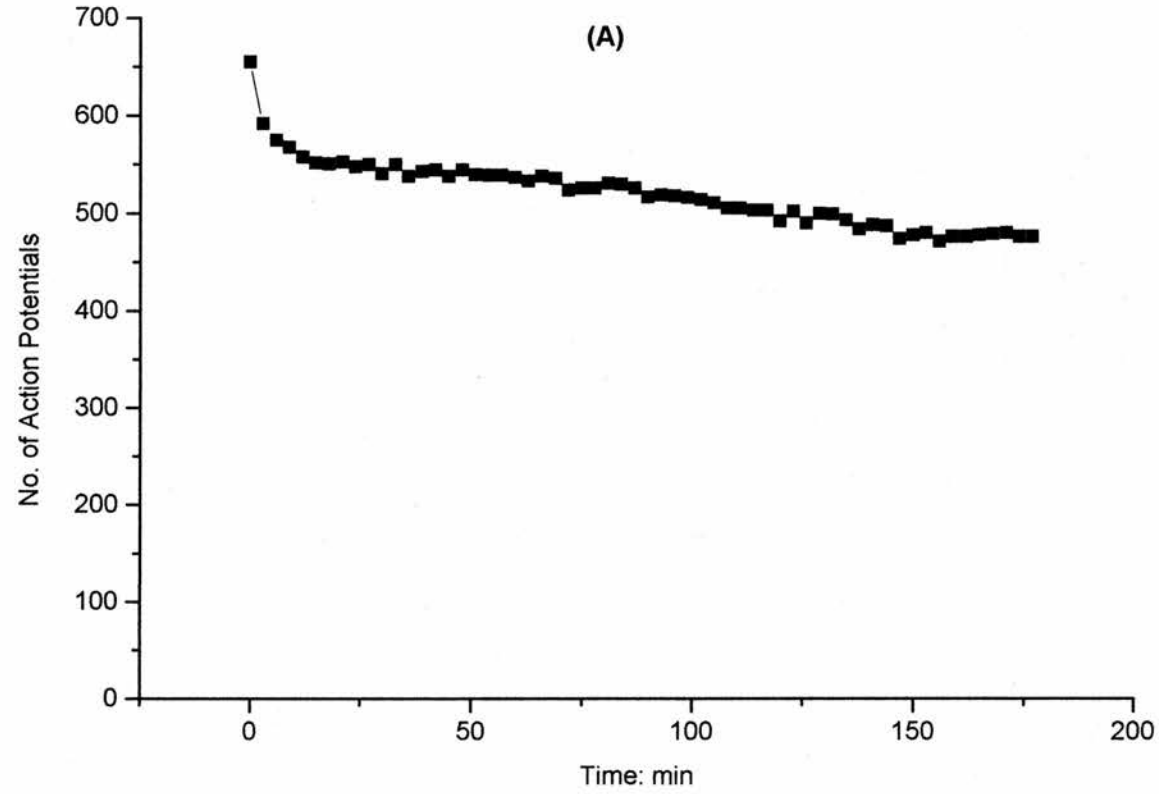
(A)
No. of Action Potentials
700
600
500
400
300
200
100
0
0
50
100
150
200
Time: min

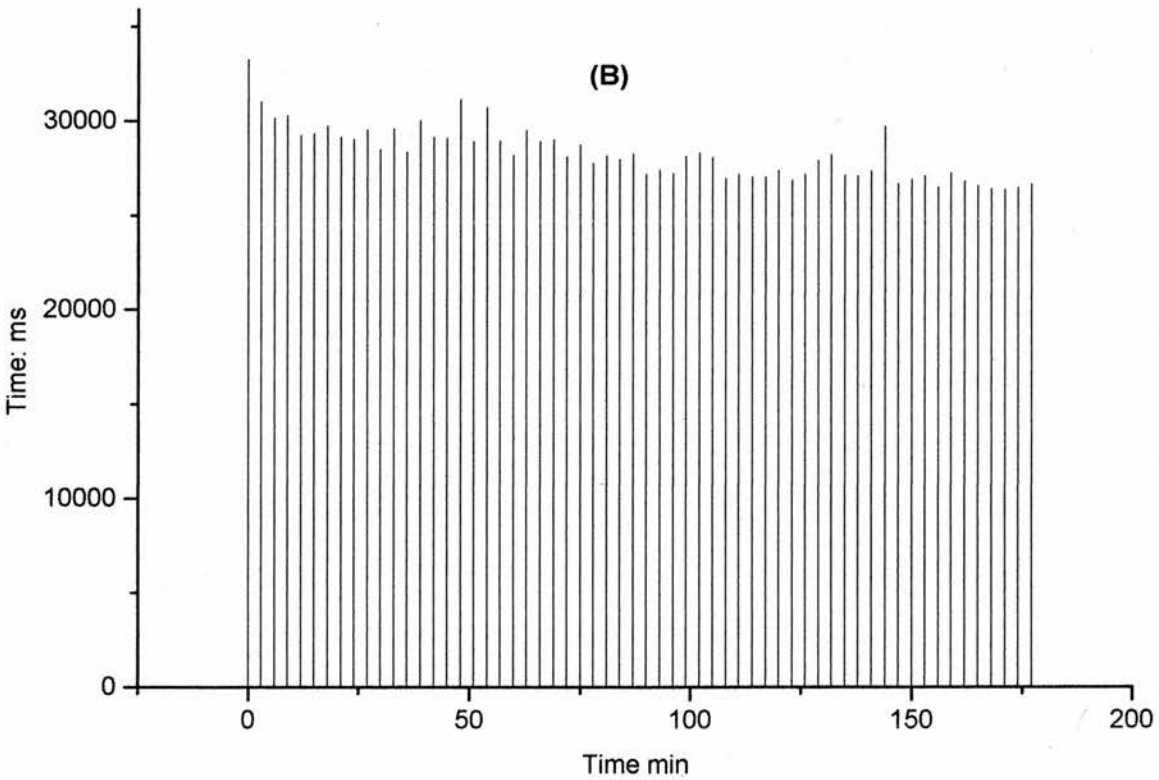
(B)
Time: ms
30000
20000
10000
0
0
50
100
150
200
Time min

Figure III.xi

Repetitive Light Stimulation of the Caudal Photoreceptor - Measurements Taken From Extracellular Recordings

Panel (A): graph to show the time of the first action potential of the photic response when the preparation was subjected to a four second light stimulus every three minutes.

Panel (B): graph to show the time of the initial peak frequency of the photic response when the preparation was subjected to a four second light stimulus every three minutes.

Panel (C): graph to show the frequency of action potential at the initial peak of the photic response when the preparation was subjected to a four second light stimulus every three minutes.

Panel (D): graph to show the frequency of action potential during the plateau phase of the photic response when the preparation was subjected to a four second light stimulus every three minutes.

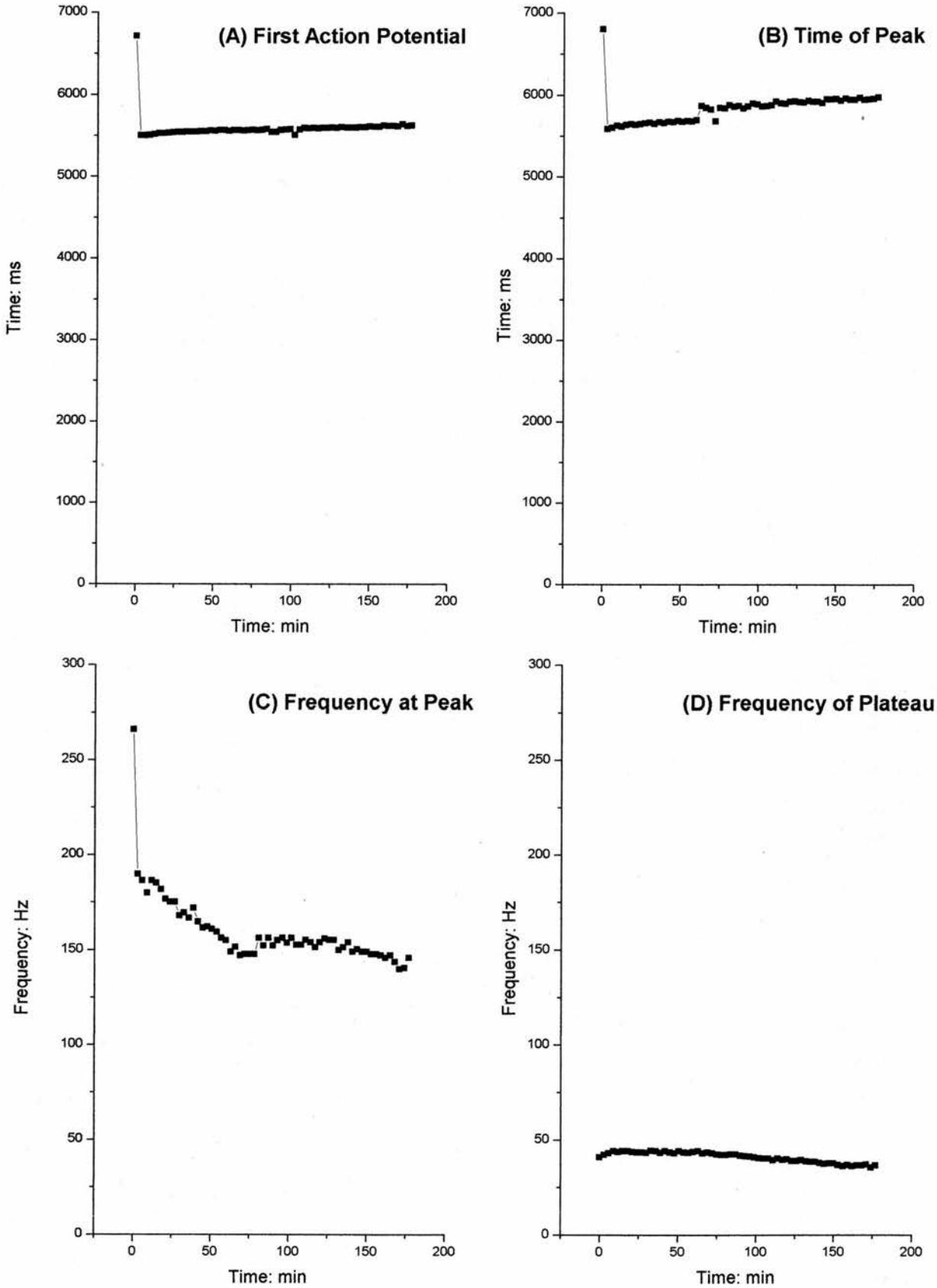
(A) First Action Potential
Time: ms
Time: min
(B) Time of Peak
Time: ms
Time: min
(C) Frequency at Peak
Frequency: Hz
Time: min
(D) Frequency of Plateau
Frequency: Hz
Time: min

Figure III.xii

Repetitive Light Stimulation of the Caudal Photoreceptor - Measuremcnts Taken From Intracellular Recordings From a Single Preparation

Panel (A): graph to show variation in the resting potential of the caudal photoreceptor when the preparation was subjected to a four second light stimulus every three minutes.

Panel (B): graph to show variation in the size of the peak of the photic response when the preparation was subjected to a four second light stimulus every three minutes.

Panel (C): graph to show variation in the size of the plateau of the photic response when the preparation was subjected to a four second light stimulus every three minutes.

Panel (D): graph to show variation in the area of the generator potential of the photic response when the preparation was subjected to a four second light stimulus every three minutes.

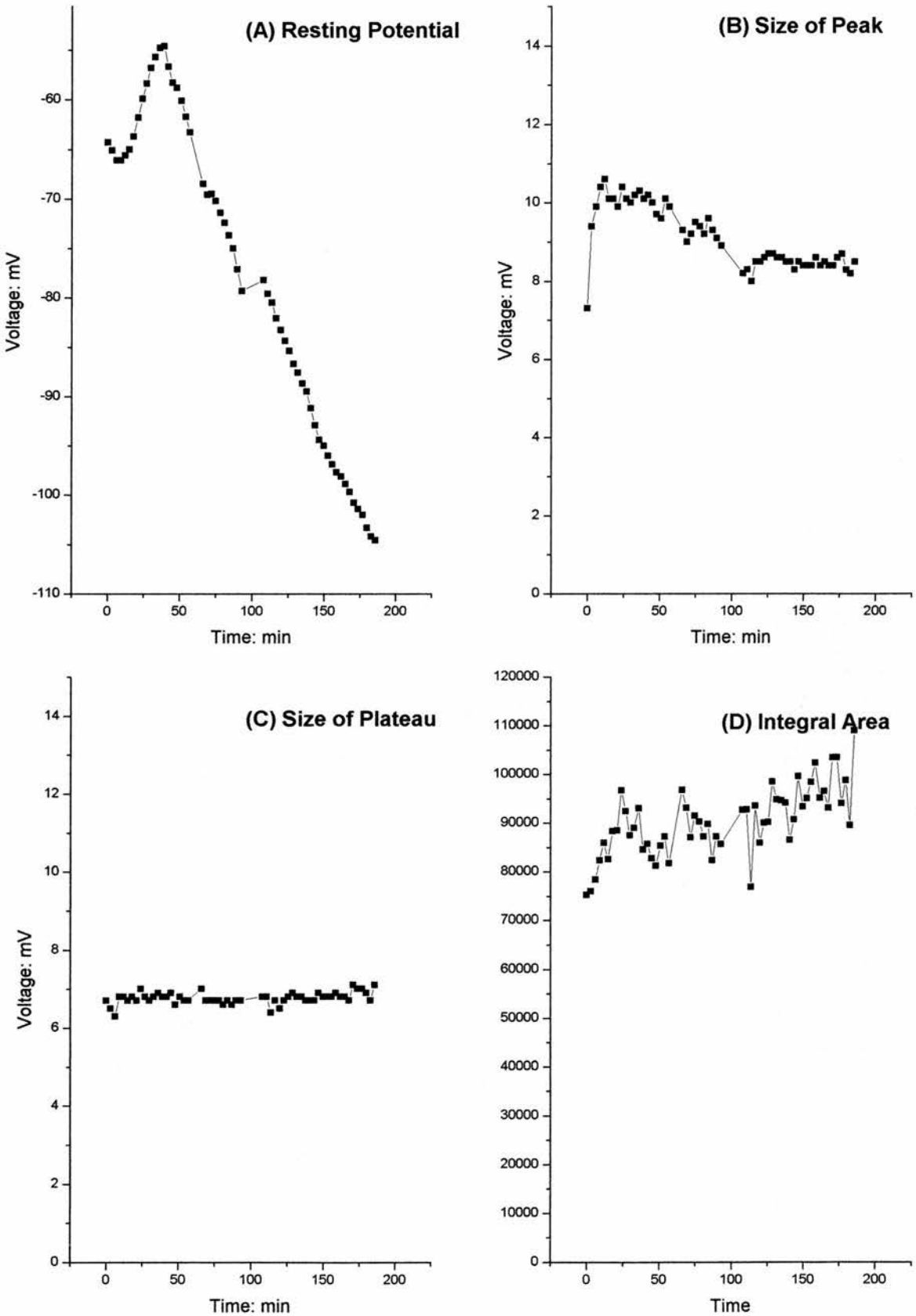
(A) Resting Potential
Voltage: mV
-60
-70
-80
-90
-100
-110
0
50
100
150
200
Time: min
(B) Size of Peak
Voltage: mV
14
12
10
8
6
4
2
0
0
50
100
150
200
Time: min
(C) Size of Plateau
Voltage: mV
14
12
10
8
6
4
2
0
0
50
100
150
200
Time: min
(D) Integral Area
120000
110000
100000
90000
80000
70000
60000
50000
40000
30000
20000
10000
0
0
50
100
150
200
Time

calculated over the duration of the response as a single metric indicating its overall "strength" (panel D). This area parameter shows a slight increase over the duration of the experiment although there is some variation.

3.8 Discussion

The existence of caudal photoreceptors have been reported throughout the decapod crustaceans (Wilkens and Larimer, 1976) including various cavernicolous crayfish (Larimer, 1966). In all of these animals the CPR is thought to be homologous neurons sharing the same morphology and the same developmental lineage which evolved before they diverged. Lucifer yellow staining in this study confirms that the morphology and position within the ganglion of the CPR in *Pacifasticus leniusculus* is the same as in other species of crayfish (Wilkens and Larimer, 1972). Physiological recordings made here also reveal that, on the whole, *Pacifasticus leniusculus* shows the same photic response an initial transient peak depolarization and intense action potential firing on exposure to bright light stimuli, followed by a decrease in depolarization and action potential firing rate to a plateau level for the duration of the light stimulus. Once light has been removed the CPR returns to its original resting membrane potential. The major difference between the CPR in this and other species of crayfish is that, in *Pacifasticus leniusculus*, there is no spontaneous tonic firing when the CPR is in the dark.

This study uses TTX to show, for the first time, the generator potential that underlies the photic response. Comparison between this and frequency curves reveal a close match leading to the conclusion that it is the generator potential that determines the frequency of the action potentials that are elicited. Both show an initial transient peak soon after the onset of the light, followed by a decrease to a plateau in constant illumination. There is often a slight increase of an off-response when light is removed.

Injected current is known to elicit tonic firing of action potentials, the frequency of which is dependent on the amount of current and the magnitude of depolarization it causes. Unfortunately it was not possible to mimic the depolarization of the generator potential, however, these experiments show there to be an initial high frequency of action potentials that plateaus off which can be explained in terms of spike adaptation. Therefore, the frequency of action potentials elicited in the photic response may be thought of as a result of the magnitude

and shape of the depolarization of the generator potential combined with the CPR's natural properties.

Having established that there is a predictable nature to the shape of the frequency curve the CPR's photic response generates it was then possible to verify the accuracy of template recognition analysis against intracellular recordings. Extracellular recordings contain action potentials from a mass of different neurons and recognition of one neuron from among many requires a tight template that captures the waveform with little of the surrounding record. Using the average of several action potentials as a template can eliminate much of the noise while enhancing the main features that characterize that neuron, thus improving the accuracy of analysis. However, no matter how tight the template or how close the accuracy criterion is set, there are always errors. Action potentials may either be falsely identified as belonging to the CPR when they don't or they may not be recognized as emanating from the CPR when they do because they collide with those of other neurons. Being able to account for these errors makes this more of a viable analytical tool therefore allowing results to be extracted from extracellular recordings which are technically much easier to perform than penetrating the CPR.

This chapter has also set out the parameters for repetitive extracellular and intracellular recordings as a baseline to be used against experiments in following chapters.

CHAPTER 4: THE EFFECT OF SEROTONIN ON THE PHOTIC AND MECHANO-SENSORY PROPERTIES OF THE CRAYFISH CAUDAL PHOTORECEPTOR

4.1 Introduction

The biological amine serotonin occurs naturally in the nervous system of all animals and it has been implicated in a variety of behaviours from mood in humans to swimming behaviour in the leech (Table 4.1). There are two means by which serotonin may acts, firstly as a focal synaptic neurotransmitter neuromodulator, and secondly as a neuro-hormone that acts further afield because it is released into the blood or haemolymph system. In the invertebrate nervous system serotonin has a wide range of effects on overt behaviours: "changes in" aggression and posture in the lobster, *Homarus americanus,* (Livingstone *et. al.*, 1980; Harris-Warrick and Kravitz, 1984; Kravitz, 2000); reduction of photo-negative behaviour in the crab *Carcinus maenas* (McPhee and Wilkens, 1989); modulation of swimming behaviour in several species of mollusc: medicinal leech, *Hirudo medicinalis,* (Willard, 1981), *Aplysia brasiliana* (Laurienti and Blankenship, 1997; McPherson and Blankenship, 1991), and *Clione limacine* (Satterlie, 1995); feeding behaviour in the medicinal leech *Hirudo medicinalis* (Lent and Dickinson, 1988); modulation of buccal musculature in molluscs (Weiss *et. al.*, 1978; Yoshida and Kobayashi, 1995).

In a decapod crustacean such as the lobster and the crayfish a major function of serotonin is thought to lie in modulation of aggression. It has well documented that crayfish fight each other in order to establish a dominance hierarchy and that this hierarchy will affect an animals ability to retain the best burrows and the best feeding and mating opportunities. These fights involve a lot of display and posturing, resulting in one animal being acknowledged as dominant and the other as submissive illustrated by the appropriate posturing. The dominant animal will take a dominant stance, flexed body posture and extended open claws. And the subordinate animal will take on a submissive stance, with its abdomen lying close to the substrate in an extended posture and with the animal walking backwards away from a more dominant animal.

In 1980, Livingstone *et al.* injected serotonin and octopamine into the haemolymph of freely moving lobsters and found that the same "aggressive-looking" and "submissive-looking" postures could be evoked, respectively, thus firmly implicating serotonin in aggression in lobsters. It was noticed that subordinate animals injected with serotonin would also confront

Table 4.1: Behavioural Importance of Serotonin in Arthropods

Animal	Behavioural importance of serotonin	Reference
Crab, *Carcinus maenas*	Stimulation of ventilatory and heart rates	Wilkens *et. al.* (1985)
Crab *Carcinus maenas*	Modifies posture – at micromolar doses: leg flexion, limb rigidity, reflected in slow walking and righting relexes; high doses: extreme flexion, rigidity and general unresponsiveness; and phototaxis – reduces photo-negative behaviour	McPhee and Wilkens (1989)
Crayfish	Depresses LG-EPSPs	Glanzman and Krasne (1983; 1986)
Crayfish	Enhancement of transmitter release at neuromuscular junction	Delaney *et. al.* (1991)
Crayfish, *Pacifasticus leniusculus*	Walking behaviour	Gill and Skorupski, (1996)
Lobster, *Homarus americanus*	Aggression/postural	Livingstone *et. al.* (1980); Harris-Warrick and Kravitz (1984); Kravitz (2000)
Lobster, *Homarus americanus*	Reduces the amplitude of command fibre evoked EPSPs recorded from both flexor inhibitor and extensor excitor motorneurons	Harris-Warrick (1985)
Lobster, *Homarus americanus*	Modulation of receptor muscles of the abdominal stretch receptor	Pasztor and Golas (1993)
Medicinal leech, *Hirudo medicinalis*	Induces prolonged spontaneous swimming and stimulates bursts of nerve impulses in motoneurons in the isolate nerve cord, implying an cxcitatory rolc	Willard (1981)
Medicinal leech, *Hirudo medicinalis*	Stimulates several aspects of feeding behaviour	Lent and Dickinson (1988)
Mollusc	Modulation of the buccal musculature	Weiss, *et. al.* (1978); Yoshida and Kobayashi (1995)
Mollusc, *Aplysia brasiliana*	Swimming behaviour	Laurienti and Blankenship (1997); McPherson and Blankenship (1991); Yu *et al.* (2001)
Pteropod mollusc, *Clione limacine*	Swimming behaviour	Satterlie (1995)
Snail, *Helisoma*	Modulation of buccal neurons	Zoran, *et al.* (1989)
Snail, *Helix aspersa*	Modulation of buccal neurons	Hill-Venning and Cottrell (1992)

opponents much bigger than themselves and from whom they would usually shy away. Subsequently, in 2001, Tierney and Mangimele furthered this study by investigating the effect of different concentrations of serotonin and serotonin analogues. Huber *et al.* (1997) said that the serotonin reduced the animals' willingness to retreat and therefore claimed that the serotonin must be enhancing the aggressive motivation. Following on from investigations into the behavioural effects of serotonin, studies were undertaken to determine what effect serotonin is having on a cellular and synaptic level, using electrophysiological recordings from excised nervous systems. Yeh *et al.* (1997) showed that high or low concentrations of serotonin had different effects on synaptic strength of sensory inputs from the tail fan onto the lateral giant fibre. They suggested that in this situation, for any naturally occurring serotonin to be having an effect on the synapses between the cells in the terminal ganglion and the LG, it must be reaching the synapse by being released into the circulatory system, possibly from the serotenergic cells in the first abdominal ganglion identified by Beltz and Kravitz (1986; 1987). Serotonin has been implicated both "as a mediator of diurnal changes in the insect visual system" (Cuttle *et al.*, 1995) and entrainment of circadian rhythms (Prieto-Sagredo and Fanjul-Moles, 2001). The CPR is also located within the abdominal section of the ventral nerve cord and therefore is also likely to be exposed to serotonin in the same way. It has also been suggested that the CPR plays a part in circadian rhythms (Amir *et.al.*,1998; Oniszk and Barbacka-Surowiak, 2003). Therefore, this chapter sets out to investigate whether serotonin has a modulatory effect on the photoreceptive properties of the crayfish CPR or on its capacity to function as a mechano-sensory integrating interneuron.

4.2 Additional Materials and Methods

In this series of experiments animals were isolated for two weeks prior to experimentation in order to eliminate the effect(s) of fighting for social dominance on the endogenous serotonin levels, which may interfere with the examination of the effects of serotonin on the photic response of the CPR. The standard light regime, outlined in chapter 2, of a 4 second pulse every three minutes was employed. Four to five light responses were recorded prior to the application of serotonin. Another four to five light responses were then recorded in the presence of serotonin. This regime was maintained while the preparation was washed with fresh saline for 10-15 min, to remove traces of the pharmacological agent, and recovery light responses recorded.

The effects of serotonin on the synaptic inputs on to the CPR from the nerve roots were also examined. For extracellular recording, two bipolar hook electrodes were placed on the connective between the last thoracic ganglion and the first abdominal ganglion, and the 3rd and 4th ganglion. In those experiments involving nerve root stimulation of the terminal ganglion a suction electrode was used in addition to the hook electrodes. The suction electrode was placed on the nerve root to be stimulated prior to the penetration of the CPR with a micro-electrode for intracellular recording.

Techniques used for analysis include template and threshold recognition as were described in Chapter 3.

4.3 Results

4.3.1 The Effect of Serotonin [100μM] on the Photoreceptive Properties of the Caudal Photoreceptor

Figure Iv.i shows main effect of serotonin, that it evokes spontaneous firing in the CPR. In panel (A) of Figure IV.i there is a single spontaneous action potential in the dark prior to the onset of the light stimulus when there is no serotonin present, whereas the spontaneous firing level in panel (B) has increased to 17 Hz. Panel (C) shows a partial recovery when the preparation was washed with fresh saline for 15 minutes.

There is no consistent or significant trend as to whether serotonin causes an increase in the number of action potential evoked as part of a photic response. In six experiments there was an increase in the number of action potential produced by the CPR in the presence of serotonin, whereas in five experiments there was a decrease in the number of action potentials evoked, and in two there was no change.

The exact number of action potentials per photic response from one preparation has been plotted out in Figure IV.ii. In this example there is an initial increase in the number of action potentials in the presence of serotonin, followed by a slight decrease. This may be compared with the control graph in panel (B) which shows the number of action potentials per photic response following the same protocol minus the application of serotonin.

Figure IV.i

The Effect of Serotonin on the Light Response of the Caudal Photoreceptor Determined by Intracellular Recording

Measurements are made from light responses stimulated every 3 minutes. The arrows indicate when serotonin was applied and washed off with normal saline.

Panel (A) A normal intracellular recording of the photic response of the CPR.

Panel (B) the photic response of the CPR in the presence of serotonin [100μM].

Panel (C) the photic response of the CPR after serotonin has been washed off the preparation.

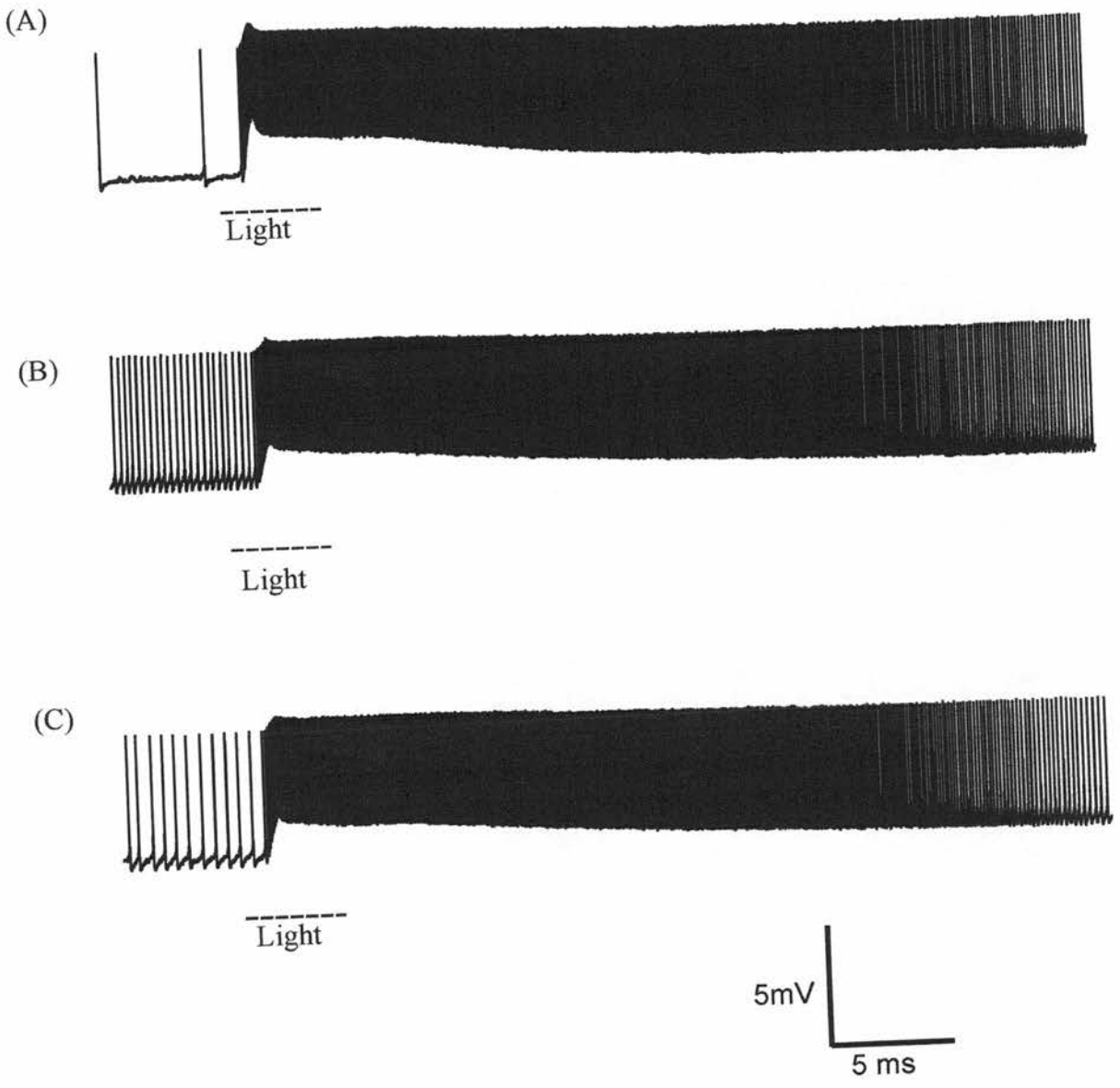
(A)
Light
(B)
Light
(C)
Light
5mV
5 ms

Figure IV.ii

The Number of Action Potentials Evoked per Photic Response

Panel (A) shows the number of action potentials evoked in each photic response over the course of the application of serotonin.

Panel (B) shows a control (repeated from chapter 3 to aid comparison) of repetitive stimulation every 3 minutes over the course of an hour.

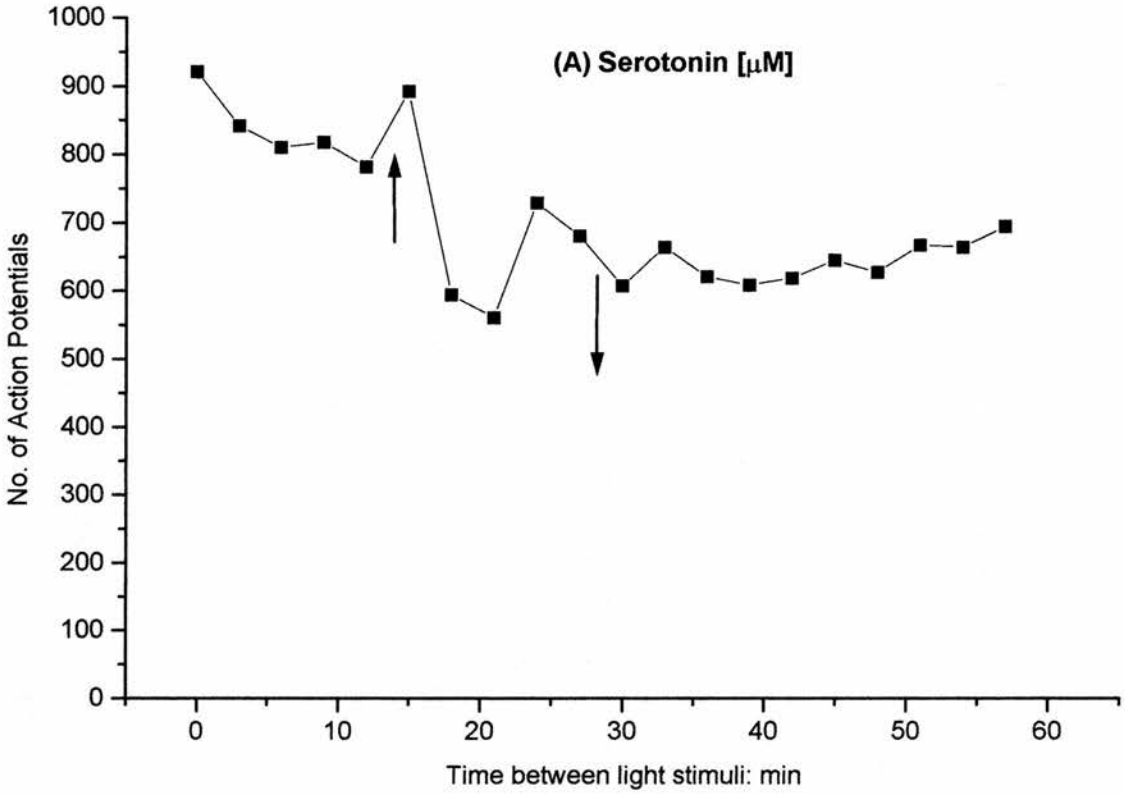
(A) Serotonin [μM]
No. of Action Potentials
1000
900
800
700
600
500
400
300
200
100
0
0
10
20
30
40
50
60
Time between light stimuli: min

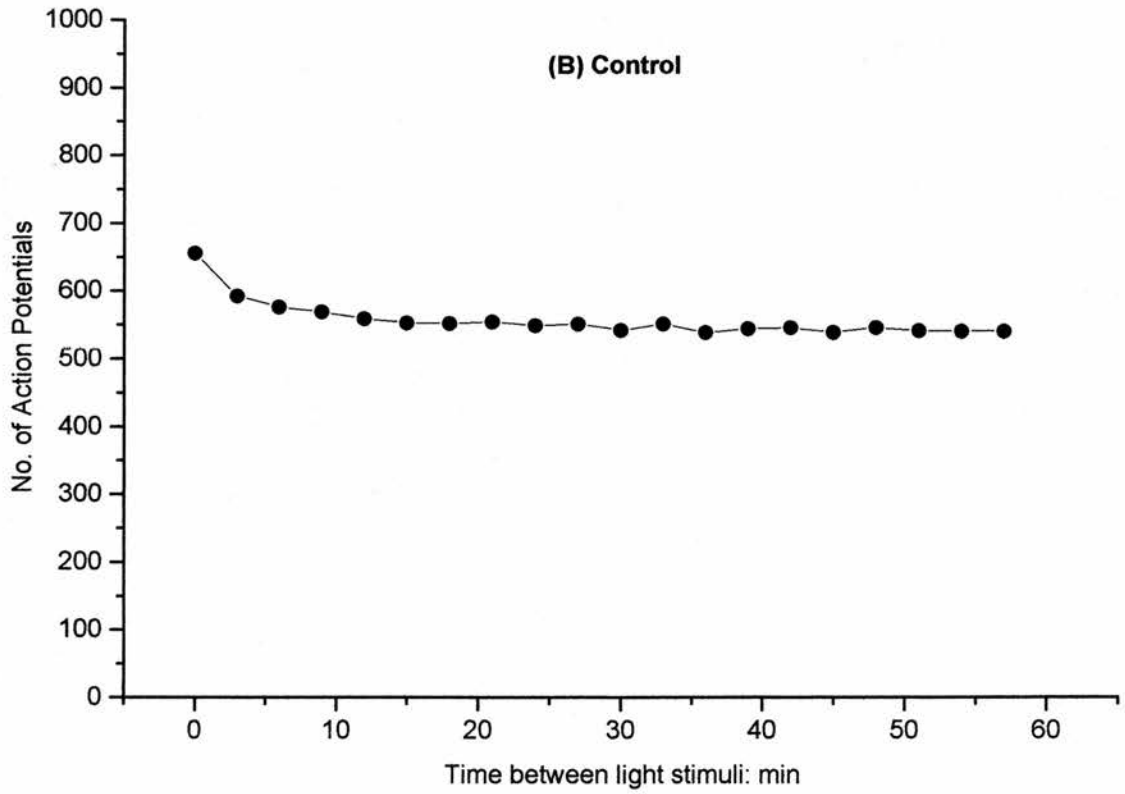
(B) Control
No. of Action Potentials
1000
900
800
700
600
500
400
300
200
100
0
0
10
20
30
40
50
60
Time between light stimuli: min

The number of action potentials may give an indication of whether or not serotonin is modulating the photic response but in order to investigate this in detail frequency distribution plots like that shown in Figure IV.iii must be constructed. It shows that there is an increase in the frequency of action potentials prior to the onset of the light stimulus which can be explained by the presence of spontaneous firing in the dark following the application of serotonin. There is also a decrease in both the initial peak frequency and the plateau phase of the photic response. However there is a slower decline in frequency once the light stimulus has been removed, accounted for by the persistent firing of the CPR at a low frequency for up to several minutes after the termination of light stimulus (data not shown).

The decrease in frequency during the photic respond correlates temporally with a decrease in the magnitude of the depolarization in the membrane potential seen in the graphs in Figure IV.iv which illustrate the effects serotonin is having on the resting membrane potential which shows a mean change of 6.78 mV (s.d=1.48) (n=5), and the size of the initial peak depolarization and the plateau phase that follows it, both of which appear to decrease in size in the presence of exogenous serotonin.

4.3.2 The Effect of Serotonin on the Generator Potential of the Light Response

The changes in the number of action potentials evoked and a change in the frequency distribution of these action potentials in the presence of serotonin suggests that this reagent may have an effect on the photic response of the CPR. Bathing the preparation in TTX in order to block voltage gated Na^+ channels allows the generator potential that underlies the photic response to become more visible by preventing the action potentials that usually appear upon it.

Figure IV.v shows no significant change in the size of the generator potential following the application of serotonin with a mean change in resting potential of 1.48 mV (s.d=4.37), exact measurements are plotted out in Figure IV.vi. This negative result was found repeatedly in five preparations.

Figure IV.iii

Frequency Plot of the Effect of Serotonin on the Action Potentials Produced by the Caudal Photoreceptor Determined by Intracellular Recording

Black Trace: frequency distribution of action potentials from one light response prior to the exposure to serotonin.

Red Trace: frequency distribution of action potentials from one light response following the application of serotonin 100μM.

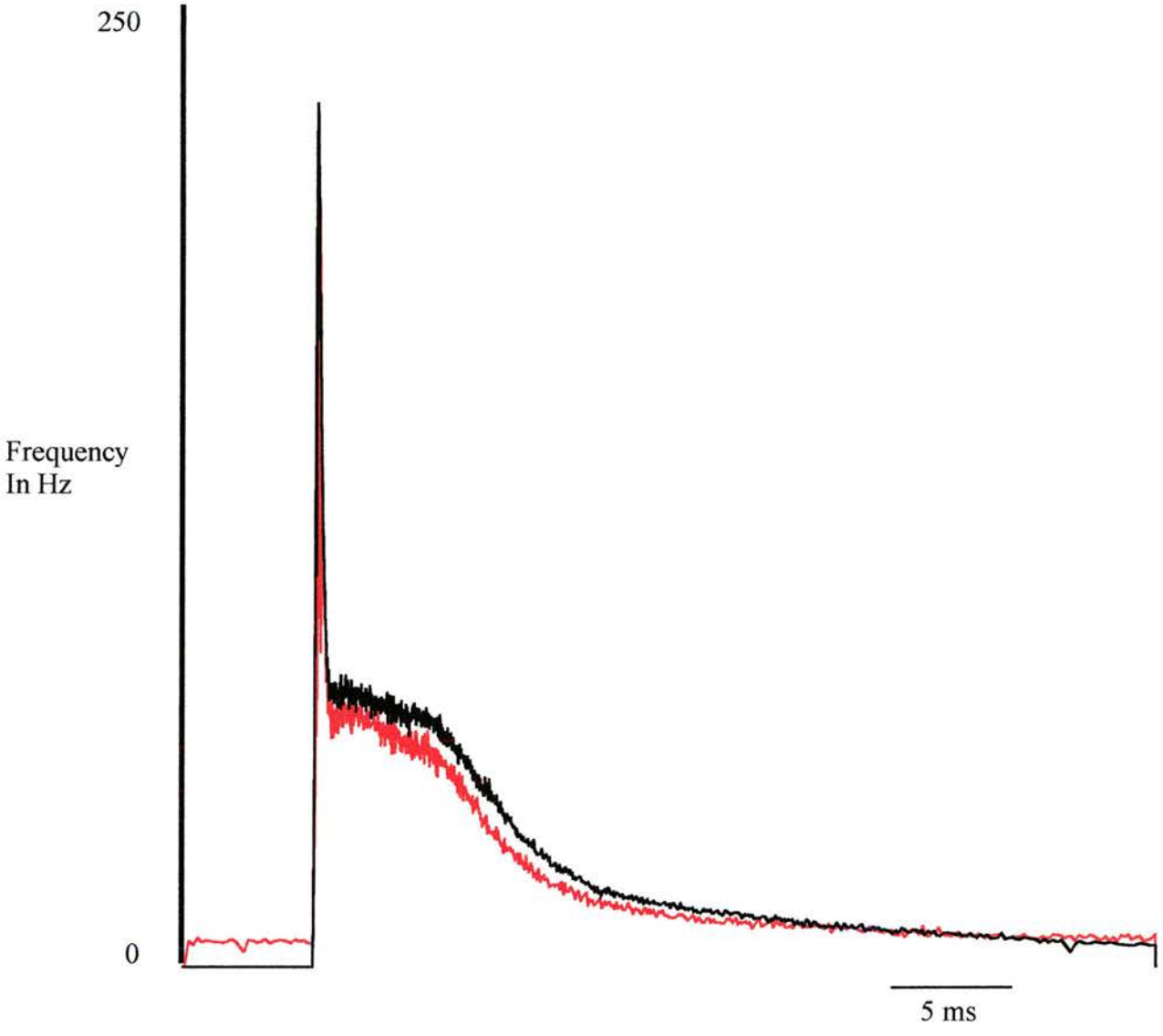
250
Frequency
In Hz
0
5 ms

Figure IV.iv

Changes in Features of the Light Response in the Presence of Serotonin [100μM] - Recorded Intracellularly

Measurements are made from the light responses stimulated every 3 minutes. The arrows indicate when serotonin was applied and washed off with normal saline.

Panel (A) shows the resting membrane potential prior to the light stimulation.

Panel (B) shows the size of the peak calculated as the difference between the membrane potential of the cell at rest and the maximum excursion at the transient peak.

Panel (C) shows the size of the plateau calculated as the difference between the membrane potential of the cell at rest and the maximum height of the plateau phase.

Panel (D) shows the variation in the area of the generator potential following the application of serotonin [100μM].

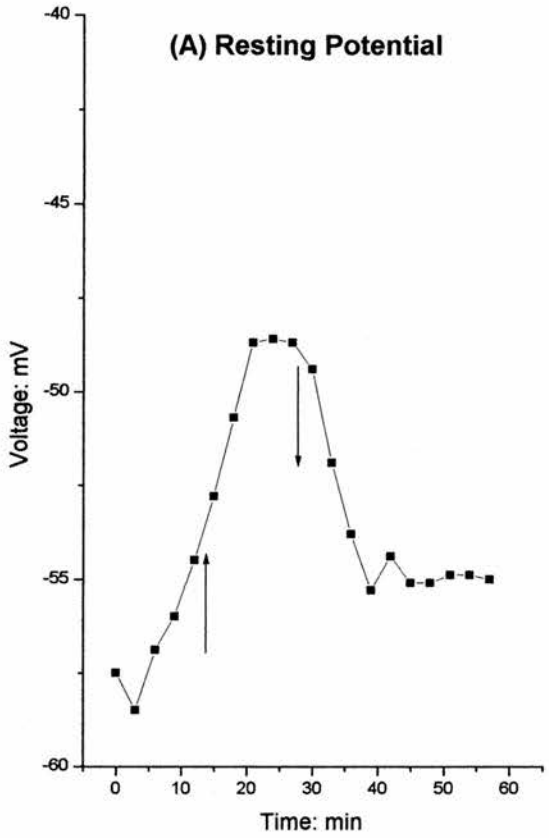
(A) Resting Potential
Voltage: mV
-40
-45
-50
-55
-60
0
10
20
30
40
50
60
Time: min

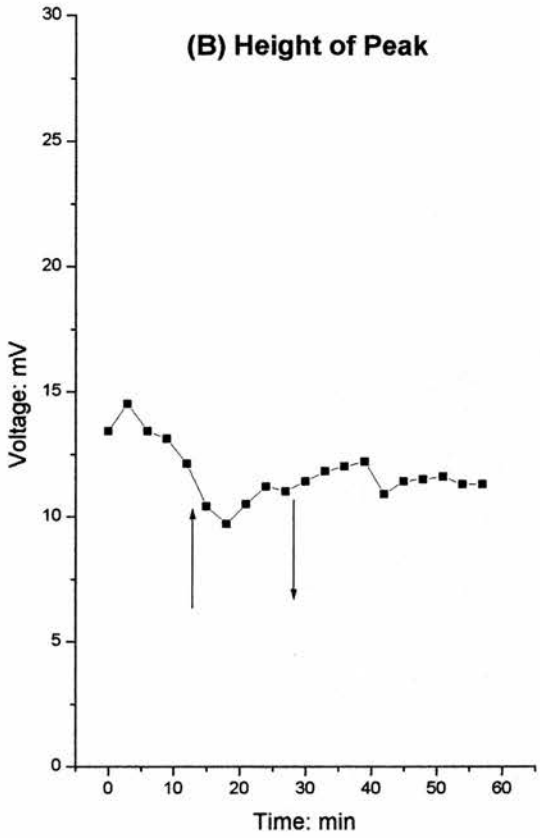
(B) Height of Peak
Voltage: mV
30
25
20
15
10
5
0
0
10
20
30
40
50
60
Time: min

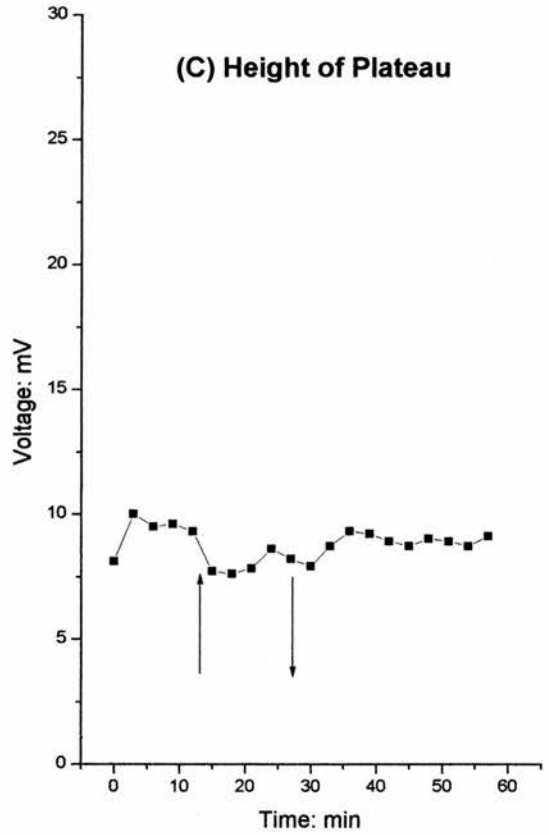
(C) Height of Plateau
Voltage: mV
30
25
20
15
10
5
0
0
10
20
30
40
50
60
Time: min

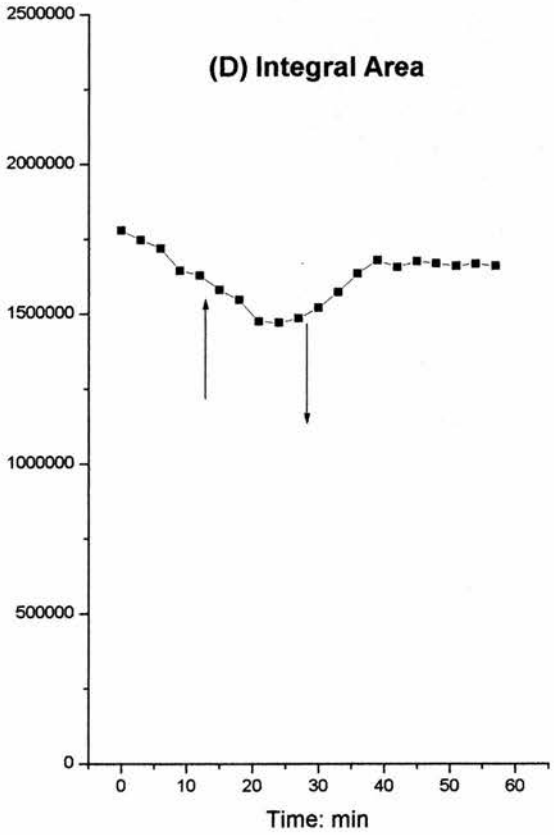
(D) Integral Area
2500000
2000000
1500000
1000000
500000
0
0
10
20
30
40
50
60
Time: min

Figure IV.v

Intracellular Recording of the Caudal Photoreceptor Generator Potential in the Presence of TTX and Serotonin [100μM]

Overlay of the generator potential in the three states: prior to application (black trace), with serotonin (red trace), and following a wash with normal saline (grey trace).

Panel (A) the overlay of the generator potentials without any sort of alignment.

Panel (B) the base-lines have been aligned to give an indication of the relative height in the three states.

(A)

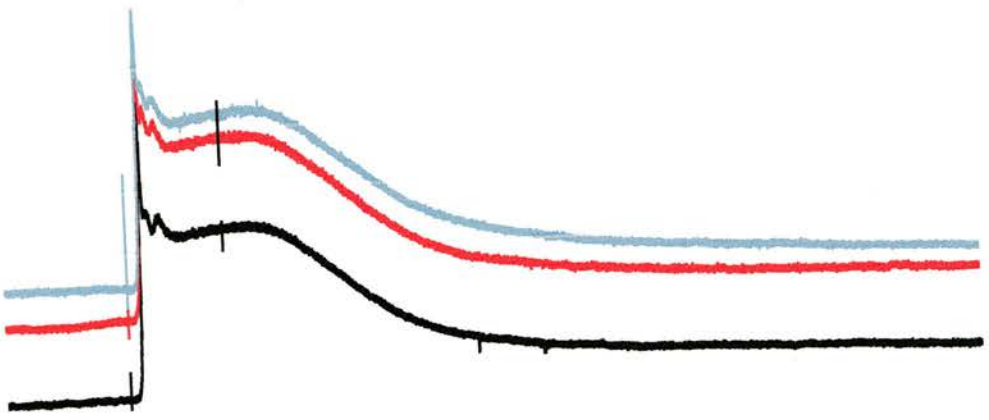

Light

(B)

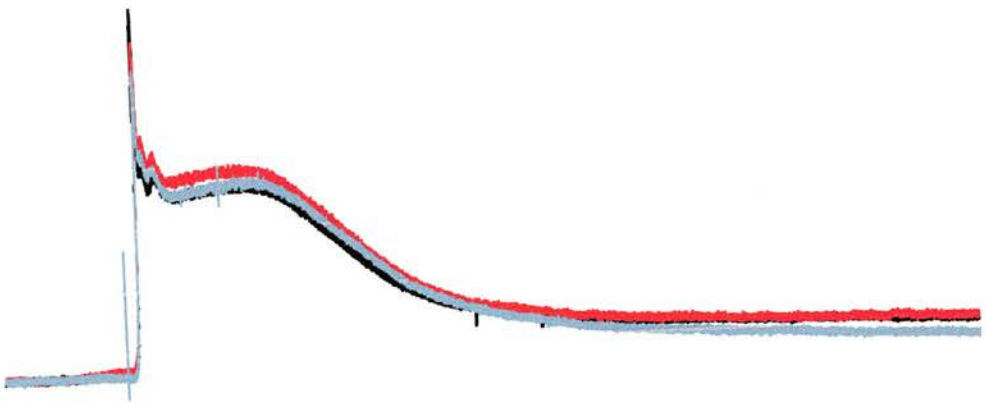

Light

10 mV

5000 ms

Figure IV.vi

Changes in Features of the Light Response following the application of Serotonin [100μM]- Recorded Intracellularly in the Presence of TTX

Measurements are made from the light responses stimulated every 3 minutes. The arrows indicate when caffeine was applied and washed off with normal saline.

Panel (A) shows the resting membrane potential prior to the light stimulation.

Panel (B) shows the size of the peak calculated as the difference between the membrane potential of the cell at rest and the maximum excursion at the transient peak.

Panel (C) shows the size of the plateau calculated as the difference between the membrane potential of the cell at rest and the maximum height of the plateau phase.

Panel (D) shows the variation in the area of the generator potential following the application of Serotonin [100μM].

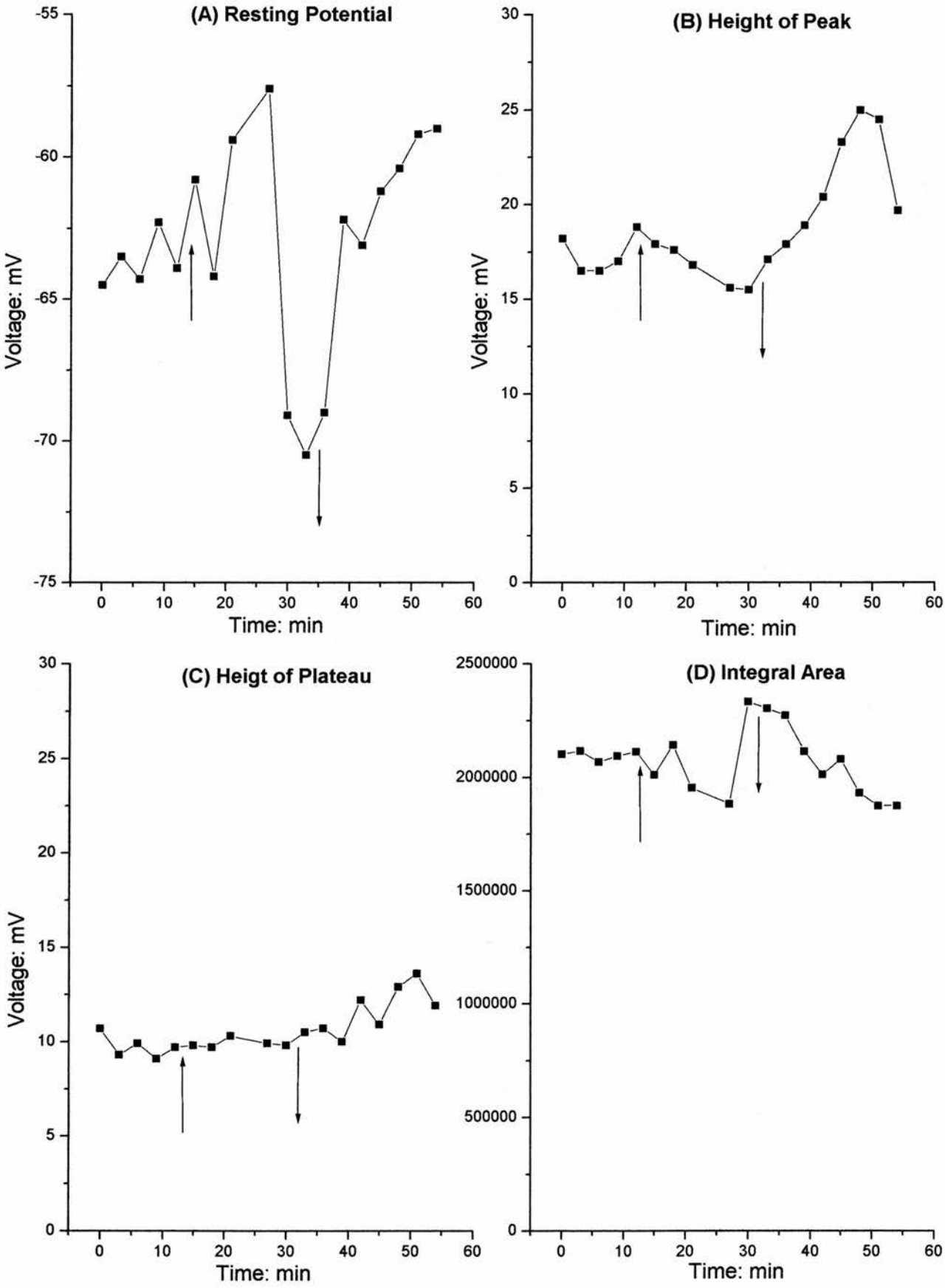
(A) Resting Potential
Voltage: mV
Time: min
(B) Height of Peak
Voltage: mV
Time: min
(C) Heigt of Plateau
Voltage: mV
Time: min
(D) Integral Area
Time: min

4.3.3 The Effect of Serotonin [100μM] on the Role of the Caudal Photoreceptor as a Mechano-Sensory Integrating Interneuron

4.3.3.1 Current evoked EPSPs and IPSPs may be modulated by serotonin

The effect of serotonin [100μM] on the synaptic inputs on to the CPR was examined though nerve root stimulation of the sensory cells entering the terminal ganglion, using a suction electrode. It has been shown by Kennedy (1963b,c) that stimulating ispilateral nerve roots produces both an excitatory and an inhibitory response in the CPR, whereas contralateral stimulation produces only an inhibitory response. In these experiments stimulation was used to drive EPSPs or IPSPs at 15 second intervals. In Figure IV.vii (panel A), the size of the EPSPs to a fixed stimulus voltage increased and summated to produce an action potential. In Figur IV.vii (panel B), a similar effect was seen for stimulus voltage driven IPSPs, which increased in size in response to the presence of serotonin.

4.3.4 The Effect of Serotonin on the Caudal Photoreceptor in the Dark

Serotonin [100μM] was applied to preparation during intracellular recording of the CPR in the absence of photic stimulus in order to examine its effects on the cell itself rather than the cells photic response (n=5).Panel (A) shows the response of the cell at rest in the dark, which, as stated previously in Chapter 3, means that in *Pacifasticus leniusculus* there is no spontaneous background level of action potentials as reported in other species of crayfish. Following the application of serotonin [100μM] there is a gradual increase in the firing of EPSPs onto the CPR 6 minutes after the application of serotonin (panel B). After 12 minutes following the application of serotonin (panel C) some of the EPSPs summate to produce action potentials. The frequency of these action potentials were measure as being between 3.5 - 4Hz. Serotonin was removed by washing the preparation with fresh saline to give a significantly reduced rate of EPSPs in the CPR and the absence of action potentials (panel D). Corresponding to the increase in level of electrical activity in the CPR in response to serotonin, there is also a change in the resting potential of the cell. There is a small, but significant depolarization in the membrane potential from -64mV to -60mV (as shown in Figure IV.viii). This change is also reversed following a wash with fresh saline.

4.4 Discussion

Initial experiments indicated that there was clearly a change in the photic response of the CPR following the application of serotonin. However, the results shown here suggest that the

Figure IV.vii

The Effect of Serotonin on Synaptic Inputs onto the Caudal Photoreceptor

Panel (A) Serotonin increases the magnitude of current evoked EPSPs causing them to summate and trigger an action potential.

Panel (B) serotonin increases the magnitude of current evoked IPSPs.

Baselines have been superimposed for the comparison of amplitude.

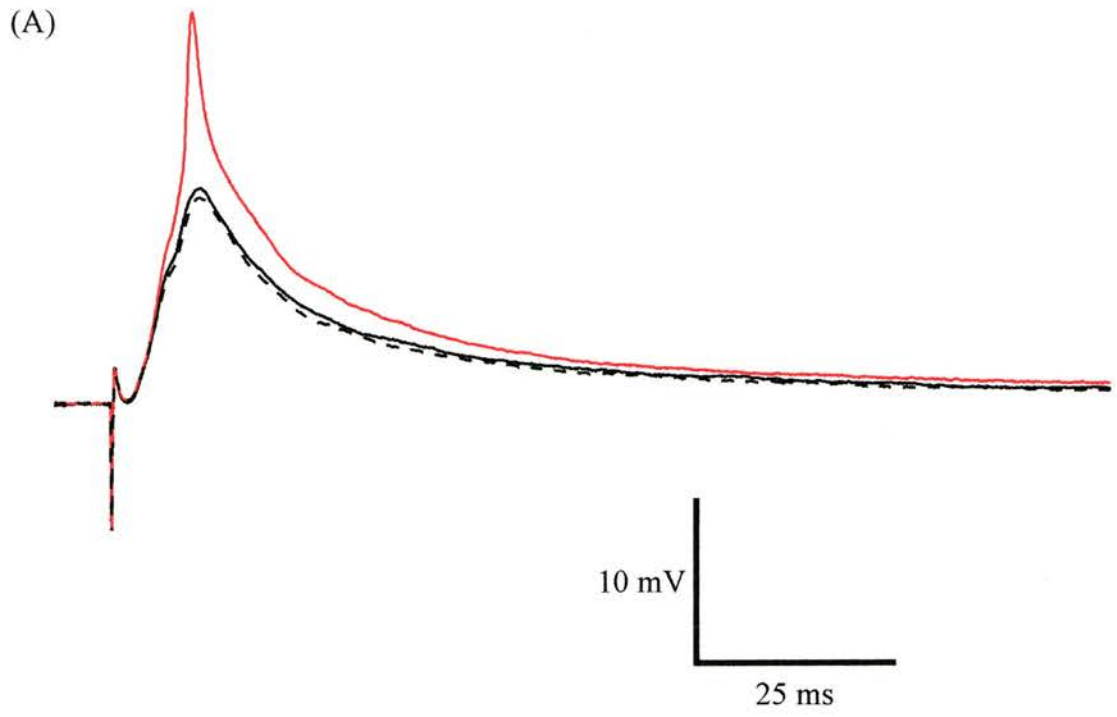
(A)
10 mV
25 ms
(B)

Figure IV.viii

The Effect of Serotonin [100μM] on Activity in the Caudal Photoreceptor in the Absence of Light

Panel (A) the cell shows no spontaneous activity prior to the application of serotonin

Panel (B) serotonin initially causes the an increasing number of EPSPs 6 min

Panel (C) these EPSP summate to produce action potential on top of the EPSPs 12 min

Panel (D) post wash shows a reduction in the level of activity but excitation persists.

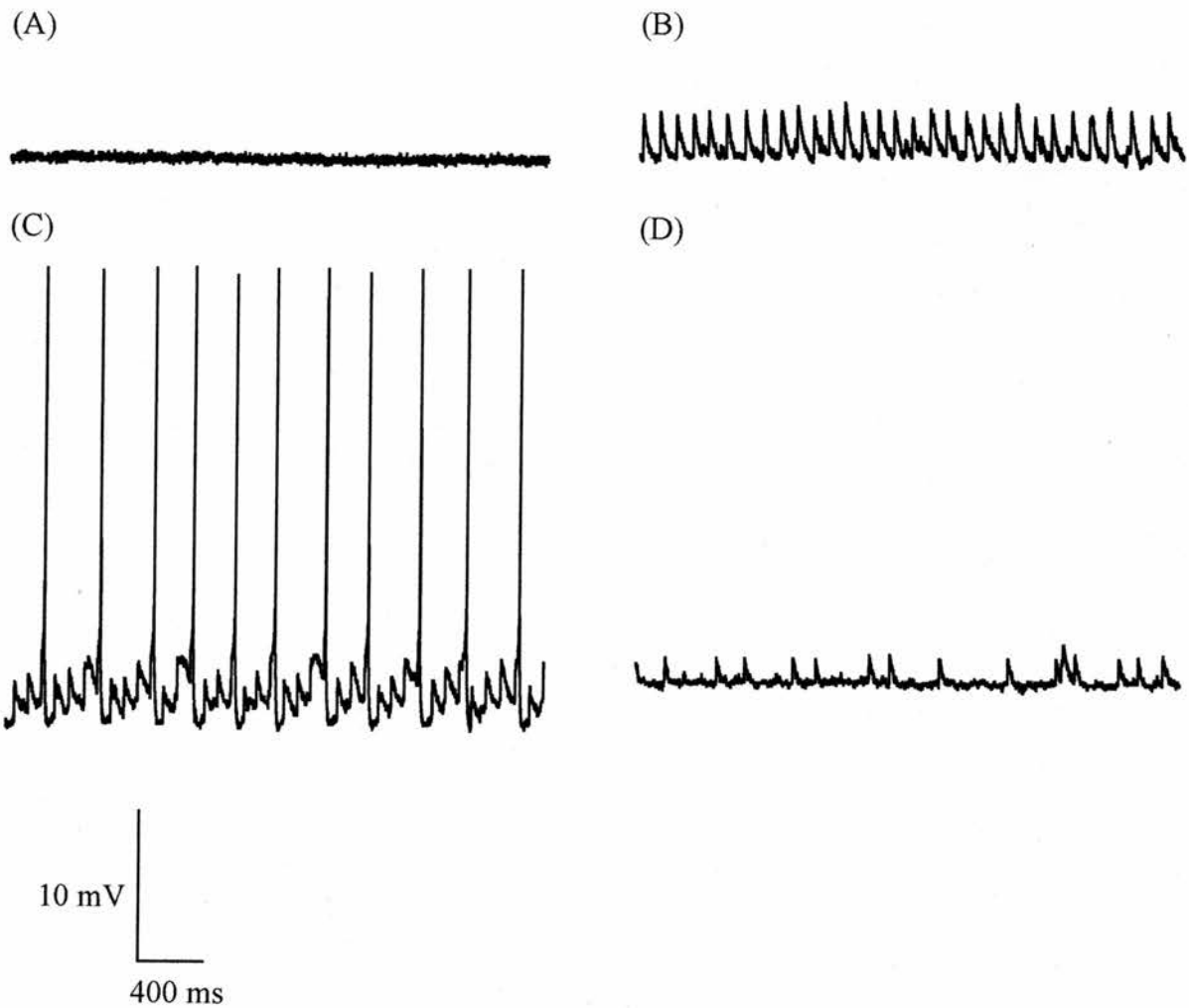
(A)
(B)
(C)
(D)
10 mV
400 ms

application of serotonin does not always lead to an increase in the number of action potentials evoked. In fact, there are examples where there has been a decrease in the number of action potentials evoked. Some of these results come from extracellular recordings from which the number of action potentials has been extracted using template recognition. This inevitably calls in to question the accuracy of such results given that as has been mentioned previously in Chapter 3, the method of template recognition is not an absolutely reliable measure of which action potentials come from any one neuron given that false positives can occur if another neuron has an action potential of a similar size or shape, and false negatives may occur if an action potential which should match the template collides with one from another neuron and appear to have a different shape on the recording. By going thorough the record it is possible to identify and account for such occurrences however given that there has been a massive increase in action potential activity from various neurons in the inter-ganglionic connective in the presence of serotonin this increases the likelihood of action potentials from other neurons being misidentified as matches for the CPR template. Serotonin may also be altering the shape or duration of the action potentials from the CPR causing them to deviate from the shape of the template and therefore not be correctly identified during the analysis. Therefore, where possible it is preferable to use intracellular data to ascertain the effects of serotonin, such as that depicted in Figure IV.i. From this data frequency distribution curves can show that there is an increase in the spontaneous firing outwith what one would consider to be the photic response. There is also a reduction in the frequency of the initial peak and the plateau phase. Following the termination of the light stimulus there is a prolonged firing of action potentials at a low frequency which may continue until the time of the next light stimulation some 3 minutes later.

Measurements of various features of the intracellular recordings (Figure IV.iv) have revealed that there is a slight positive (1-2mV) change in the resting membrane potential and a small decrease in the magnitude of the depolarization underlying the photic response. It is possible that these two features are linked, and it is likely that this more positive resting potential is, in someway, responsible for the increased firing of the CPR during the supposed resting phase when the preparation is in the dark.

There are two possible ways in which serotonin could be effecting the CPR:

1. Serotonin could be lowering the threshold for the photic response i.e. the CPR is able to respond to light at lower levels. For this to be the case, serotonin must be acting on the transduction cascade underlying the photic response of the neuron.
2. or Serotonin is increasing the excitability of the CPR either by lowering the threshold of the CPR to excitation or by increasing the number or intensity of excitations on to the CPR from other neurons.

4.4.1 The Effect of Serotonin on the Caudal Photoreceptor Generator Potential

The positive shift in membrane potential and the decrease in the magnitude of the depolarization seen in intracellular recordings suggest that serotonin may be having an effect on the transduction cascade underlying the photic response; however, the application of serotonin in the presence of TTX does not support this theory. No significant changes in the size or shape of the generator potential have been discerned. If serotonin apparently alters the photic response but has no affect on the generator potential itself then by what means is it able to alter the excitability of the neuron?

It is well established that, in addition to its photoreceptive properties, the CPR also acts as a mechano-sensory integrating interneuron (Kennedy, 1958a). Sensory hairs on the tail-fan of the animal detect changes in local water currents that could indicate the proximity of predators and imminent danger for the crayfish. Sensory information from these hairs are brought together in this interneuron, as with many other mechano-sensory interneurons found in the terminal ganglion, before being transmitted on to other parts of the ventral nerve cord. Kennedy (1958a) described the asymmetry seen in the inputs the interneuron receives from sensory hairs on the tail fan. Synaptic inputs from the contralateral side of the terminal ganglion gave inhibitory inputs and inputs from the ipsilateral side gave excitatory inputs.
Stimulus driven EPSPs were found to increase in size and reach spike threshold in the presence of serotonin while IPSPs were also found to increase in size. This modulation of synaptic inputs is thought to be responsible for the increase in spontaneous action potential activity that has been seen in the CPR and lead to the false assumption that serotonin was increasing the photic response. By applying serotonin to the preparation whilst recording from the CPR in the dark (in five preparations) it has been possible to confirm that there is an increase in excitable input on to the CPR (Figure IV.viii) which, after 12 minutes reaches a sufficient threshold for spontaneous action potentials (panel C). This effect is removed when

the preparation is washed with fresh saline adding credence to serotonin being the cause of this increased excitation. There are, of course, two ways in which serotonin could be effecting this change in excitability. Firstly, it could be lowering the threshold of the CPR causing inputs of the same strength to have an increased effect on the interneuron. Or secondly, serotonin could be, and this is thought more likely, increasing either the size, or number, of inputs onto the CPR.

4.4.2 What Would be the Effects of Serotonin *in vivo*?

Serotonin levels are known to fluctuate according to the social status of the crayfish. Livingstone *et al.* (1981) showed that injecting serotonin into the haemolymph of a subordinate animal could induce it to behave in a dominant manner. Beltz and Kravitz (1986; 1987) identified more than 100 serotonergic neurons in the decapod (lobster) ventral nerve cord. They mapped the position of the cell body, and traced the fibres and neuropil for each of these neurons. The function of the serotonergic neurons is on the whole not fully understood, however, in 1987, Beltz and Kravitz proposed that the two pairs of large neurons in the fifth thoracic ganglia (T5) and the first abdominal ganglia (A1) may be the source of neurosectretory serotonin released into the hemolymph. They proposed that serotonin-immunoreactive varicosities from these two pairs of larges cells were found in the central neuropil regions of the ventral nerve cord as well as in two peripheral neurosectretory sites: the pericardial organ and the proximal regions of the thoracic second roots. It was suggested that the neurosectretory endings in the central neuropil acted on the central-pattern generating neurons, whilst those endings in the peripheral regions had more peripheral targets. A similar distribution pattern of seroternergic neurons have been described in the crayfish. Therefore, there would be a natural source of serotonin were the CPR to be exposed to it *in vivo*. Yeh *et al.* (1997) showed that serotonin affected the synaptic strength of sensory neurons which synapse on to the lateral giant escape response, in the same way that we have seen it do here on the CPR. Therefore, it is likely that the function of modulatory effect serotonin can have on the CPR is part of the bigger picture in which serotonin, along with other neurohormones, are able to affect the behaviour of animals according to their social status.

CHAPTER 5: THE PHOTOTRANSDUCTION PATHWAY OF THE CAUDAL PHOTORECEPTOR OF THE CRAYFISH *PACIFASTICUS LENIUSCULUS*

5.1 Introduction

The gross anatomy of the crayfish caudal photoreceptor does not resemble that of a typical photoreceptor, rather it has the morphology of an ascending integrating interneuron (Wilkens and Larimer, 1972). It has, therefore, been concluded that the cell's ability to detect light has evolved as a secondary function. Furthermore, the physiological properties of the CPR are very different from those of standard "image-forming" visual receptors, especially in regard to the very long latency of the response and the extreme temperature dependence of this latency (see below). This strongly suggests that there may be differences in the transduction pathways of this extra-ocular photoreceptor and visual photoreceptors.

5.1.1 The Site of Photoreception in the Caudal Photoreceptor

There have been several studies examining the ultrastructure of the ventral nerve cord for evidence of photoreceptive properties of the CPR. The first, performed by Hama (1961), incorrectly identified a lamellated compound body, which, he claimed resembled photoreceptive structures in other systems. However, such structures were found in every ganglion of the abdominal nerve cord and this was inconsistent with physiological evidence that the site of the light response was restricted to the terminal ganglion. One year later, Uchizono (1962) described layered, or lamellated, structures similar to those found in *Drosophila* (Wolken *et al.*, 1957) and ommatidium of the compound eye of *Limulus* (Miller, 1957) and concluded that this was the site of photoreception. These studies have subsequently been shown to be incorrect. A more recent study by Krusewska (1991) involving ultra structural examination of colloidial-gold filled cells found that some of the dendritic processes of the CPR contain, and are surrounded by, densely packed membranous layers thought to be the site of photoreception.

5.1.2 Light-sensitive Pigment

There has been no positive identification of the light sensitive molecule in the CPR although it is thought to be a rhodopsin-like molecule similar to that commonly found in other photoreceptive systems. Antibodies against retinal rhodopsin of the Australian crayfish, *Cherax destructor* were injected into the CPR of the crayfish *Procambarus clarkii* with negative immunocytochemical results (Kruszewska, 1991). This has been attributed to either

a limited cross-reactivity of the antibody over the phylogenic distance between the two species, or to minor differences in the molecular structure of the photo-pigment in the CPR making it incompatible to the antibody, rather than evidence for absence of a rhodopsin-like molecule.

Analysis of the spectral sensitivity of the CPR revealed that the photosensitive pigment of the CPR is different from that of the crayfish compound eye (Kennedy and Bruno, 1961; Bruno and Kennedy 1962). The sensitivity of the CPR ranges from 420mμ to 620mμ, with a peak sensitivity at 500mμ. This indicates that there is a shift of 70mμ towards the shorter end of the spectrum from that of the compound eye which has a wider range, *i.e.*, from 440mμ to 700mμ with a maximum of 430mμ. The general shape and position of the maximum of the spectral sensitivity function for the CPR has been confirmed as consistent with the rhodopsins of other crustaceans (Wald and Hubbard, 1957; Briggs, 1961; Bruno and Kennedy, 1962). Therefore, it is reasonable to assume that the photosensitive pigment of the CPR is a member of the carotenoid-protein family of pigments commonly associated with photoreception.

5.1.3 Transduction Cascade

The transduction cascade underlying the photic response of the crayfish caudal photoreceptor has not been fully elucidated. A number of studies have reported a long latency period (in the order of 500ms) between the onset of a light stimulus and the depolarization of the generator potential and the production of action potentials, which indicates a multi-stage second messenger pathway (Kennedy, 1958a; Kennedy, 1963b, 1963c; Kennedy and Preston, 1960). This latency period can be further elongated by lowering the temperature from 25 ± 0.05°C to 10 ± 0.05°C (Larimer, 1967) which adds credence to the theory. Furthermore, the latency of the response shows strong temperature dependence at the lower temperatures (Larimer, 1967; Kivivuori, 1982; Belanger, 1988).

The nature of this second messenger pathway is thought to resemble that of the invertebrate visual transduction cascade rather than that of vertebrates (both of which are redrawn in Figure V.i), based on the study by Kruszewska (1991). IP_3 and Ca^{2+} were injected into the CPR with the effect of inducing a photic-like response, suggesting that they may both play a role in the innate transduction cascade of the CPR as previously demonstrated in the retinal photoreceptors of other invertebrates.

Figure V.i

Visual Phototransduction Cascades

Panel (A) vertebrate phototransduction cascade

Panel (B) invertebrate phototransduction cascade

Vertebrate Transduction Cascade

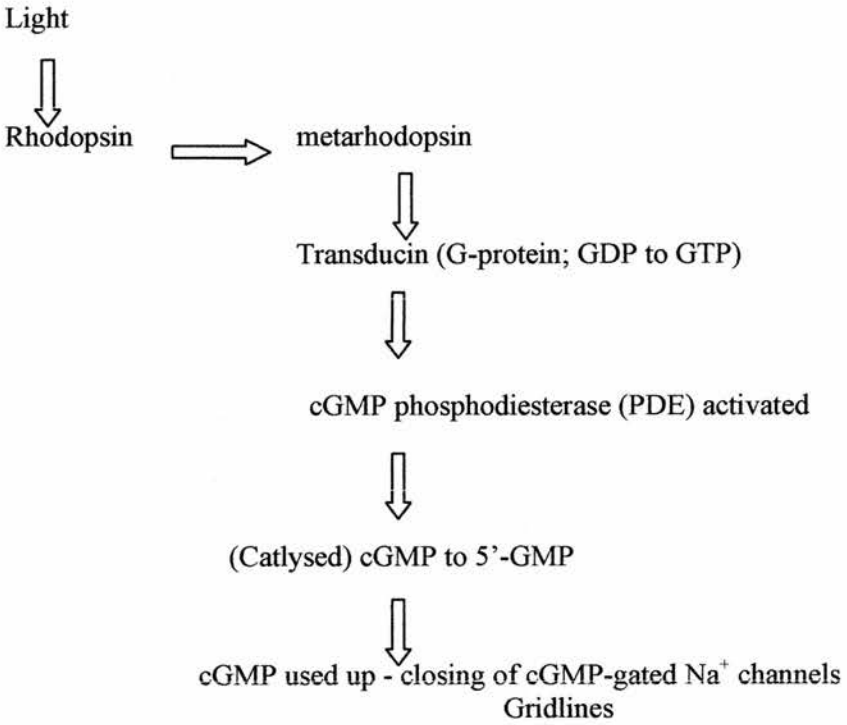

Invertebrate Transduction Cascade

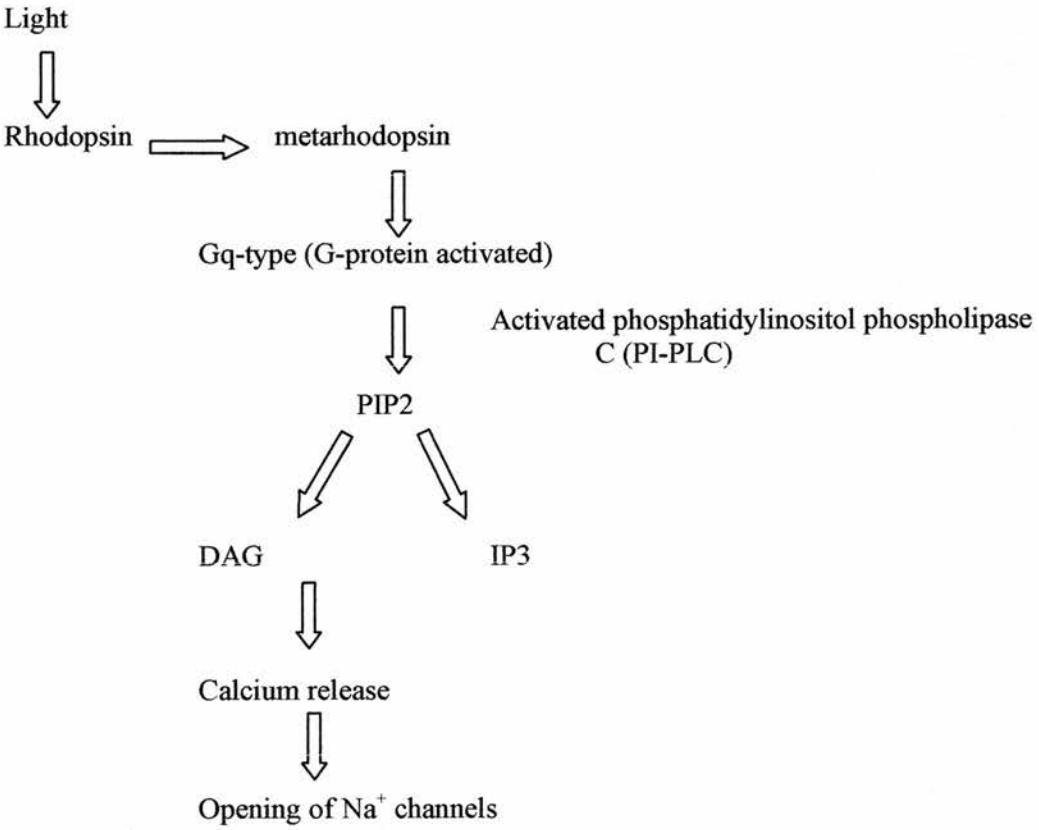

The resting potential and depolarizing generator potential of the CPR are also consistent with the invertebrate model as opposed to the vertebrate model, which has a much more positive resting potential and a hyperpolarizing generator potential. However, in both cases sodium ions are involved in the photic response, and it is thought that the same ion is responsible for the potential change in the CPR. Whether this is the case will be discussed further in the next chapter.

The proposed phototransduction cascade of the crayfish caudal photoreceptor, based on the findings of Kruszewska (1991) and Kruszewska and Larimar (1993), is shown in Figure V.ii. Photons of light are absorbed by, and activate, a rhodopsin-like molecule resulting in a guanosine di-phosphate (GDP) to guanosine tri-phosphate (GTP) transformation in an unspecified G-protein, because injection of GTP also induces a photic-like response (Kruszewska, 1991; Kruszewska and Larimer, 1993). This triggers the activation of phospholipase-C (PLC), which in turn causes the release of inositol 1,4,5-triphosphate (IP_3) which acts a cytoplasmic second messenger inducing the release of calcium from intracellular stores. It is not known whether the increase in Ca^{2+} causes a permeability change directly or indirectly, or whether there is another mechanism altogether.

5.1.4 Reagents Applied to the Caudal Photoreceptor

Based on the assumption that the photic response of the CPR is indeed similar to that of retinal photoreceptors in invertebrates rather than vertebtrates, it should be possible to inhibit, or excite the transduction pathway at different points depending upon the exogenous reagent applied. Injecting IP_3, Ca^{2+} and GTP induces spikes in the CPR, and this suggests that these agents may be involved in the phototransduction cascade. We applied various pharmacological agents to elucidate this cascade further.

5.1.4.1 Staurosporine

IP_3 is known to be a product of the phosphatidylinositide (PI) pathway in the invertebrate visual photoreceptor. In that system phosphatidylinositide phospholipase C (PI-PLC) catalyses the breakdown of phosphatidylinositol diphosphate (PIP_2) into diacylglycerol (DAG) and inositol triphosphate (IP_3). While IP_3 acts as a cytoplasmic second messenger releasing Ca^{2+} from intracellular stores, DAG remains membrane bound and activates protein kinase-C (PKC) which is responsible for the opening of Na^{+} channels. The application of staurosporine, a broad spectrum kinase inhibitor, was intended to provide evidence for any

Figure V.ii

The Phototransduction Cascade of the Caudal Photoreceptor

The pathway depicted is based on the published work of Kruszewska (1991), and Kruszewska and Larimer (1993).

Caudal Photoreceptor Cascade

Light

Light sensitive molecule assumed to be rhodopsin-like

GTP G-protein

Phospholipase C catalyses the hydrolosis

DAG/IP3

Intracellular calcium release

Assumed this results in a permeability change

kinase activity in the photic response of the CPR.

5.1.4.2 Lithium

Inositol lipids play a major role in cell signalling by functioning as precursors of second messengers. Of the three common inositol-containing lipids found in the plasma membrane, phosphatidylinositol (4,5)-biphosphate is hydrolysed to give diacylglycerol, which stimulates protein kinase-C, and inositol 1,4,5-triphosphate, which diffuses into the cell to release intracellular calcium. Inositol 1,4,5-triphosphate is metabolised to give free inositol by two separate pathways. Lithium inhibits the final desphosphorylation step of both pathways, thus reducing the supply of the inositol required to maintain the lipid precursors used for signalling.

5.1.4.3 Caffeine

Caffeine is a central nervous system stimulant believed to act through adenosine receptors and monoamine neurotransmitters as an adenosine receptor antagonist and adenosine 3'5'-cyclic monophosphate (cAMP) phosphodiesterase inhibitor. Thus, levels of cAMP increase in cells following treatment with caffeine. Caffeine has also been reported to affect cellular calcium levels by releasing calcium from intracellular stores. Evidence suggests that calcium is released from intracellular stores in the CPR in response to light, therefore addition of exogenous caffeine may cause the CPR to produce a depolarizing potential even in the dark response by inducing the cell to release calcium from its intracellular stores.

5.2 Additional Materials and Methods

5.2.1 Staurosporine

The light stimulus regime may be summarized as:

Stimuli 1-4	in normal saline
Stimuli 5-8	with staurosporine [10μM]
Stimuli 9-12	normal saline wash
Stimuli 13-16	in normal saline/recovery

5.2.2 Lithium

The light stimulus regime may be summarized as:

Stimuli 1-4	in normal saline
Stimuli 5-8	with lithium [100μM]

Stimuli 9-12	normal saline wash
Stimuli 13-16	in normal saline/recovery

5.2.3 Caffeine

The light stimulus regime may be summarized as:

Stimuli 1-4	in normal saline
Stimuli 5-8	with caffeine [5mM]
Stimuli 9-12	normal saline wash
Stimuli 13-16	in normal saline/recovery

5.3 Results

5.3.1 The Effect of Staurosporine on the Light Response of the Crayfish Caudal Photoreceptor

Addition of exogenous staurospaurine [100μM] and [10μM] was found to have no significant effect on the photic response of the CPR in n=5 preparations. From extracellular recordings the number and frequency of action potentials produced by each light stimulus was examined using template recognition. The number of action potentials produced does not vary significantly with the presence of staurosporine. The P value from the two-tailed T-test for the data shown (n=3) in Figure V.iii is 0.055. There were no significant changes in the shape of the frequency curve in the presence of staurosporine (Figure V.iv) either. Intracellular recordings in the presence of TTX also show no significant changes in the shape of the generator potential that underlies the photic response of the CPR (Figure V.v). There was however a slight depolarization in resting potential but this is thought to be an artefact of electrode drift as it is very small and the post wash resting potential is also more positive than the initial value.

5.3.2 The Effect of Lithium on the Light Response of the Crayfish Caudal Photoreceptor

Overall lithium has an inhibitory effect on the photic response of the CPR in n=6 extracellular recordings. Initially there was an increase in the number of spikes recognized by the template; however it is thought that many of these are misrecognized spikes emanating from other neurons. There is a general increase in activity in the connective during 3 to 6 minutes after the application of lithium chloride [100μM] (Figure V.vi), after which the general activity seems to return to normal levels whilst activity in the CPR reduces to almost nothing.

Figure V.iii

The Effect of Staurosporine [10μM] on the Number of Action Potentials Evoked by the Photic Response

Measurements are made from light responses stimulated every 3 minutes. The arrows indicate when staurosporine was applied and washed off with normal saline.

Panel (A) variation in the number of action potentials with the application of staurosporine.

Panel (B) control – the number of action potentials produced under standard conditions over the same time course.

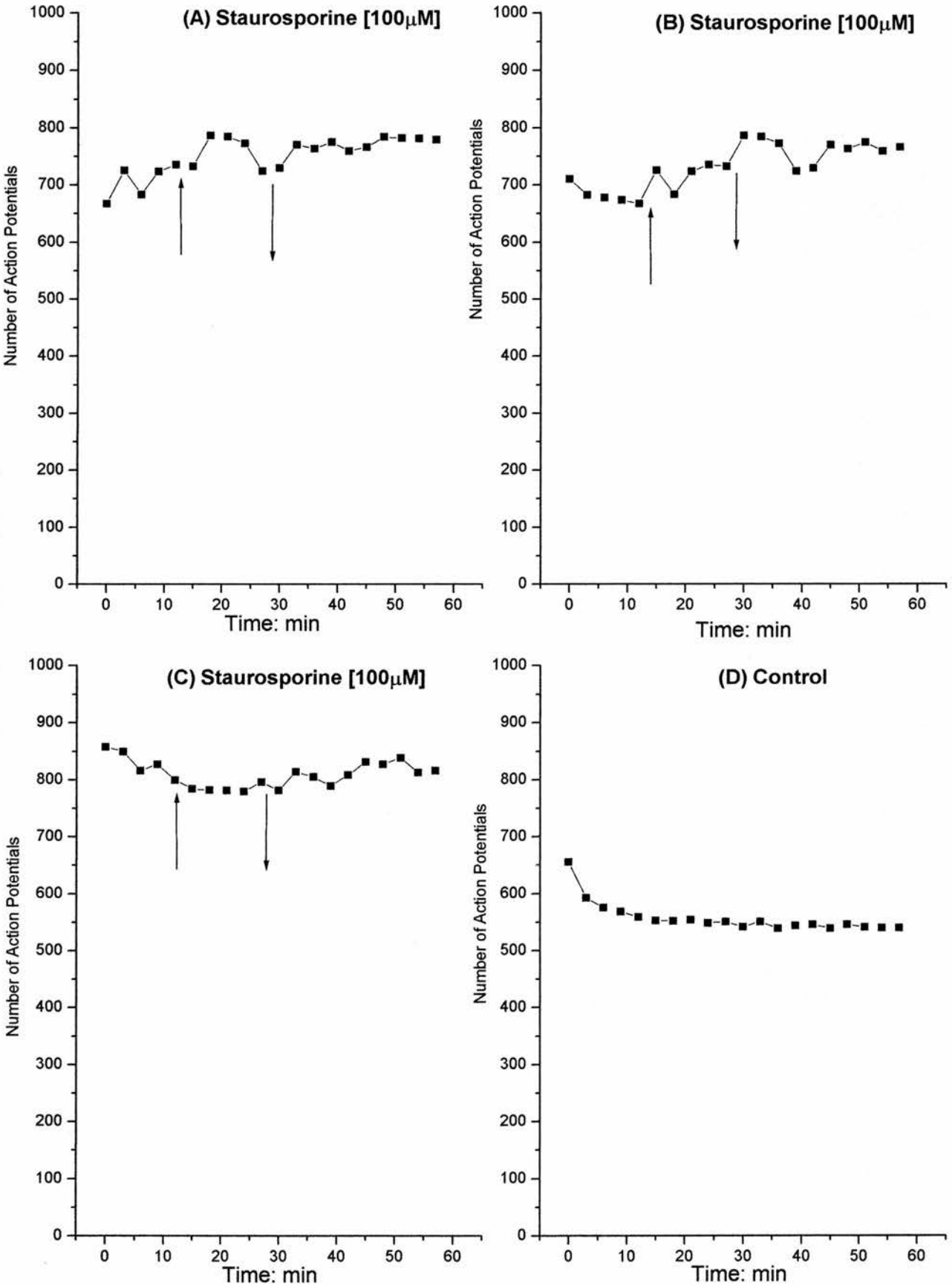
(A) Staurosporine [100μM]
(B) Staurosporine [100μM]
(C) Staurosporine [100μM]
(D) Control
Number of Action Potentials
Time: min
0
100
200
300
400
500
600
700
800
900
1000
0
10
20
30
40
50
60

Figure V.iv

The Effect of Staurosprine [100μM] on the Frequency Distribution of Action Potentials Produced in Response to Light

Panel (A) shows the spike frequency of standard light response prior to the application of staurosporine.

Panel (B) shows the spike frequency of the light response in the presence of staurosporine (10μM)

Panel (C) shows the spike frequency of the light response when staurosporine has been washed off with normal saline.

The broken line under each trace represents the light stimulus.

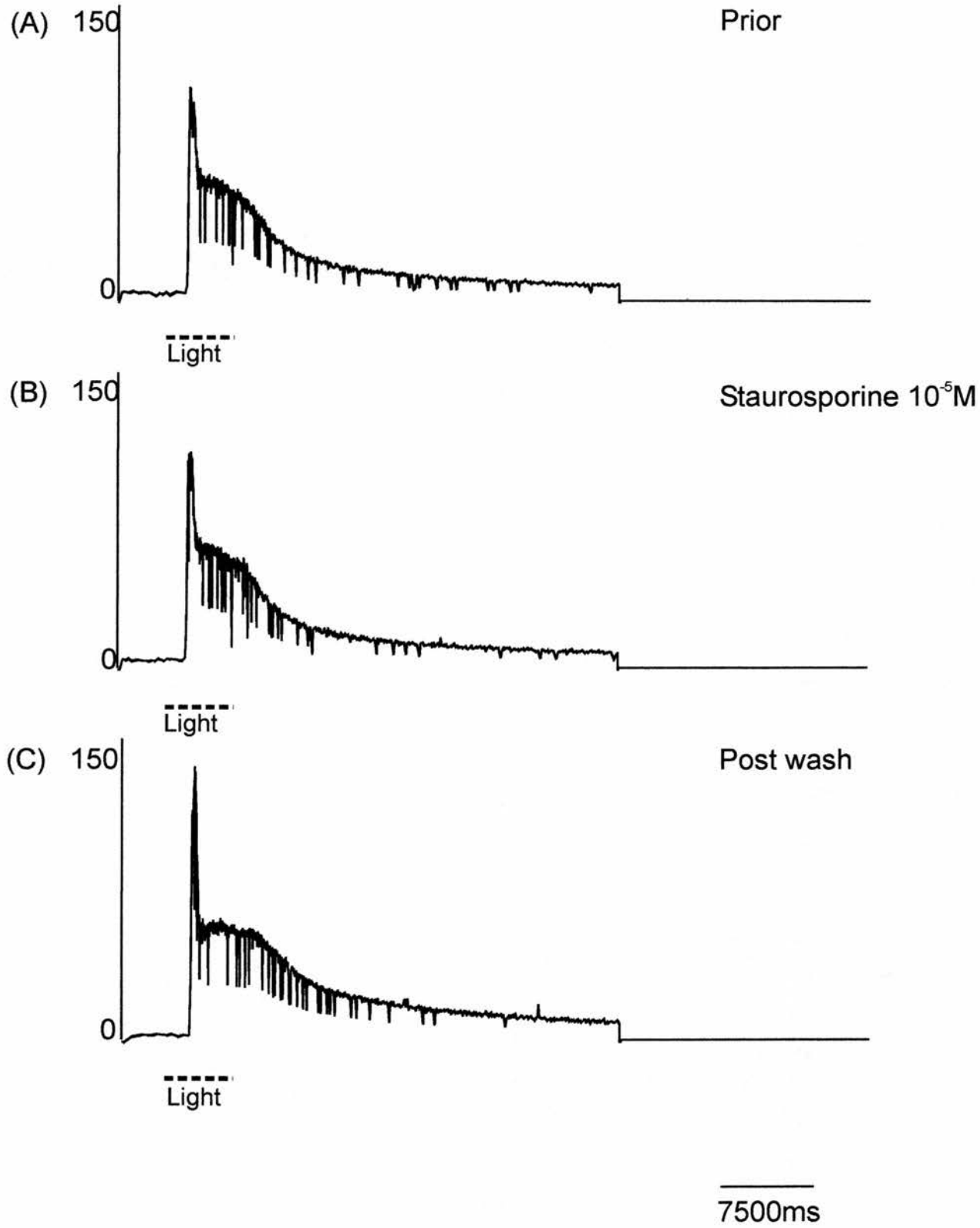
(A) 150
Prior
0
Light
(B) 150
Staurosporine 10^{-5}M
0
Light
(C) 150
Post wash
0
Light
7500ms

Figure V.v

Intracellular Recording of the Caudal Photoreceptor Generator Potential in the Presence of TTX and Staurosporine [10μM]

Overlay of the generator potential in the three states: prior to application (black), with staurosporine (red).

Panel (A) the overlay of the generator potentials without any sort of alignment.

Panel (B) the base lines have been aligned to give a indication of relative height in the three states.

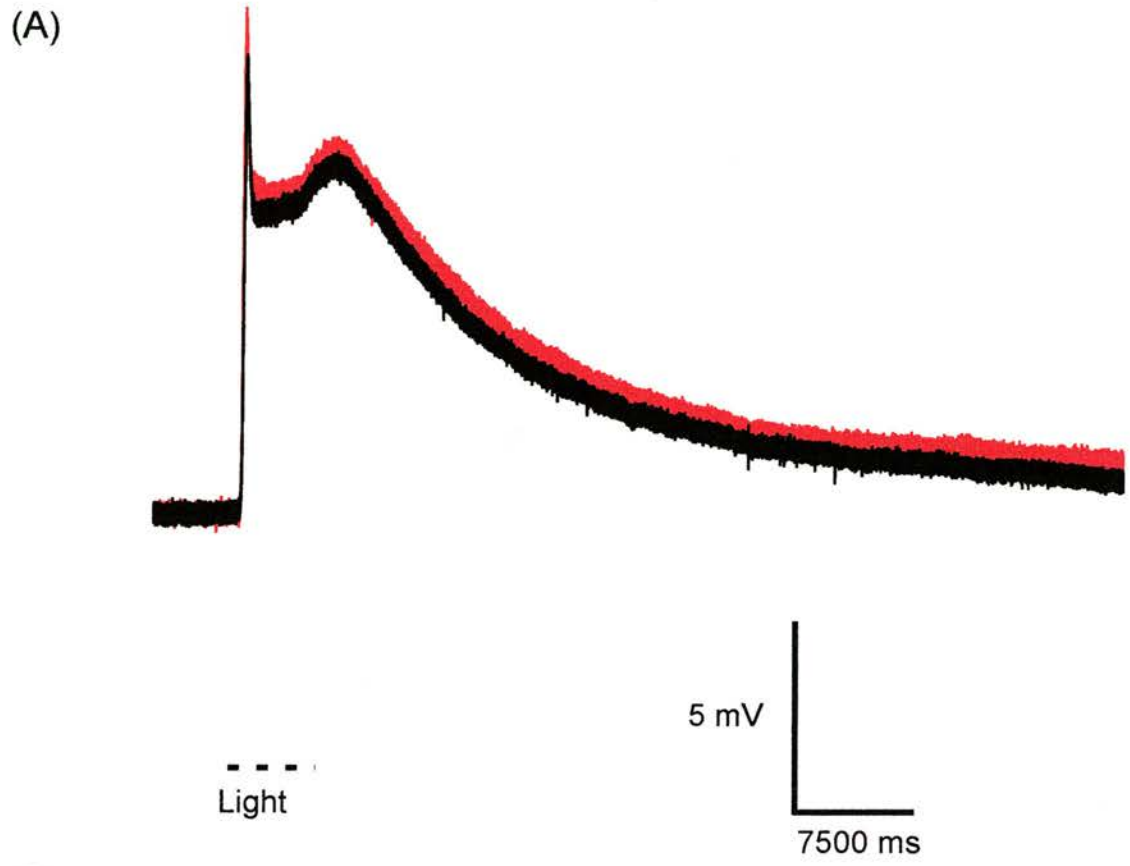
(A)
5 mV
Light
7500 ms
(B)
5 mV
7500 ms
Light

Figure V.vi

Extracellular Recording of the Caudal Photoreceptor Light Response in the Presence of Lithium [100μM]

Panel (A) shows the activity in the connective prior to the application of lithium.

Panel (B) shows an increase of activity in the presence of lithium.

Panel(C) shows the level of activity in the connective when lithium has been washed off with normal saline.

The broken line under each trace represents the light stimulus.

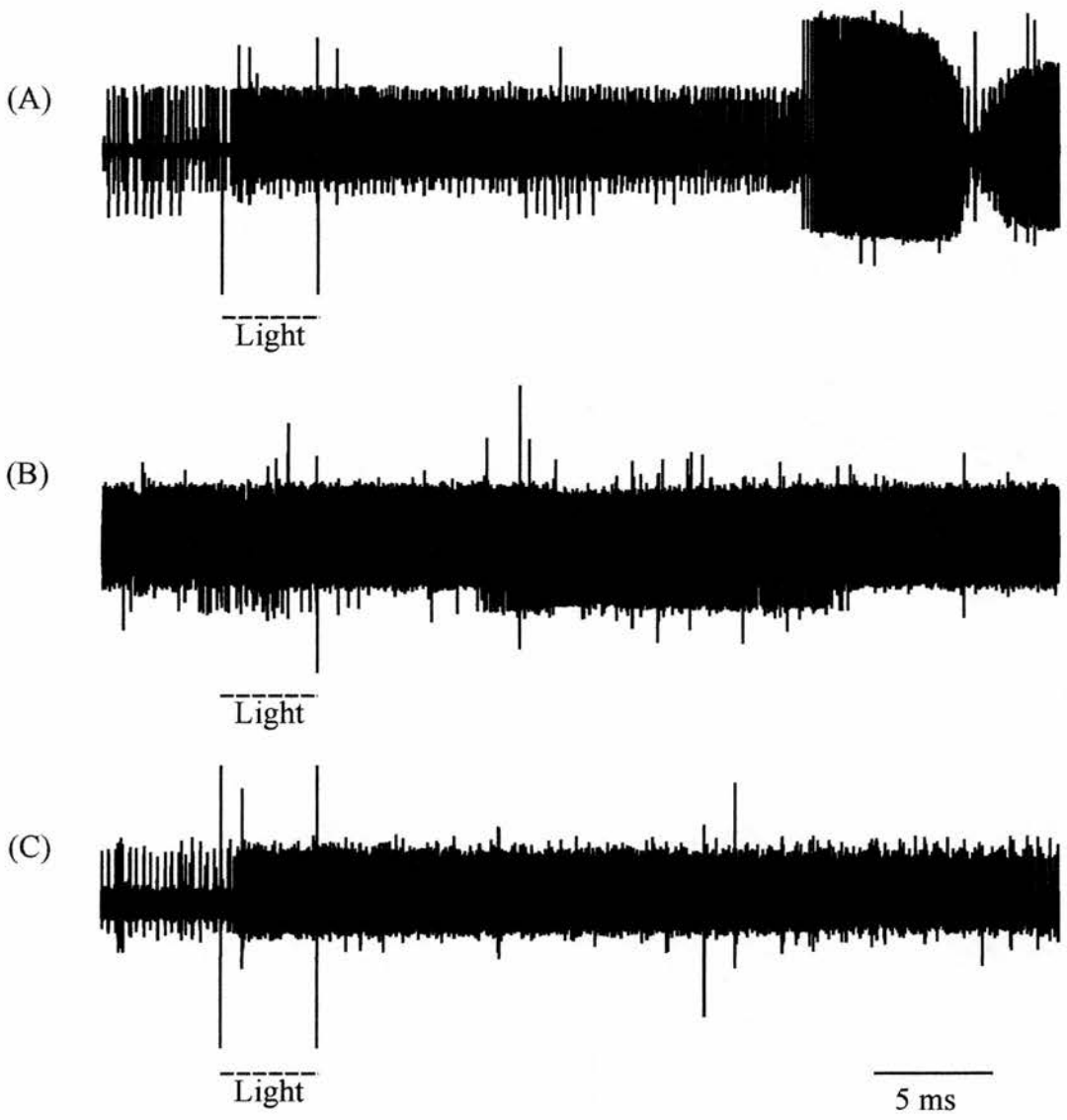
(A)
Light
(B)
Light
(C)
Light
5 ms

This is illustrated very clearly when the number of action potentials in each photic response is plotted out in Figure V.vii.

The shape of the spike frequency curves (Figure V.viii) shows an almost uniform decline in the distribution of the action potentials produced. Prior to the application of lithium there is the standard shape, initial peak in frequency, followed by a plateau phase in the presence of the light stimulus, which tails off when the stimulus is removed. Once lithium is applied the frequency at the peak is lost and the whole of the curve is reduced considerably as the action potentials that are produced become more and more spaced out. Following a wash with fresh saline the photic response recovers, and the shape of the frequency curve returns to that seen prior to the lithium although the initial peak never quiet regains its intensity again.

Intracellular recordings provide information about possible changes in resting potential as well as the size and shape of the depolarization of the generator potential. Lithium has no obvious effect on the waveform of the generator potential (Figures V.ix and V.x). There were sometimes changes in resting potential with the application of lithium, but these were not consistent between preparations. The mean difference in resting potential prior to adding lithium and in the presence of lithium was 0.77 mV (sd. 3.14 mV, n=5). Both Figure V.ix and Figure V.x show there to be very little variation in the height of the peak or plateau in the presence of lithium suggesting that the inhibitory effect it is having on the action potential of the photic response is not determined by the extent of the depolarization of the generator potential.

5.3.3 The Effect of Caffeine on the Light Response of the Crayfish Caudal Photoreceptor

Intracellular recording of the light response of the crayfish caudal photoreceptor showed there to be an increase in action potentials following the application of caffeine [5mM] into the bath saline (Figure V.xi). Panel (A) shows the standard light response to a four second pulse of light. Following the application of caffeine the light response is extended such that the CPR is firing continuously in the dark when the cell is resting as well as during the generator potential (panel (B)). Panel (C) shows an effective recovery when the preparation was washed with fresh saline. The action potentials for a complete experiment is shown in Figure V.xii, panel (A), and may be compared with the number of action potentials per response of the control where repetitive stimulations have been made under standard

Figure V.vii

The Effect of Lithium [100μM] on the Number of Action Potentials Evoked by the Photic Response

Measurements are made from light responses stimulated every 3 minutes. The arrows indicate when lithium was applied and washed off with normal saline.

Panel (A) variation in the number of action potentials with the application of lithium.

Panel (B) control – the number of action potentials produced under standard conditions over the same time course.

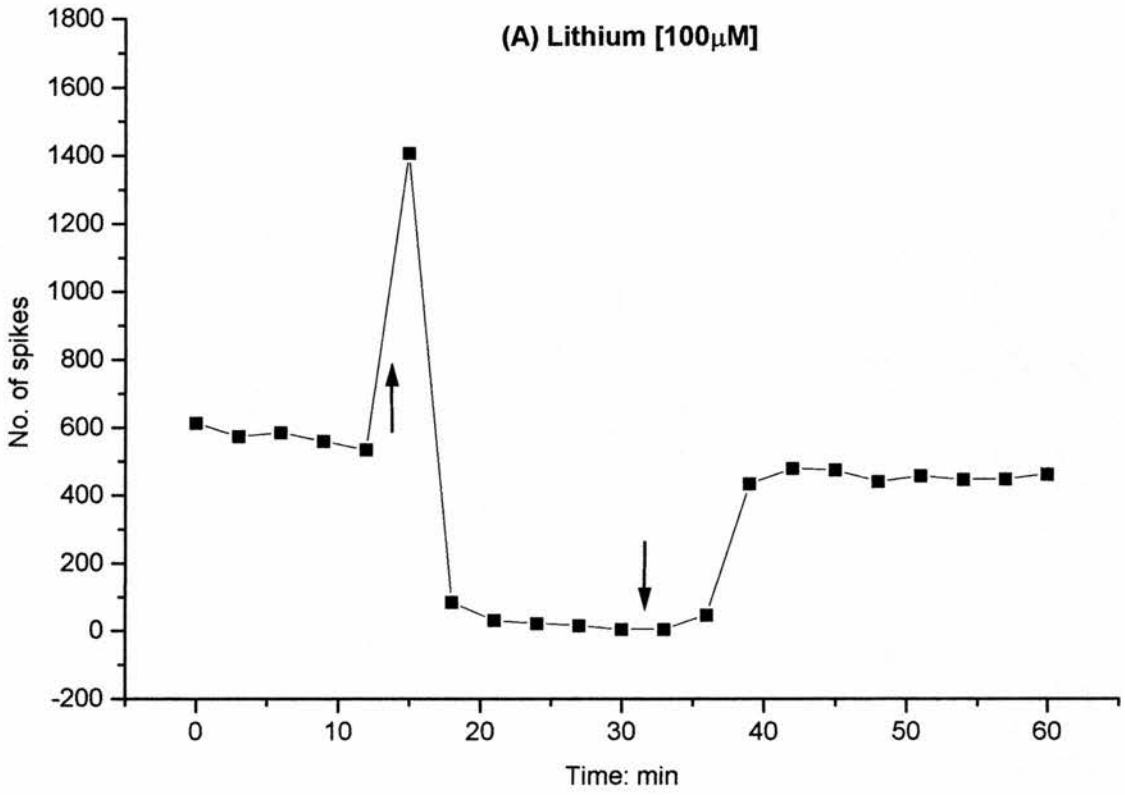
(A) Lithium [100μM]
No. of spikes
1800
1600
1400
1200
1000
800
600
400
200
0
-200
0
10
20
30
40
50
60
Time: min

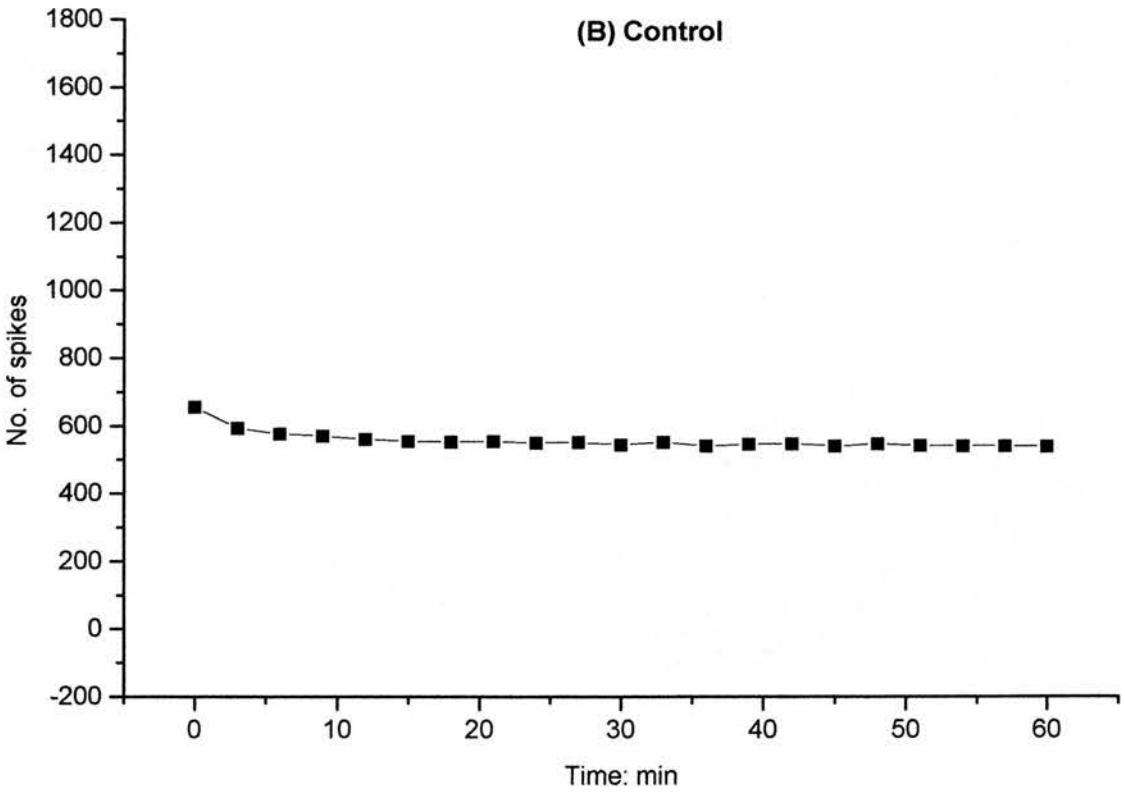
(B) Control
No. of spikes
1800
1600
1400
1200
1000
800
600
400
200
0
-200
0
10
20
30
40
50
60
Time: min

Figure V.viii

The Effect of Lithium [100μM] on the Frequency Distribution of Action Potentials Produced in Response to Light

Panel (A) shows the spike frequency of standard light response prior to the application of lithium.

Panel (B) shows the spike frequency of the light response in the presence of lithium (100μM).

Panel (C) shows the spike frequency of the light response when lithium has been washed off with normal saline.

The broken line under each trace represents the light stimulus.

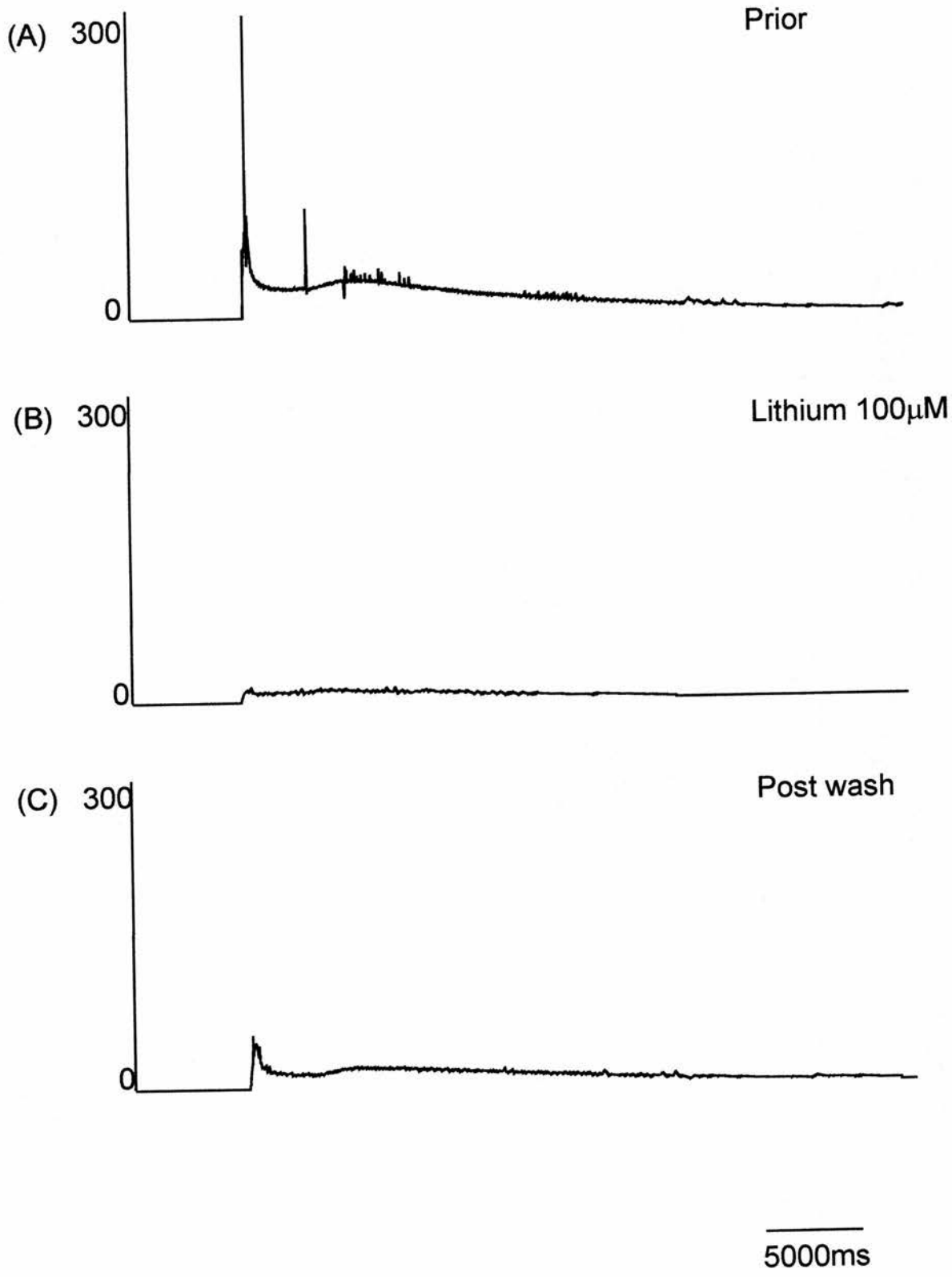
(A) 300
Prior
0
(B) 300
Lithium 100μM
0
(C) 300
Post wash
0
5000ms

Figure V.ix

Measurements of the Generator Potential in the Presence of Lithium [100μM]

Measurements are made from light responses stimulated every 3 minutes. The arrows indicate when lithium was applied and washed off with normal saline.

Panel (A) shows the resting membrane potential prior to the light stimulation.

Panel (B) shows the size of the peak calculated as the difference between the membrane potential of the cell at rest and the maximum excursion at the transient peak.

Panel (C) shows the size of the plateau calculated as the difference between the membrane potential of the cell at rest and the maximum height of the plateau phase.

Panel (D) shows the variation in the area of the generator potential following the application of lithium.

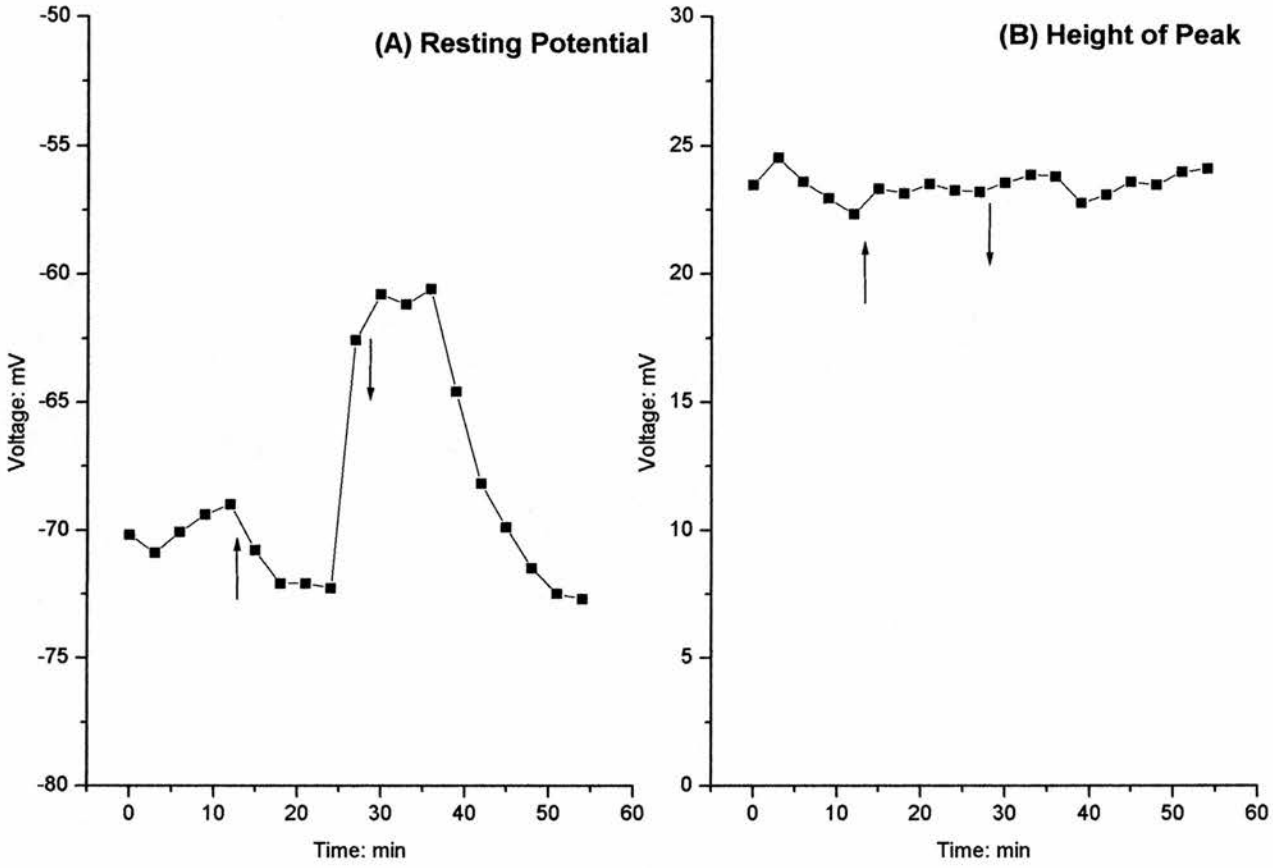
(A) Resting Potential
Voltage: mV
-50
-55
-60
-65
-70
-75
-80
0
10
20
30
40
50
60
Time: min

(B) Height of Peak
Voltage: mV
30
25
20
15
10
5
0
0
10
20
30
40
50
60
Time: min

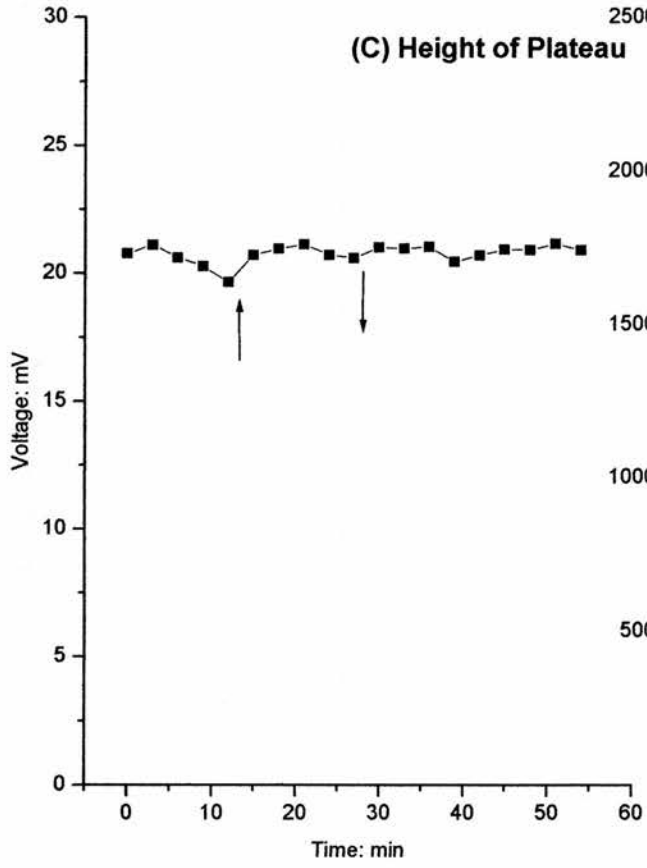
(C) Height of Plateau
Voltage: mV
30
25
20
15
10
5
0
0
10
20
30
40
50
60
Time: min

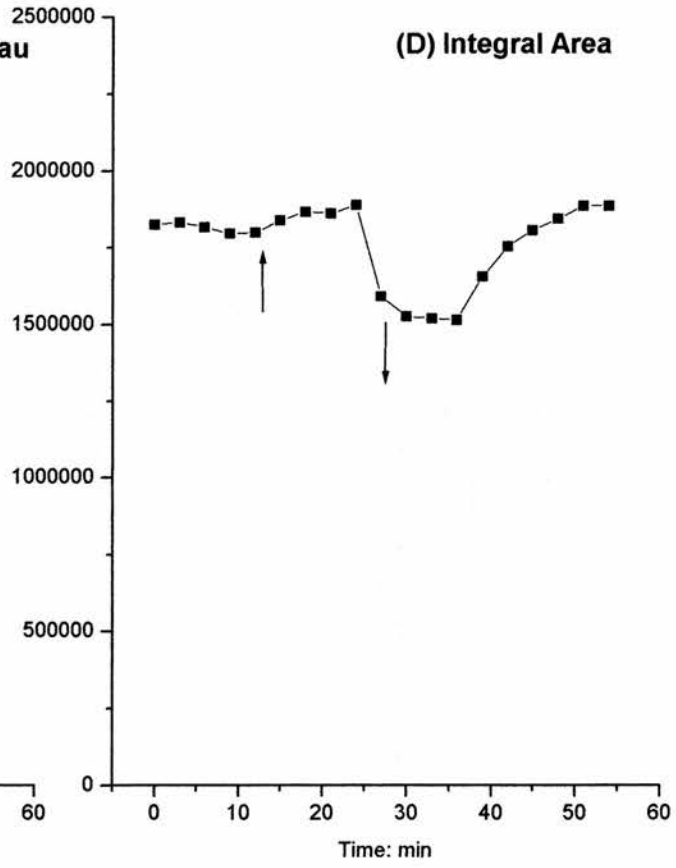
(D) Integral Area
2500000
2000000
1500000
1000000
500000
0
0
10
20
30
40
50
60
Time: min

Figure V.x

Intracellular Recording of the Caudal Photoreceptor Generator Potential in the Presence of TTX and Lithium [100μM]

Overlay of the generator potential in the three states: prior to application (black), with lithium (red), and following a wash with normal saline (grey).

Panel (A) the overlay of the generator potentials without any sort of alignment.

Panel (B) the base lines have been aligned to give a indication of relative height in the three states.

(A)

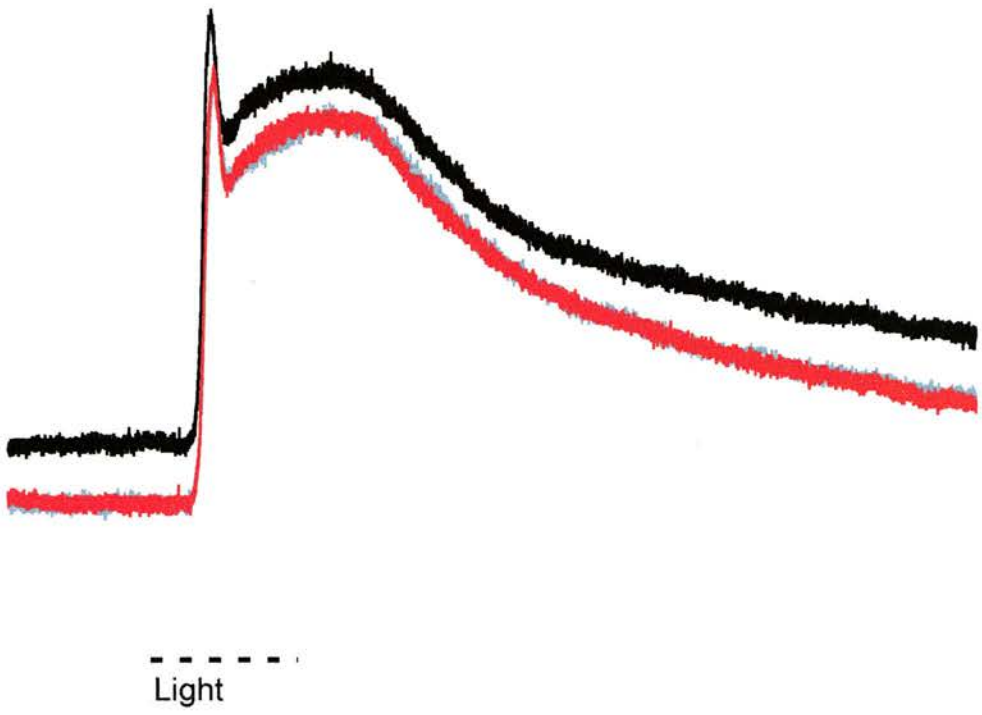

(B)

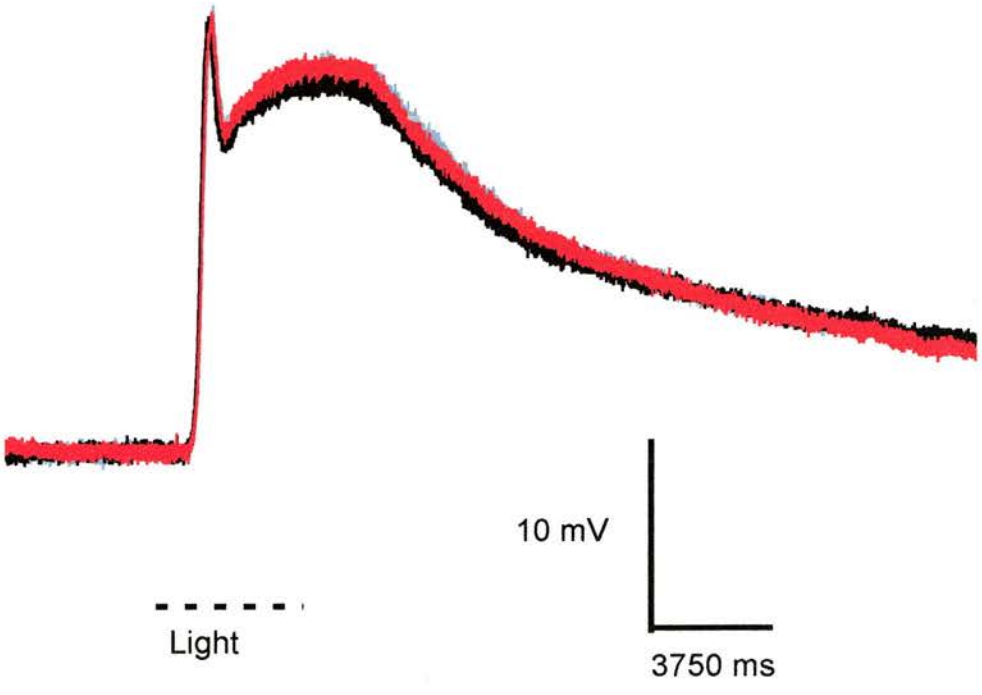

Figure V.xi

Intracellular Recording of the Caudal Photoreceptor Light Response in the Presence of Caffeine [5mM].

Panel (A) shows the activity in the connective prior to the application of caffeine.

Panel (B) shows an increase of activity in the presence of caffeine [5mM].

Panel (C) shows the level of activity in the connective when caffeine has been washed off with normal saline.

The broken line under each trace represents the light stimulus.

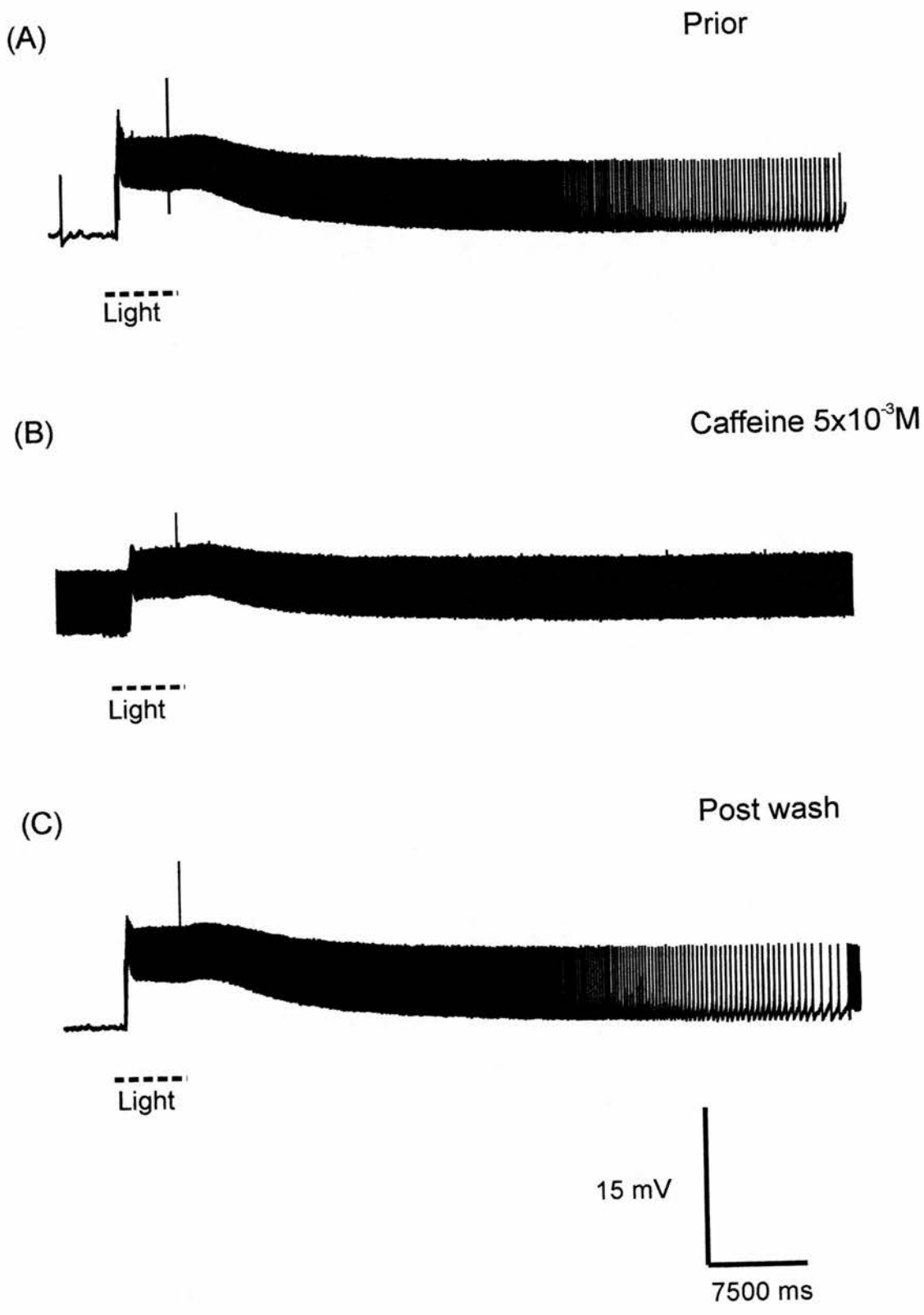
(A)
Prior
Light
(B)
Caffeine 5x10-3M
Light
(C)
Post wash
Light
15 mV
7500 ms

Figure V.xii

The Effect of Caffeine [5mM] on the Number of Action Potentials Evoked by the Photic Response

Measurements are made from light responses stimulated every 3 minutes. The arrows indicate when caffeine was applied and washed off with normal saline.

Panel (A) variation in the number of action potentials with the application of caffeine [5mM].

Panel (B) control – the number of action potentials produced under standard conditions over the same time course.

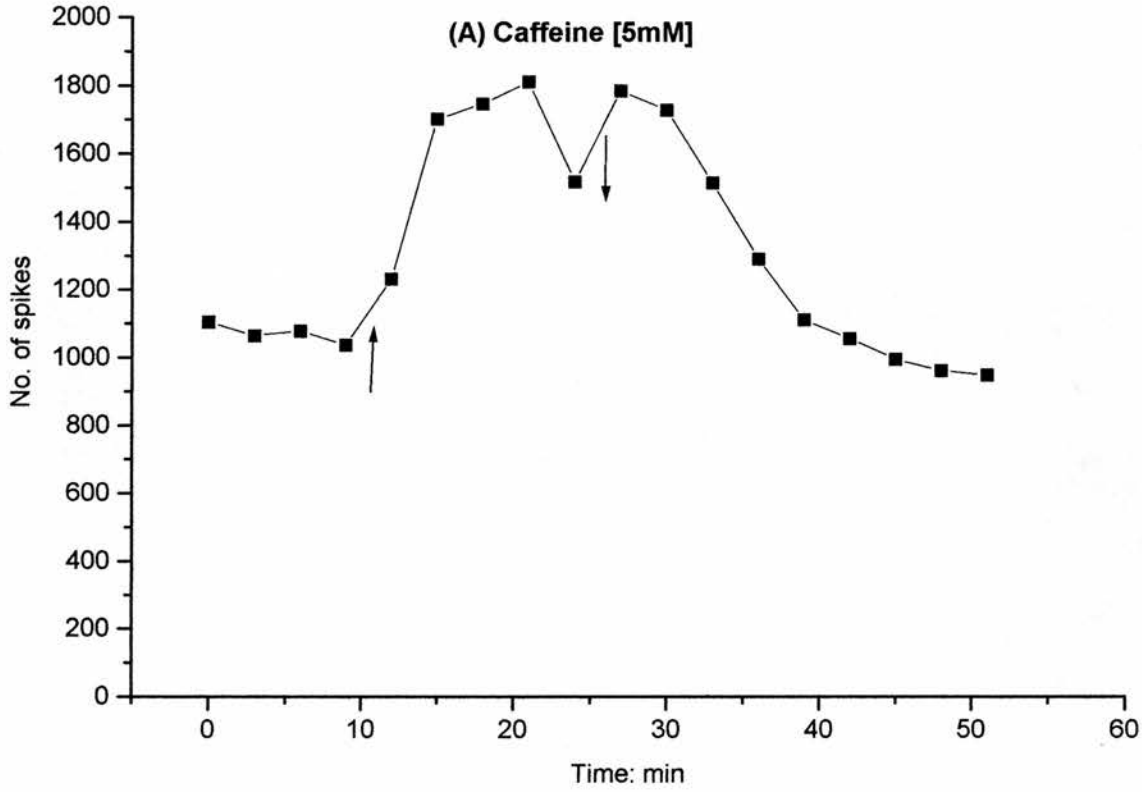
(A) Caffeine [5mM]
No. of spikes
Time: min
0
200
400
600
800
1000
1200
1400
1600
1800
2000
0
10
20
30
40
50
60

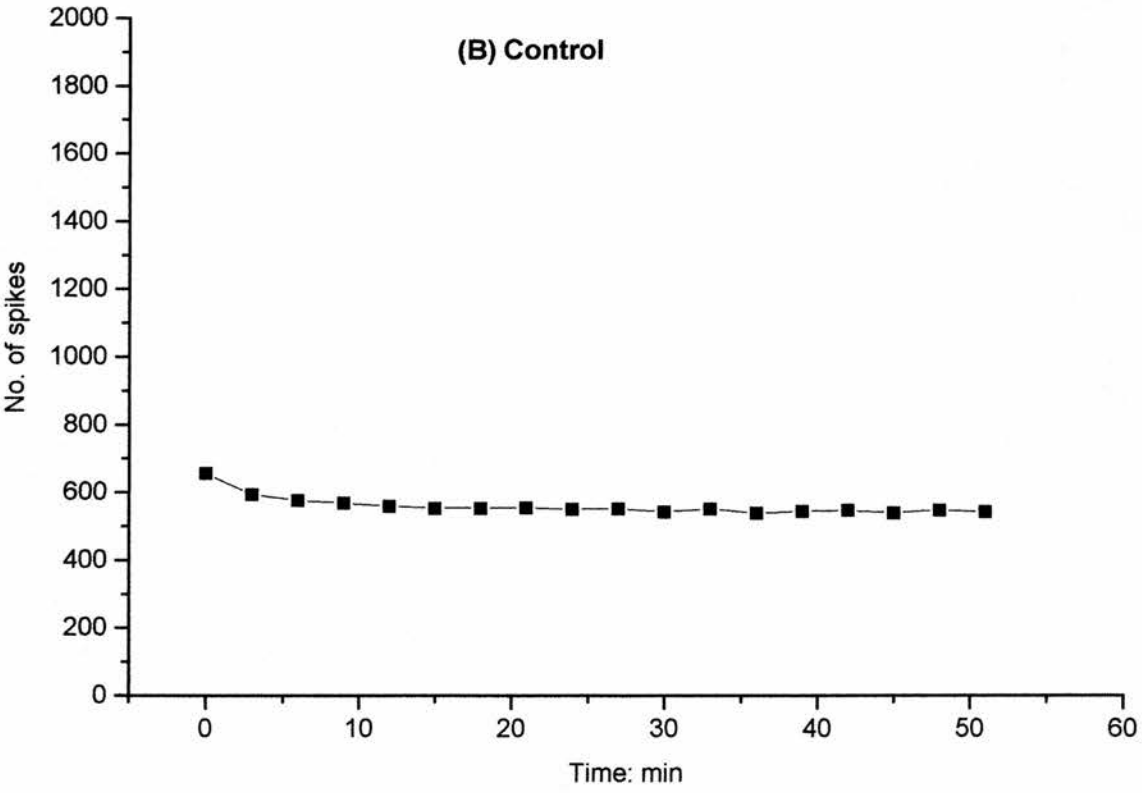
(B) Control
No. of spikes
Time: min
0
200
400
600
800
1000
1200
1400
1600
1800
2000
0
10
20
30
40
50
60

conditions panel (B). There is a 52.4% increase in the number of action potentials in the presence of caffeine which returns to normal when the preparation is washed with fresh saline.

It has been shown that there is an increase in the number of action potentials exhibited by the CPR in the presence of caffeine, however the frequency plots show that this is not a uniform increase across the time frame of the light response (Figure V.xiii). There is a large decrease in frequency at the transient peak, from 243Hz to 118Hz, whereas, the frequency during the plateau phase remains between 60 and 66Hz.

In the dark phase, the spontaneous firing frequency was raised from 0Hz to 17Hz which is approximately the same as if the CPR was in constant light. Following the light response the spike frequency returns to 17Hz with the same time course that the frequency returns to 0Hz in the standard state light response. This frequency of action potentials is maintained in the 3 minutes between light stimuli (data not shown).

There appears to be no shift in the onset of the light response following the onset of the light stimulus, with the latency remaining in the order of 500ms throughout.

In addition to the decrease in peak spike frequency there was a reduction in the size of the generator potential. The graphs in Figure V.xiv are plots of the changes in the resting potential as well as the size and area of the generator potential. There is an overall depolarization in the resting membrane potential following the application of caffeine from -72mV to -54mV, which returns to -69mV following a wash with fresh saline.

There is a drop in the size of the transient peak from 22.0mV to 13.3mV (Figure V.xiv, panel B) and less of a reduction in the size of the plateau from 18.5mV to 13mV (panel C). Both the peak and plateau phases of the response decrease in height, the peak more so than the plateau. Changes in both features appear to be time correlated with the overall depolarization of the resting membrane potential in the presence of caffeine (Figure V.xiv, panel A). The graph in Figure V.xiv, panel (D), shows an obvious reduction in the area of the generator potential which recovers following the removal of caffeine with fresh saline.

Repeating the experiment in a TTX background shows a significant reduction in the size of

Figure V.xiii

The Effect of Caffeine [5mM] on the Frequency Distribution of Action Potentials Produced in Response to Light

Panel (A) shows the spike frequency of standard light response prior to the application of caffeine.

Panel (B) shows the spike frequency of the light response in the presence of caffeine at 5mM

Panel (C) shows the spike frequency of the light response when caffeine has been washed off with normal saline.

The broken line under each trace represents the light stimulus.

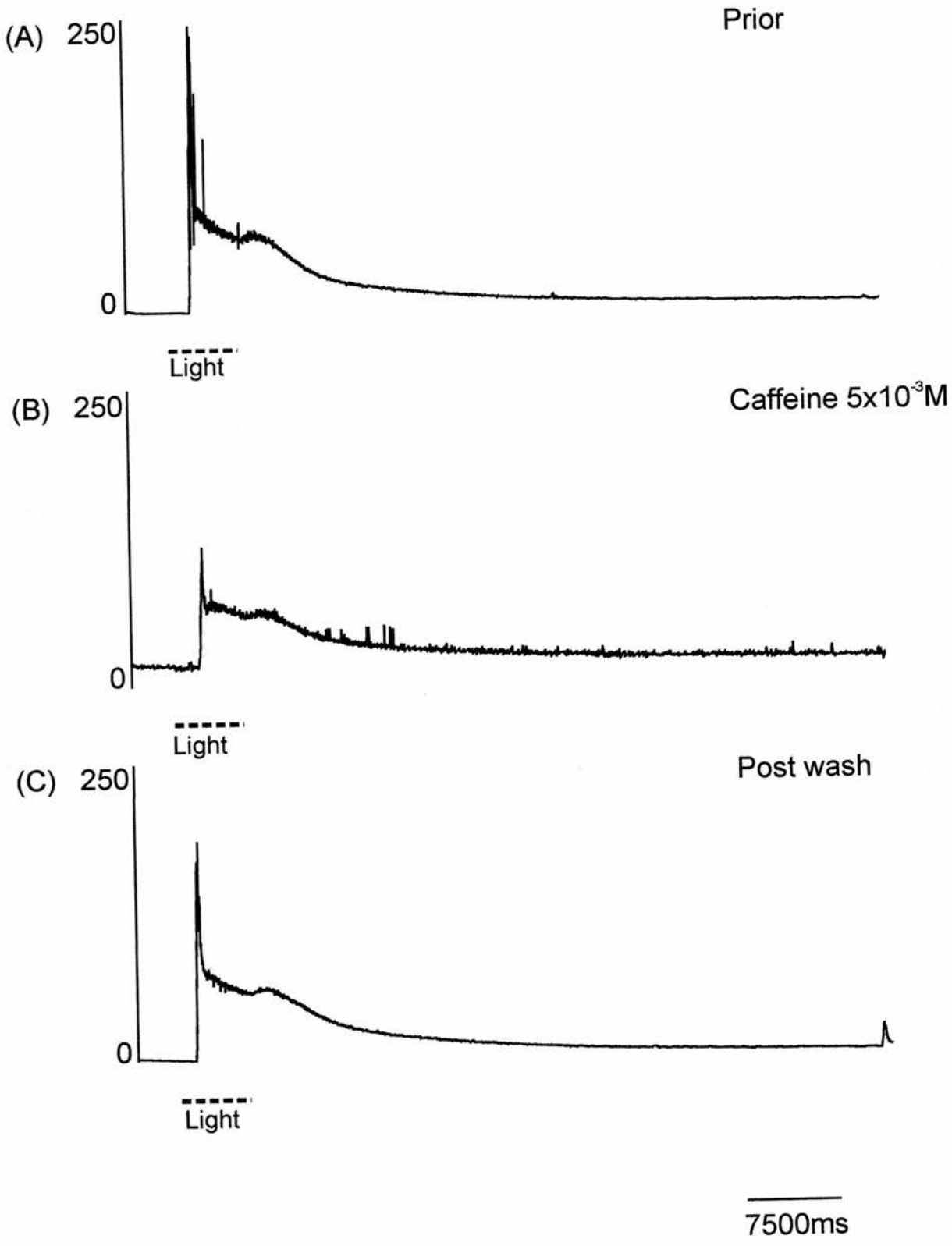
(A) 250
Prior
0
Light
(B) 250
Caffeine 5x10^{-3}M
0
Light
(C) 250
Post wash
0
Light
7500ms

Figure V.xiv

Measurements of the Generator Potential in the Presence of Caffeine [5mM]

Measurements are made from the light responses stimulated every 3 minutes. The arrows indicate when caffeine was applied and washed off with normal saline.

Panel (A) shows the resting membrane potential prior to the light stimulation.

Panel (B) shows the size of the peak calculated as the difference between the membrane potential of the cell at rest and the maximum excursion at the transient peak.

Panel (C) shows the size of the plateau calculated as the difference between the membrane potential of the cell at rest and the maximum height of the plateau phase.

Panel (D) shows the variation in the area of the generator potential following the application of caffeine [5mM].

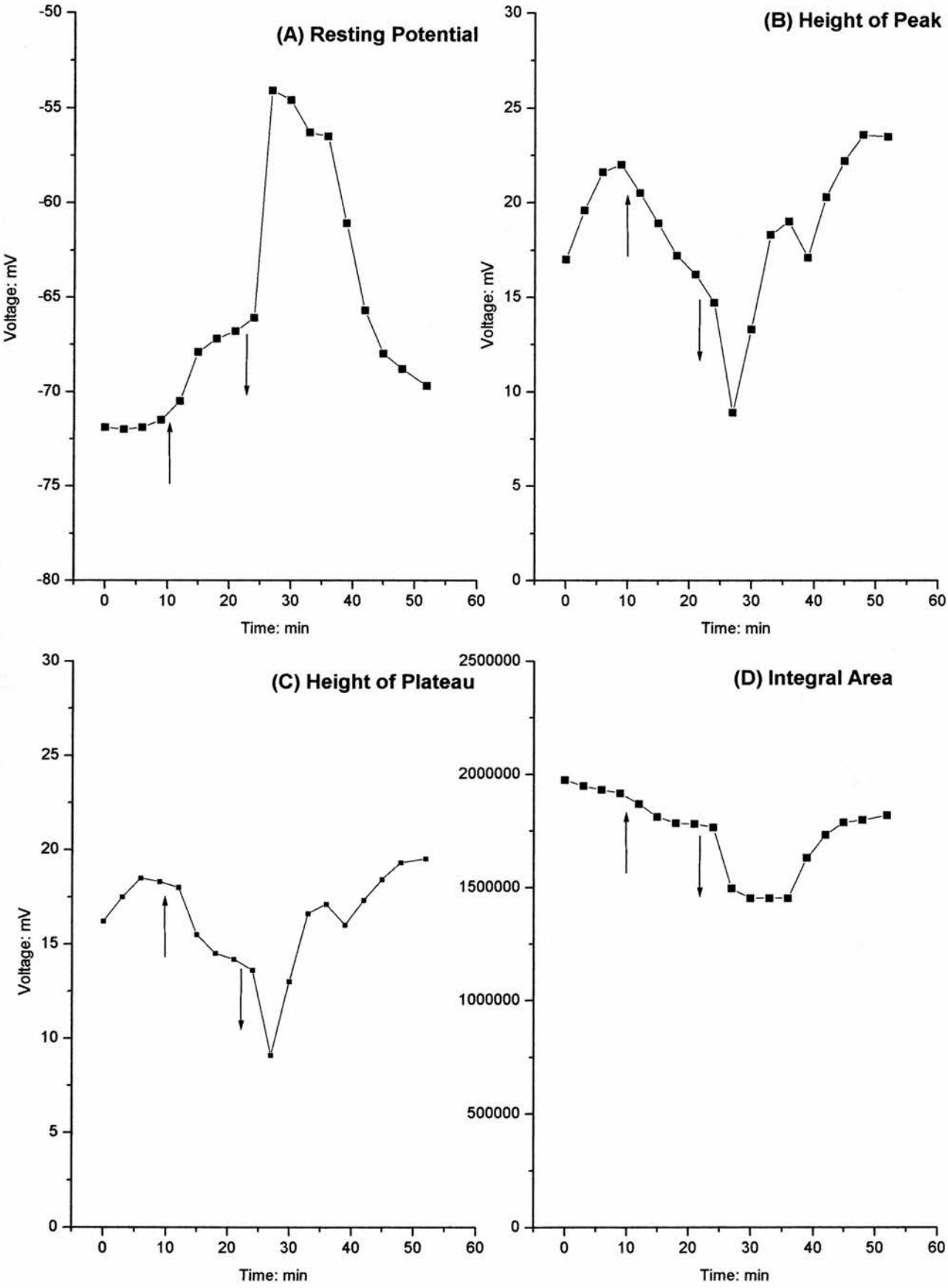
(A) Resting Potential
Voltage: mV
-50
-55
-60
-65
-70
-75
-80
0
10
20
30
40
50
60
Time: min
(B) Height of Peak
Voltage: mV
30
25
20
15
10
5
0
0
10
20
30
40
50
60
Time: min
(C) Height of Plateau
Voltage: mV
30
25
20
15
10
5
0
0
10
20
30
40
50
60
Time: min
(D) Integral Area
2500000
2000000
1500000
1000000
500000
0
0
10
20
30
40
50
60
Time: min

the generator potential. In the overlay (Figure V.xv) the base-lines have been aligned so that the size of the generator potential can be easily compared. This figure shows a significant decrease in both the initial peak and the plateau, which recovered following a wash with fresh saline mixed with TTX.

5.4 Discussion

Understanding of the biochemical pathways underlying the photic response is dependent upon identifying the various steps involved using known agonist and antagonists.

5.4.1 Staurosporine

In this series of experiments staurosporine had no discernable effect on the photic response of the CPR suggesting that there is no phosphorylation step involved in the transduction pathway. If there were such a step inhibition with an exogenous reagent, such as staurosporine, would reduce the size of the generator potential produced within the normal protocol used here.

The negative results obtained cannot, however, be considered to be absolute proof that there is no kinase involved in the transduction pathway because there are possible experimental reasons why staurosporine had no significant effect. Firstly, the concentration applied to the bath saline may be insufficient to evoke a measurable response. An initial concentration of 10μM was used as it has been shown to produce physiologically significant changes in other invertebrate systems (Butt, 1998). However, an increase in staurospaurine concentration to 100μM also failed to produce any effect. Secondly, the staurosporine may not penetrate far enough into the tissue to reach the CPR. To minimize this possibility, not only was the dorsal section of the sheath around the ganglion was removed (which was routine to allow microelectrode penetration, but in this series of experiments the terminal roots and the posterior section of the terminal ganglion were also removed. Finally, staurospaurine may have species-specific properties that render it ineffective in crayfish. However, changes in the overall activity of the connective following the application of staurosporine in the absence of TTX suggest that staurosporine does indeed have an effect on at least some systems in the crayfish nervous system. Therefore, either the transduction pathway of the CPR has no kinase step, or, despite our best efforts staurosporine may not diffuse sufficiently into the ganglion to reach the dendritic branches of the cell.

Figure V.xv

Intracellular Recording of the Caudal Photoreceptor Generator Potential in the Presence of TTX and Caffeine [5mM]

Overlay of the generator potential in the three states: prior to application (black trace), with caffeine (red trace), and following a wash with normal saline (grey trace).

Panel (A) the overlay of the generator potentials without any sort of alignment.

Panel (B) the base-lines have been aligned to give an indication of the relative height in the three states.

(A)

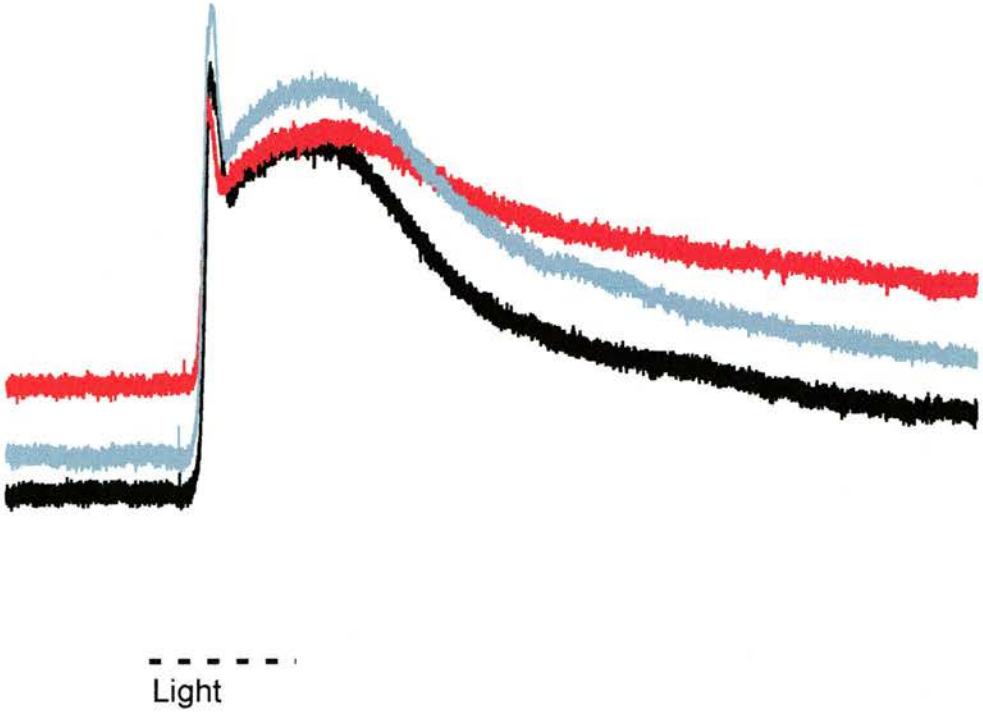

(B)

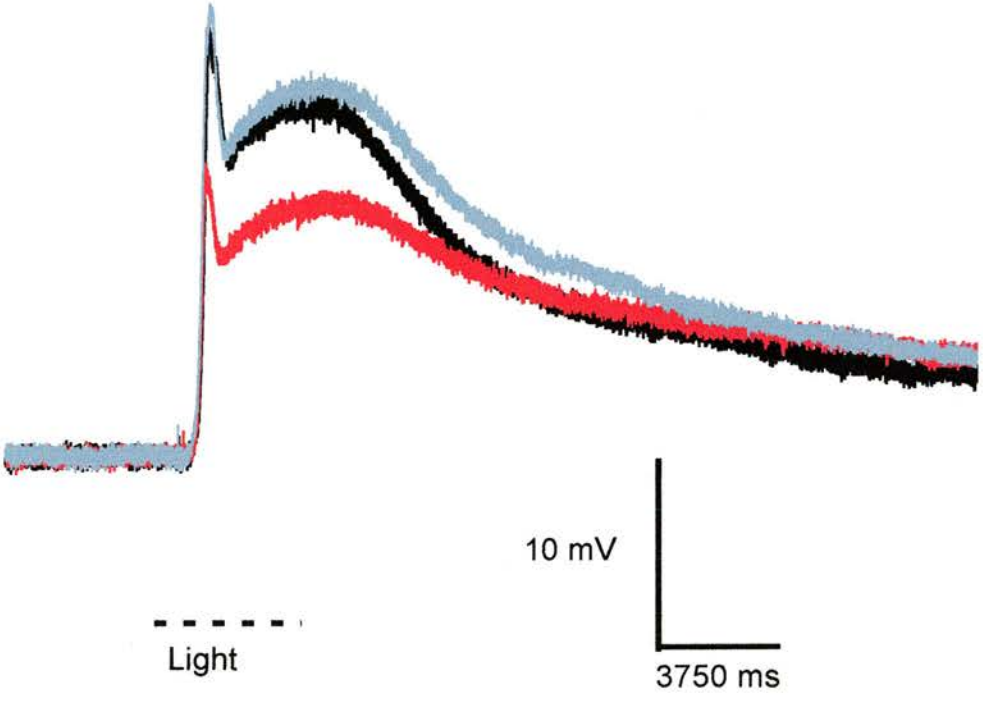

5.4.2 Lithium

The evidence provided by Kruszewska (1991) and Kruszewska and Larimer (1993) from IP_3 injections into the CPR, strongly suggests that the transduction pathway of the CPR contains an IP_3 step. Exogenous application of lithium in this study reduced the photic response, and this inhibitory effect is consistent with the previous finding.

5.4.3 Caffeine

There is a notable increase in action potential activity of the CPR in the presence of caffeine, in line with a more general increase in activity in the inter-ganglionic connective which is to be expected as caffeine is a central nervous system stimulant. This increase in activity in the CPR is, however, not uniform across the photic response; in fact at the initial peak there is a decrease in spike frequency whilst the response itself is elongated and after a few minutes in caffeine the photoreceptor is firing at a steady 17Hz in the dark phase between light stimulations.

This drop in spike frequency at the initial peak is also matched by a decrease in the height of the generator potential at this point. There are two possible explanations for this. Firstly, caffeine could be causing a general increase in the release of calcium from intracellular stores of the CPR, so that when it comes time for the cell to respond to a light stimulus there isn't as much calcium available therefore the photic response/generator potential is diminished. Or, secondly, the general increase in action potential activity with the CPR firing in the dark phase means that the cell physically cannot produce the same intense frequency of action potentials. Refractory periods between the firing of one action potential and the onset of the next could be having a limiting effect on the spike frequency achievable. Repeating the experiment in the presence of TTX has shown that caffeine does affect the generator potential by reducing its size, presumably by using up much of the calcium from the cells intracellular stores.

CHAPTER 6: IONIC DEPENDENCE OF THE LIGHT RESPONSE OF THE CRAYFISH CAUDAL PHOTORECEPTOR

6.1 Introduction

In 1984, Wilkens proposed that the light response of the caudal photoreceptor was dependent upon sodium ions. He based this conclusion on experiments using a reduced sodium concentration saline and extracellular recording in which he found that endogenous spikes and the photic discharge were blocked in the presence of low sodium saline. Subsequently, Kruszewska (1991) and Kruszewska and Larimer (1993) reported that "preliminary experiments indicate that in a sodium-free saline bath, light sensitivity is lost within a few minutes". However, they do not state whether these experiments actually involved the generator potential, or the CPR spikes. In the latter case, as with the lithium experiments, the loss of response might be due to the loss of sodium-dependent spikes rather than loss of photosensitivity *per se*.

In the experiments undertaken here evidence was sought to confirm the sodium dependence of the generator potential itself. Recordings were made intracellularly and in the presence of TTX [7.5×10^{-10} M], which blocks all known voltage-gated sodium channels in crayfish neurons, in order to ascertain the effect of reducing sodium ion concentration on the underlying generator potential. Conductance measurements were made using the injection of constant current pulses into the CPR, in order to determine whether there was an opening or closing of ion channels in response to photic stimulation. The voltage deflection produced by the injected current pulses would become smaller if there was an increase in conductance.
The simplest explanation of the generator potential would be a light dependent increase in sodium conductance resulting in a Nerstian influx of Na^+ into the CPR. Such an influx of positive ions would account for the depolarization of the neuron, and would fit the evidence that removal of sodium from the saline disrupts the photic response.

Alternative Nerstian mechanisms that could account for the generator potential are an increase in Ca^{2+} conductance or a decrease in K^+ conductance. Krueswka (1991) showed that the intracellular injection of Ca^{2+} into the CPR produced a response that mimicked the generator potential, but that the generator potential remains undisrupted when calcium is removed from the extracellular milieu. In this study cadmium is added to the saline so that changes in the

photic response of the CPR when calcium channels are blocked may be detected. This also has the effect of isolating the CPR from communication from other neurons.

The other positive ion involved in the maintenance of a neurons membrane potential is potassium (K^+). It is not unheard of for potassium to be the ion responsible for the photic response in extra-ocular photoreception. In the Opisthobranch Mollusc *Onchidium veruculatum* (Gotow, 1989) K^+ efflux from the photoreceptor in accordance with diffusion gradient and driving force establishing a dark current which, when the cell is illuminated, ceases, and the membrane potential hyperpolarizes.

The obvious difference between this mollusc and the crayfish CPR is that the CPR depolarizes rather than hyperpolarizes, thus suggesting that there isn't a dark current although blocking of the potassium channels in the CPR can be used to prove this.

Kennedy (1958b) and Kruszewska (1991) both reported that the photic response remains unaffected by the reduction/removal of K^+ from the extracellular milieu.

6.2 Additional Materials and Methods

6.2.1 Reduced Sodium Saline

Following penetration of the CPR and establishing a repetitive light stimulus regime, *i.e.*, light stimuli of a 4 seconds duration given every 3 minutes as described for the "standard protocol" in Chapter 2, tetrodotoxin (TTX) [7.5×10^{-10} M] was added to the bath to block the voltage-gated sodium channels and eliminate the action potentials of the light response.

The normal bath saline was replaced by drip application from a reservoir containing low sodium saline and TTX [7.5×10^{-10} M] in order to minimise any mechanical disruption that might lead to the loss of the penetration. It was found empirically that at least 15 minutes are required for the bath saline to be replaced by the liquid from the reservoir using this method. The light stimulus regime was maintained during the drip application and during the subsequent wash with normal saline/TTX. Attempts were also made to reduce any possible electro-chemical effect that changes in the ionic make-up of the saline would have by using an agar bridge earth wire. Control experiments indicated that changing the ionic composition of the saline had negligible direct effects upon the electrode potential.

The light stimulus regime may be summarized as:

Stimuli 1-5	in normal saline and TTX
Stimuli 6-10	in a low sodium saline and TTX wash
Stimuli 11-15	in low sodium saline and TTX
Stimuli 16-20	in a normal saline and TTX wash
Stimuli 21-25	in normal saline and TTX

6.2.2 Conductance Measurements

In order to examine conductance changes over the course of the light response of the CPR the voltage-gated sodium channels responsible for spike production were blocked by tetrodotoxin (TTX) [7.5×10^{-10} M]. Current pulses of a constant size, usually 0.5 nanoamps and 150ms in duration, were injected into the CPR at 1-1.5 second intervals via the intracellular electrode under bridge balanced conditions. An average of 42 current pulses were injected over the course of a 60 second light response, as illustrated in Figure VI.i, panel (A). Negative pulses were generally used and the bridge balanced by adjusting the voltage deflection so as to resemble that depicted in Figure VI.i, panel (B). However, in order to eliminate any possibility that a negative voltage deflection was interfering with TTX-insensitive voltage dependent ion channels within the membrane, the experiments were repeated using positive current pulses.

Two methods have been used in this study to investigate changes in conductance to the current injected into the CPR. The first focuses on the size of the deflection by comparing it with the membrane potential both before and after injection of the current pulse. The second examines the time constant of the cell's recovery curve from the current pulse. Both of these methods are capable of identifying any change in conductance that may be occurring in response to light stimuli.

6.2.2.1 Method one – Voltage deflection

Figure V.i, panel (B) shows a single voltage deflection overlaid with four cursors from which measurements of the membrane potential were made. The first cursor is set before the start of the pulse, and gives a baseline voltage. The second cursor is used to mark the beginning of the current pulse and line up the other cursors. The third cursor is placed during the pulse, but after the falling phase of the initial deflection, and the fourth after the current pulse, when the

Figure VI.i

Conductance Measurements During the Generator Potential

This figure illustrates a typical light response and indicates the points at which conductance measurements were made.

Panel (A) shows the overall response of the cell to a 4 second light stimulus, indicated by a broken line, during a 60 second period of applied current pulses (total of 42 pulses). Each pulse is indicated by a current transient artefact (vertical lines). A scale bar illustrating the membrane potential, in mV, and time, in ms, is superimposed.

Panel (B) illustrates a single current pulse deflection from the same tissue preparation used for the above figure. The cursors (represented by vertical lines drawn over the recording trace) illustrate the points at which measurements were made for subsequent quantitative analysis.

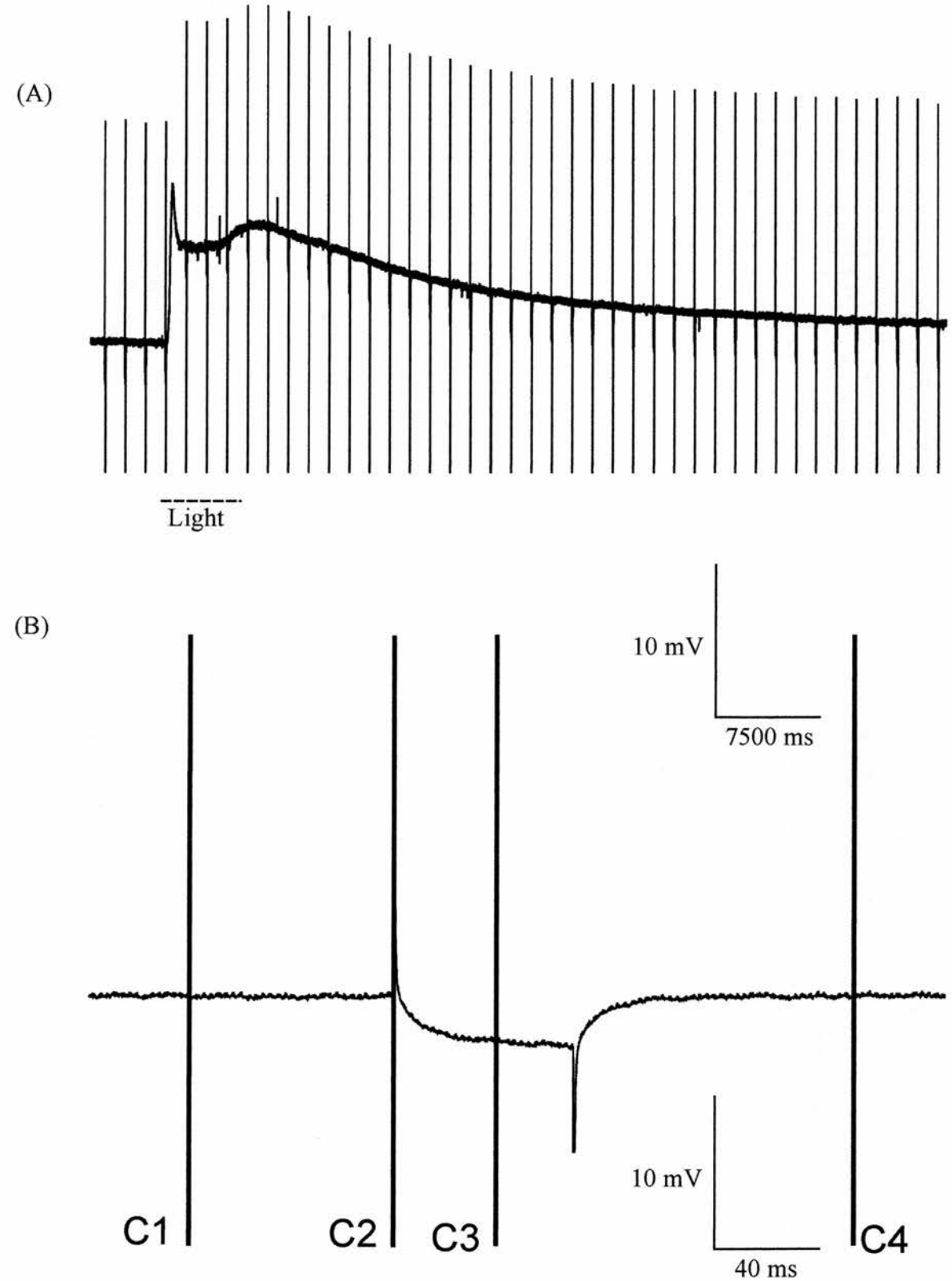
(A)
Light
(B)
10 mV
7500 ms
10 mV
40 ms
C1
C2
C3
C4

cell has recovered from the current injection.

The voltage deflection elicited by each current pulse was calculated using the equation:

$$V_{diff} = V_1 - \frac{T_3 - T_1}{T_4 - T_1}(V_4 - V_1) - V_3$$

Where:

- V_{diff} is the voltage difference between the membrane potential and the deflection produced by the injected current pulse.
- V_1 is the voltage at cursor 1.
- T_1 is the time cursor 1 has been placed at.
- V_3 is the voltage at cursor 3.
- T_3 is the time cursor 3 has been placed at.
- V_4 is the voltage at cursor 4.
- T_4 is the time cursor 4 has been placed at.

This equation was used because sometimes the current pulse was injected at a time when the generator potential was causing a relatively large change in base-line voltage. The equation estimates the current-induced voltage deflection by linear interpolation.

It is not essential to measure accurately the current passed through the electrode, only that it should remain constant throughout the light response/60 second recording period. Similarly, the absolute value of the voltage deflection in the CPR is less important than the relative changes that may be recorded in any given deflection during the light response. It is known that, given a constant current, a change in the size of the voltage deflection produced by that current pulse can be explained in terms of a change in resistance because:

$$Voltage\,(V) = Current\,(I) \times Resistance\,(R)$$

Which can be re-written as:

$$Voltage\,(V) = \frac{Current(I)}{Conductance(g)}$$

Therefore, because current is kept constant we can state that conductance is inversely proportional to resistance:

Conductance (g) = 1 / Resistance (R)

Resistance is the measure of the amount of ions moving across the cell membrane at any given moment. Therefore, if there is an increase in the amount of ion channels that are open in the lipid bi-layer of the membrane there will be a decrease in resistance of that neuron because more ions will be free to move across the membrane and there will be less 'resistance' to this movement. Therefore, for a constant current, if the voltage deflection of the neuron to the current pulses increases in size, this would be represent an increase in resistance explained by a closing of ion channels in the membrane. Conversely, if the voltage deflection were to decrease in size, there would be a proportional decrease in resistance explained by the opening of ion channels.

6.2.2.2 Method two – Measuring the time constant of current pulses during the light response of the Caudal Photoreceptor

The second method used to determine changes in conductance during the light response of the CPR was to measure the time constant of the relaxation curve. In time constant analysis the curvature of the relaxation curve of the membrane potential following the termination of the current pulse is used in the calculations rather than taking measurements during the actual current pulse. This improves the accuracy of conductance detection because it does not rely on accurate balancing of the bridge. When current pulses are injected into a cell, the recovery curve from that current pulse can be broken down into two (or more) components whose shape are determined by the time constants of two elements: the electrode, through which the current was passed, and the cell membrane. The value of the time constant is important because it is inversely proportional to conductance, and may be represented as:

Time Constant of a cell membrane = membrane resistance * membrane capacitance

The membrane capacitance is considered invariant. Therefore, changes in the time constant of the relaxation curve that occur during the light response give a measure of changes in the membrane conductance over this period.

Measuring the time constant of the cell membrane is complicated, as it is difficult to determine how much of the relaxation curve is a portrayal of the time constant of the

electrode, and how much is that of the cell itself. The initial part of the relaxation curve contains the time constant of both the electrode and the cell membrane. This segment is steep due to the fast time constant of the electrode, meaning that the relaxation curve of the electrode is very fast, and will be over much quicker than that of the cell membrane. In order to separate the two elements one must judge the point at which the curves for these two time constants meet, and measure only that of the membrane. The exact value for the electrode time constant may, however, change with time, as the resistance of the electrode can change over the course of an experiment, especially if there is any blockage of the tip by adsorption of protein molecules.

Time constant measurements are made by matching the relaxation curve to a model, but the model requires that certain assumptions be made about the anatomy of cell geometry.

6.2.2.2.1 Exponential Curve

When a current pulse is injected into a spherical cell the relaxation curve would resemble that of the exponential waveform defined by:

$$Vt = V\ final + (V\ start - V\ final) * exp\ (-t/TC)$$

Where:

Vt	is the voltage of any given point along the curve
Vfinal	is the voltage at the final point on the curve
Vstart	is the voltage at the beginning of the curve
Exp	is the exponential function
t	is the time in milliseconds at which a given voltage is measured
TC	is the time constant of the curve.

The time constant of an exponential curve is the time, in milliseconds, when the curve has reached 63% of its final value.

A large time constant will give a shallow, slow relaxation curve, and conversely, a small time constant with give a steep, fast relaxation curve.

6.2.2.2.2 Error function curve

When a current pulse is injected into an infinitely-long non-spiking axon from which a recording is made in the middle the relaxation curve would resemble that of an error function waveform as defined by:

$$Vt = V\ start + (V\ final - V\ start) * erf(\text{square root}(t/TC))$$

Where:

Vt	is the voltage of any given point along the curve
Vfinal	is the voltage at the final point on the curve
Vstart	is the voltage at the beginning of the curve
erf	is the error function
t	is the time in milliseconds at which a given voltage is measured
TC	is the time constant of the curve.

The time constant of an error function curve is the time, in milliseconds, when the curve has reached 84% of its final value.

The same parameters apply; a large time constant will give a shallow, slow relaxation curve, and conversely, a small time constant with give a steep, fast relaxation curve.

The exponential and error function curves give different values for the time constant of the cell membrane for any given pulse. This is something to be aware of but considering that a relative change in time constant is sought rather than the absolute value, it is still possible to extract the necessary information about conductance changes during the light response of the CPR.

6.2.3.1 The effects of tetraethyl ammonium on the light response of the caudal photoreceptor

Tetraethyl ammonium (TEA) blocks the voltage-sensitive K^+ channels involved in the action potential (Armstrong and Binstock, 1965; Armstrong and Hille, 1972; Pepose and Lisman 1978). In this set of experiments evidence for involvement of a potassium channel in the generator potential of the CPR is sought, therefore TEA was applied in a TTX background. Removal of the action potential of the light response meant that the effect on the generator potential itself would be more easily apparent.

The light stimulus regime may be summarized as:

Stimuli 1-4	in saline and TTX
Stimuli 5-8	with TEA [25mM] or [50mM]
Stimuli 9-12	saline and TTX wash
Stimuli 13-16	in saline and TTX

There are two salts of TEA: TEA bromide and TEA chloride. Both have the same effect of blocking voltage-gated K^+ ion channels, and so both may be used when performing this type of experiment. It is, however, known that the two types may have differing side-effects on the system to which they are applied and to this end both were used in this series of experiments but no evidence of any different effect(s) due to the chloride or bromide radical was found.

6.2.3.2 TEA controls

The lateral giant fibre was penetrated in the 3rd abdominal ganglion. The ganglion was de-sheathed and the left-hand LG penetrated. Extracellular electrodes were placed at slightly different positions (*i.e.*, between the last thoracic ganglion and the 1st abdominal ganglion; and, between 4th and 5th abdominal ganglia). The anterior electrode was used to stimulate the nerve cord whilst the posterior electrode recorded the neurons recruited by this stimulation. The LG is, due to its size and conduction velocity, the first and the largest unit to be recruited making it easily identifiable. Random non-CPR neurons were penetrated in the terminal ganglion close to where the CPR was penetrated.

6.3 Results

6.3.1 Low Sodium

Reducing the sodium concentration in physiological saline from 200mM to 40mM (*i.e.*, to 20% of the standard concentration) has a dramatic effect on the light response of the CPR in the presence of TTX. As illustrated in Figure VI.ii the size of the generator potential is reduced considerably in intracellular recordings. In normal saline (panel A) the resting potential of the CPR in this particular preparation had a mean value of -76.7 mV (s.d=0.60), increasing to -83.8 mV (s.d=3.20) when the sodium concentration was decreased. A trace profile has been consistently recorded in experiments using different tissue preparations, whereby the plateau reduces initially from a mean of 20 mV (s.d=1.22) to 12.1 mV (s.d=3.14) (n=5), while the peak remains approximately the same size 21.2 mV (s.d=2.75) compared with 22.9 mV (s.d=5.88) (panel B). In every instance there was a slower reduction in the

Figure VI.ii

The Effect of Low Sodium (20%) Saline on the Light Response of the Caudal Photoreceptor in a Background of TTX

Panel (A) shows the generator potential of the standard light response in normal saline.

Panel (B) shows the generator potential in low sodium (20%) saline. 3 minutes after exposure to low sodium saline and TTX.

Panel (C) shows the generator potential 9 minutes after exposure of the preparation to low sodium saline and TTX.

Panel (D) the generator potential after the preparation was washed with fresh normal saline TTX.

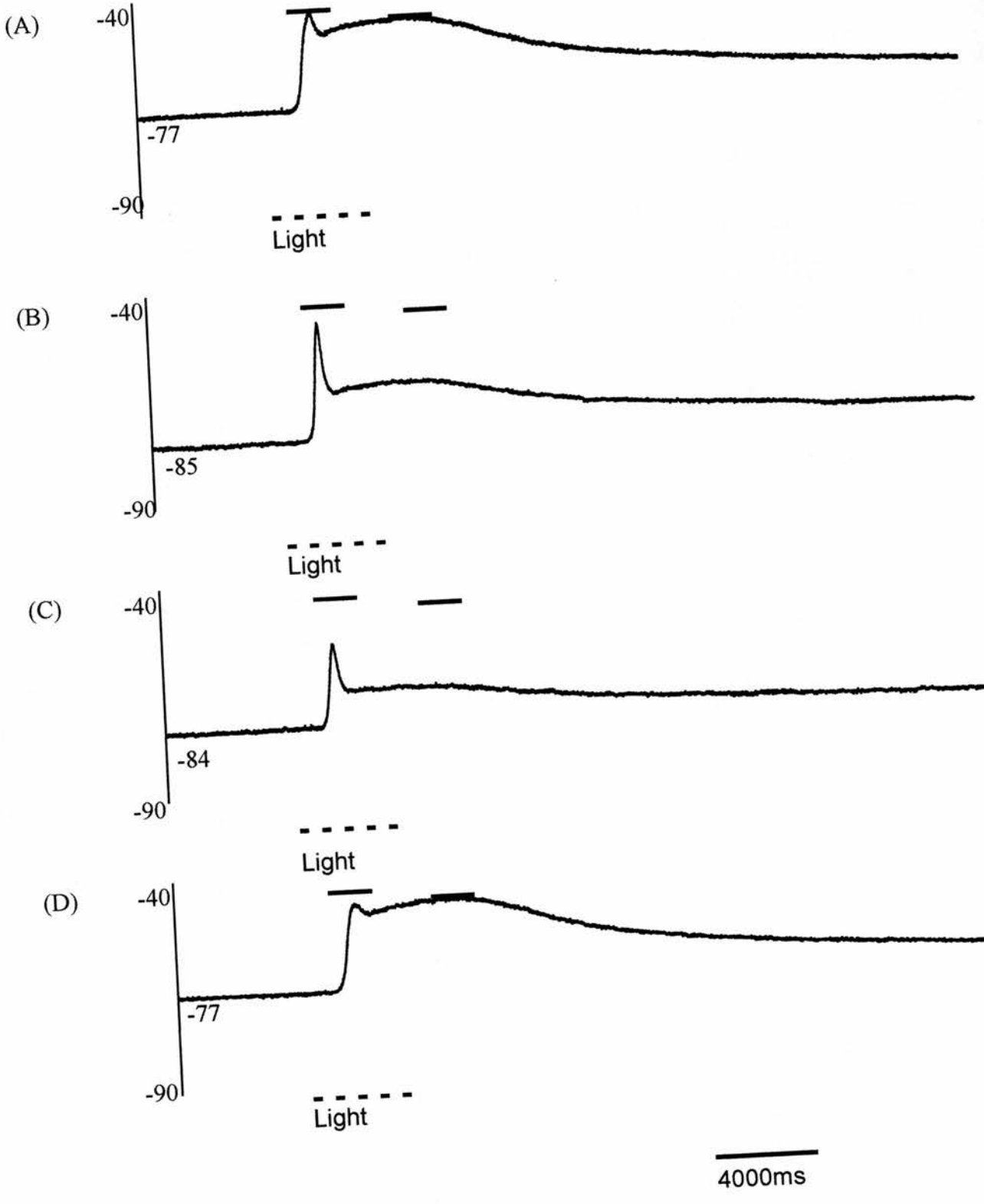
(A)
-40
-77
-90
Light
(B)
-40
-85
-90
Light
(C)
-40
-84
-90
Light
(D)
-40
-77
-90
Light
4000ms

magnitude of the peak than in the plateau, but both were eventually reduced in the presence of low sodium saline (panel C). Returning the sodium ion concentration to normal by replacing the bath medium with fresh normal saline containing TTX resulted in a restoration of the size of both the peak and plateau of the generator potential (panel D) although the plateau phase had a tendency to recover faster than the transient peak.

In order to quantify these changes in the size of the generator potential, the membrane potential at the transient peak and at the highest point of the plateau were subtracted from the values of the resting membrane potential and plotted out in panels (B) and (C) of Figure VI.iii. Panel (B) shows that following the start of perfusion with reduced sodium saline there is an initial increase in the size of peak from 22-23mV to a maximum of 28.2mV, and then a drop in size to a minimum of 14.4mV before a partial recovery in normal saline and TTX to 20.9mV. The plateau, however, shows no increase in size, rather there is a decrease from a maximum height of 21.2mV to a minimum of 9.2mV in the presence of reduced sodium saline and a complete recovery when the sodium level of bath saline was returned to normal (panel C). Given the difference rates of reduction shown by the two components of the generator potential it was necessary to calculate and plot the area from integral measurements under the curve of the graph. This has been plotted in panel (D) of Figure VI.iii and shows a reduction in the overall area of the generator potential during a time course matching the reduction in the size of the plateau. In addition to a reduction in the size of the generator potential, there is also an overall hyperpolarization in the resting membrane potential (Figure VI.iii, panel A), with a mean of 5.73 (s.d= 5.84, n=5).

6.3.2 Conductance Measurements

Three methods of analysis were employed in extracting conductance data from the voltage deflections. None of which produced any consistent results from the n=52 recordings from n=9 preparations. Figure VI.iv shows all three methods applied to one recording from the same preparation. The voltage deflections produced by the current pulses decrease (panel A) in a manner that mirrors the generator potential (panel B), suggesting that there is a conductance increase over the course of the photic response. The other two methods, exponential curve (panel C) and error function curve (Panel D),show decreases in time constant which, although not as smooth as the curve in panel A, also mirror the generator

Figure VI.iii

Measurements of Features of the Generator Potential in the Presence of Low Sodium (20%) Saline

Panel (A) shows the effect of low sodium saline on the resting membrane potential measured during the first 5 seconds of the recording prior to the onset of light stimulus.

Panel (B) shows the effect of low sodium saline on the size of the transient peak calculated by subtracting the membrane potential at the peak from the resting membrane potential.

Panel (C) shows the effect of low sodium saline on the size of the plateau calculated by subtracting the membrane potential at the highest point of the plateau from the resting membrane potential.

Panel (D) shows the effect of low sodium saline on the area of the generator potential calculated from integral measurements under the curve of the graph.

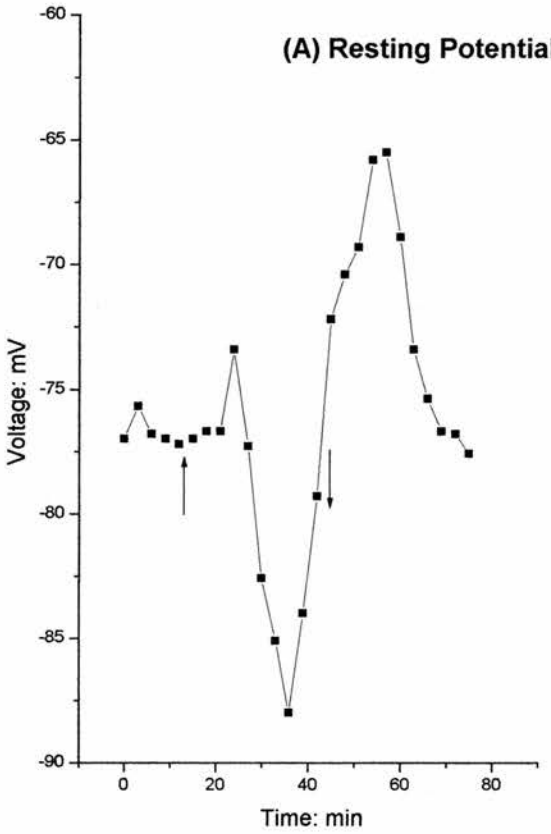
(A) Resting Potential
Voltage: mV
Time: min
-60
-65
-70
-75
-80
-85
-90
0
20
40
60
80

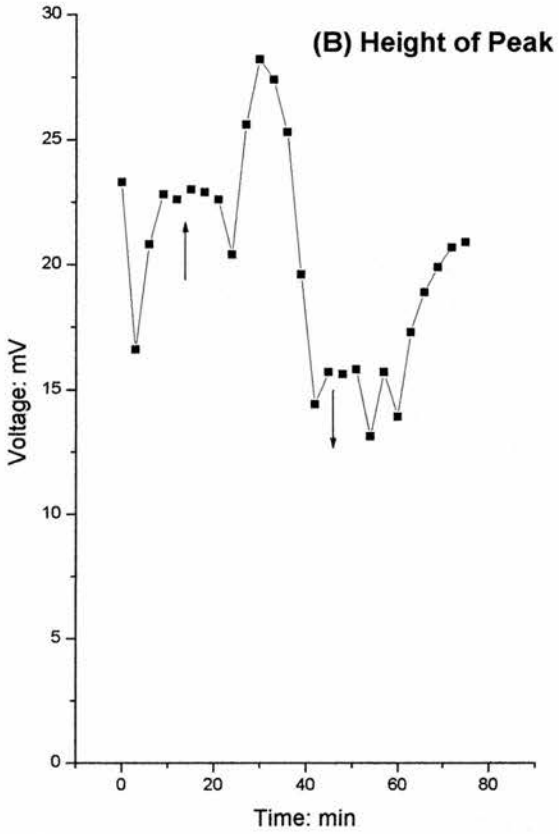
(B) Height of Peak
Voltage: mV
Time: min
30
25
20
15
10
5
0
0
20
40
60
80

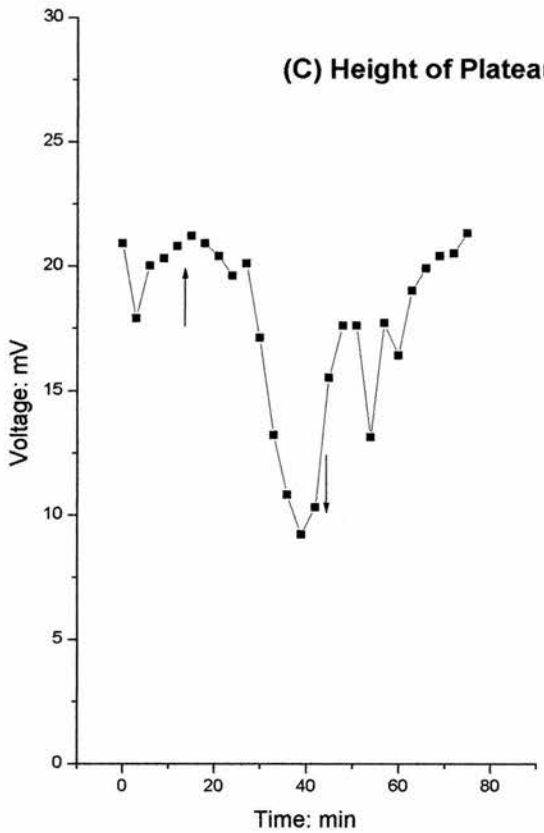
(C) Height of Plateau
Voltage: mV
Time: min
30
25
20
15
10
5
0
0
20
40
60
80

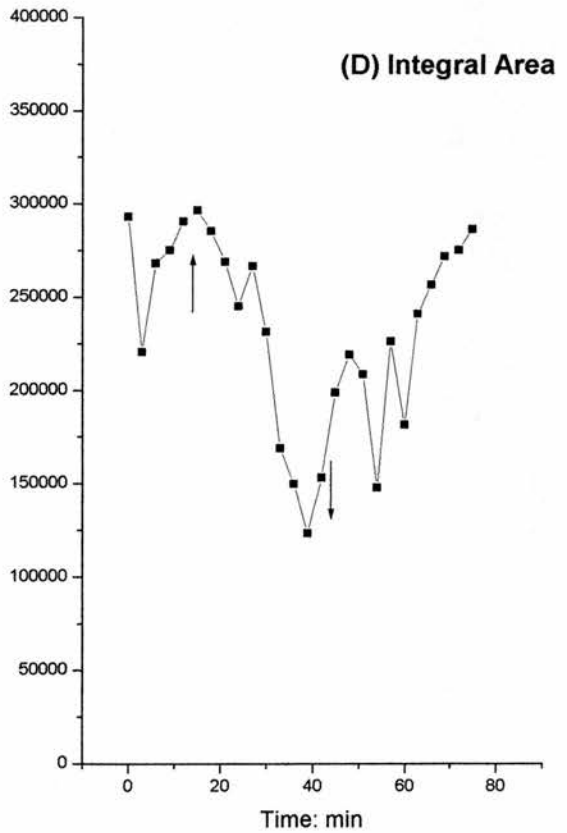
(D) Integral Area
Time: min
400000
350000
300000
250000
200000
150000
100000
50000
0
0
20
40
60
80

Figure VI.iv

Comparing the Different Ways of Analysing

Panel (A) shows changes in the voltage deflection of the CPR in response to 0.5 nanoamp current pulses (total of 42) applied over the course of 60 seconds.

Panel (B) is a diagrammatic representation of the generator potential constructed from measurements made prior the current pulse (*i.e.*, cursor 1 shown in Figure V.i). These measurements were made approximately 1.5 seconds apart, therefore specific membrane potential information was lost, hence there is no transient peak shown on this graph.

Panel (C) shows changes in membrane conductance over the course of the light response using exponential curve calculations.

Panel (D) shows changes in membrane conductance over the course of the light response using error function curve calculations.

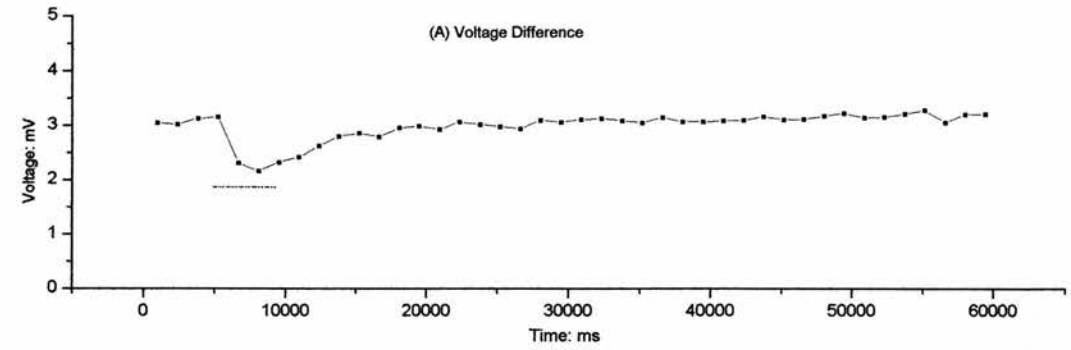
(A) Voltage Difference
Voltage: mV
5
4
3
2
1
0
0
10000
20000
30000
40000
50000
60000
Time: ms

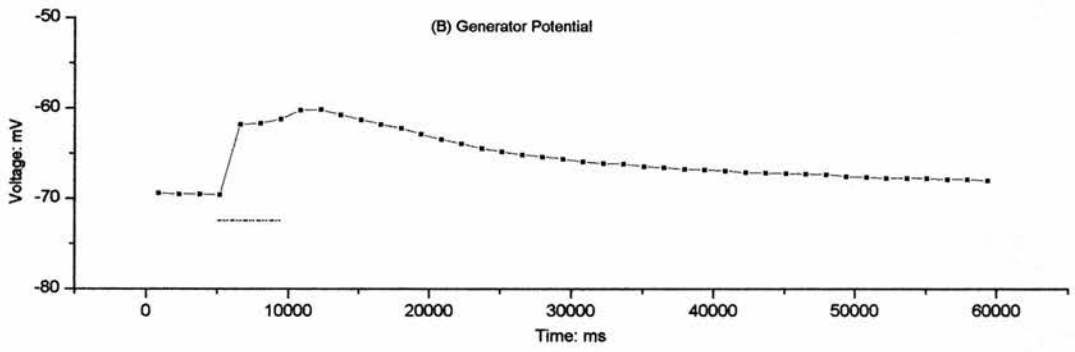
(B) Generator Potential
Voltage: mV
-50
-60
-70
-80
0
10000
20000
30000
40000
50000
60000
Time: ms

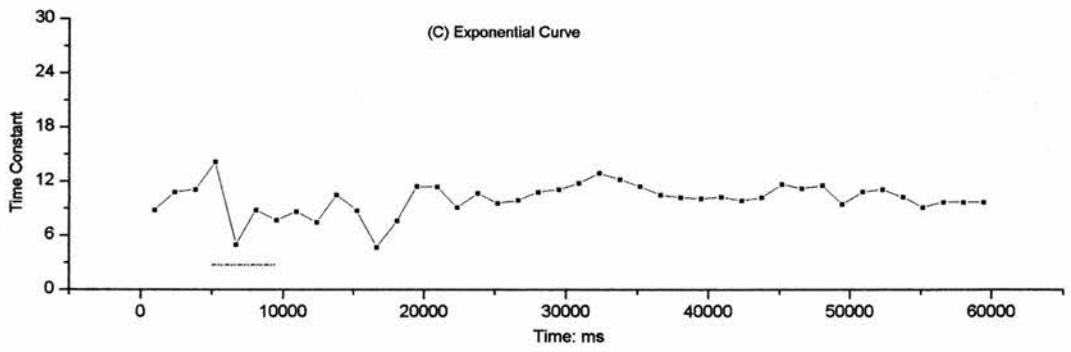
(C) Exponential Curve
Time Constant
30
24
18
12
6
0
0
10000
20000
30000
40000
50000
60000
Time: ms

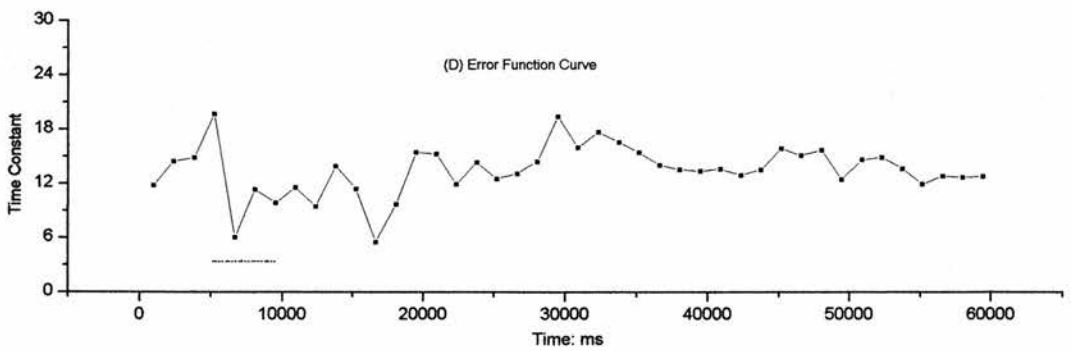
(D) Error Function Curve
Time Constant
30
24
18
12
6
0
0
10000
20000
30000
40000
50000
60000
Time: ms

Figure VI.v

The Size of Voltage Deflection Due to Current Pulses Over the Course of a Light Response

Panel (A) shows changes in the voltage deflection of the CPR in response to 0.5 nanoamp current pulses (total of 42) applied over the course of 60 seconds. The voltage change (vertical axis) is represented in mV and time (horizontal axis) in ms.

Panel (B) is a diagrammatic representation of the generator potential constructed from measurements made prior the current pulse (*i.e.*, cursor 1 shown in Figure V.i). These measurements were made approximately 1.5 s apart, therefore specific membrane potential information was lost, hence there is no transient peak shown on this graph.

The data points on both graphs represent a single pulse and are temporally correlated between these two graphs.

Light is indicated in both graphs by a broken line.

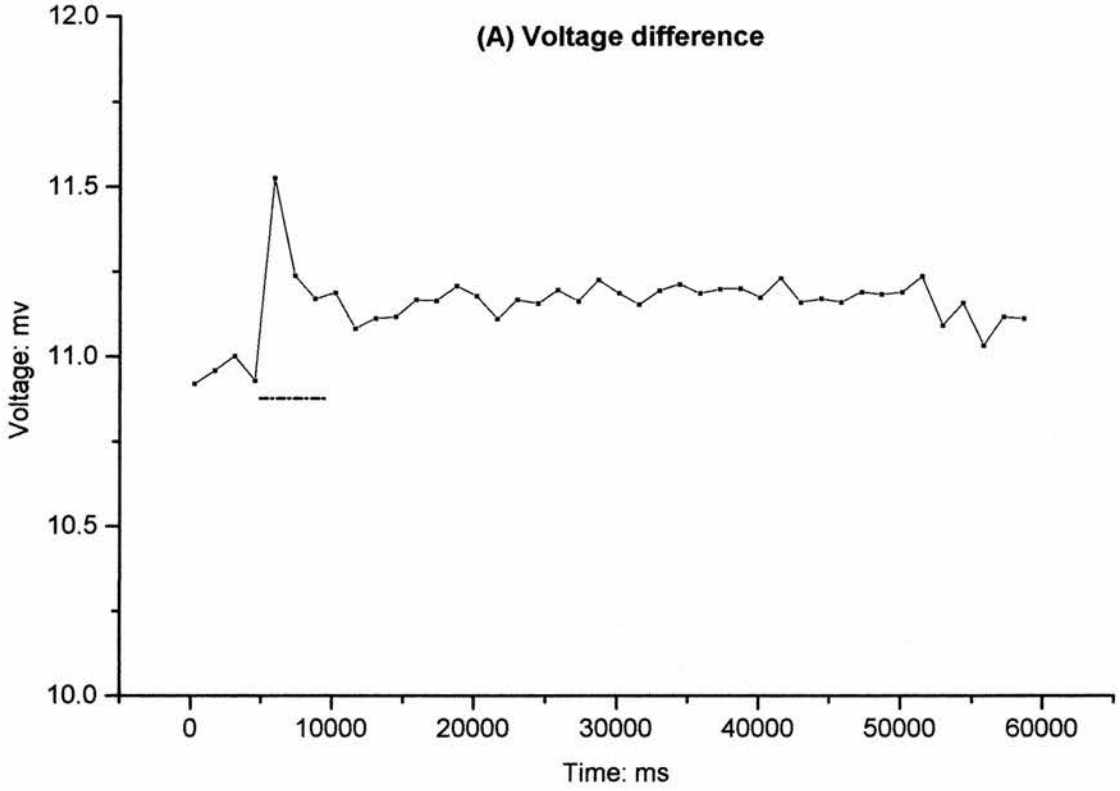
(A) Voltage difference
12.0
11.5
11.0
10.5
10.0
Voltage: mv
0
10000
20000
30000
40000
50000
60000
Time: ms

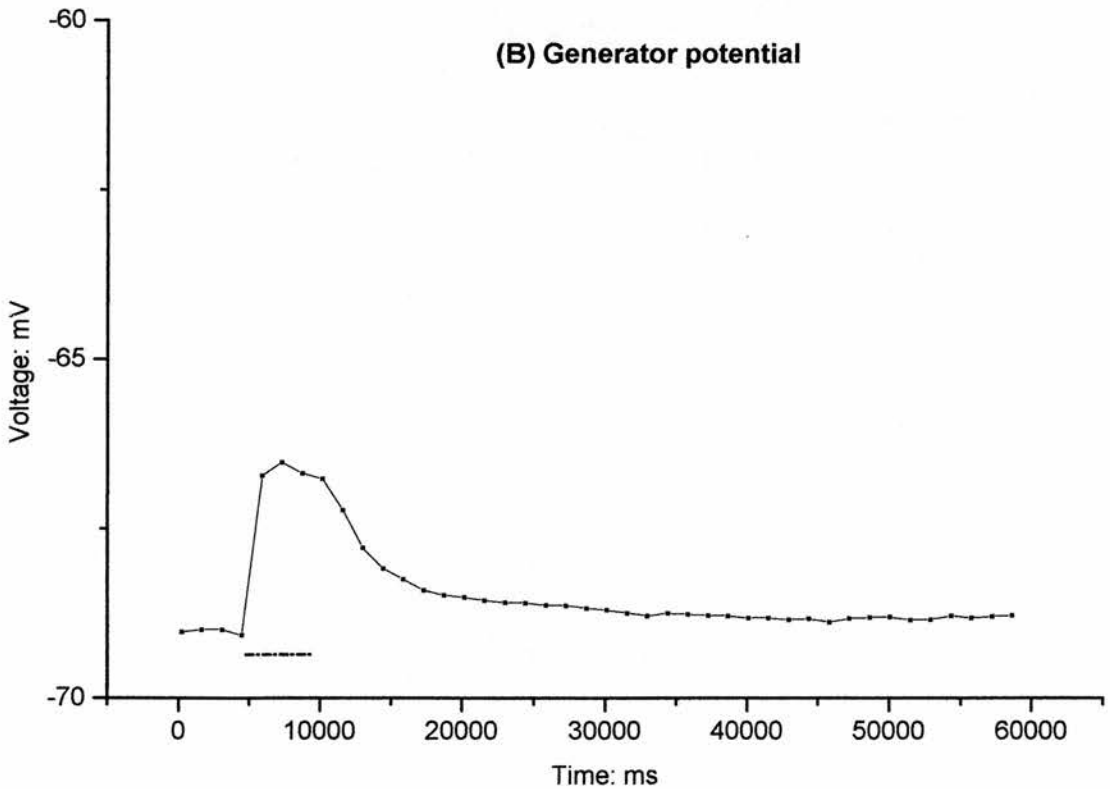
(B) Generator potential
-60
-65
-70
Voltage: mV
0
10000
20000
30000
40000
50000
60000
Time: ms

potential and provide evidence for a conductance increase. Unfortunately, this pattern has not been consistently reproducible throughout this series of experiments. In 14 recordings, voltage deflections over the course of the photic response have increased suggesting a conductance decrease an example of which is illustrated in Figure VI.v. 16 recordings showed a decrease in voltage deflections and thus a conductance increase while 22 recordings showed no consistent trend in either direction (data not shown). When recording current induced voltage deflections over the course of the photic response only four or five of these deflections actually occur during the light stimulus, making it difficult to get an accurate picture of what is happening. It is especially misleading when one of the voltage deflections falls on the transient peak. Allowances have been made in the equation for differences in the baseline membrane before and after the voltage deflection, however making conduction measurements during constant light stimulation both when the CPR was penetrated and with the electrode in the bath as a control (data not shown) showed no consistent difference.

6.3.3 TEA

6.3.3.1 Effect of TEA on the light response of the Caudal Photoreceptor

Blocking potassium channels with TEA [25mM] in a TTX background had a profound effect on the shape of the generator potential of the CPR in response to a 4 second light stimulus (see Figure VI.ix). The most obvious effect being that the smooth line of the generator potential (shown in panel A) is disturbed in the presence of TEA. In panel (B) the generator potential is broken up by numerous little 'jagged' negative deflections measuring 1 to 2mV which are detectable even in the dark phase between light stimulations. The generator potential shown in panel (B) also contains two larger negative deflections, the first following on directly from the transient peak. This deflection has been noted to occur at the same time point using different preparations, although there was some variation in the magnitude of the deflection. The other large deflection measures 5 to 6mV and occurred at different points within the time frame of the light response. Occasionally more than one deflection was present within the space of 60 seconds and, furthermore, these deflections are seen when the cell is a rest between light stimuli.

In addition to the deflections that are interspersed within the generator potential, there was a relatively large depolarization in resting potential from -86mV (in panel A) to -54mV (in panel B), and an increase in the transient peak. This trend has been seen in 5 experiments.

All of these effects were removed, and a full recovery of the tissue was apparent once the preparation had been washed with normal saline/TTX (see panel C). The exact membrane potential values from one experiment were plotted (see Figure VI.x, panel A), and show the dramatic depolarization of the CPR in the presence of TEA [25mM]. Alongside the resting potential, the size of the transient peak and size of the plateau have also been plotted (see Figure V.x, panels B and C respectively). These graphs show that whilst there was a dramatic increase in the size of the transient peak but there was less change in the size of the plateau. The area under the curve of the generator potential was calculated using integral measurements, and is shown in panel (D), but this failed to reveal any significant changes in the size of the generator potential, most probably due to the presence the large drops in the membrane potential of the cell.

6.3.3.2 Control: The effect of TEA on the action potential of the lateral giant

The action potential of the lateral giant neuron (LG) is the largest action potential seen in the crayfish. The example shown in Figure VI.viii (black) was electrically stimulated. In the presence of TEA [25mM], which blocks the voltage sensitive potassium channels responsible for the falling phase of the action potential, the height of the action potential increases and thewidth of the action potential increases (red). This was reversible (data not shown).

6.3.3.3 Control: The effects of TEA on the resting potential of non-Caudal Photoreceptor neurons

The extreme (20-35mV) depolarization of the resting membrane potential seen when the CPR is exposed to TEA Figure VI.ix (panels A and B) appears to be unique to the CPR. None of the five random non-CPR neurons from the terminal ganglion that have been used as controls showed anywhere near this degree of depolarization (panels C and D). At no time were the deflections and 'jagged' seen when the CPR was exposed to TEA present in the recordings of these other of neurons.

6.4 Discussion

6.4.1 The Effect of Low Sodium Saline on the Generator Potential of the Caudal Photoreceptor

Reducing the concentration of sodium ions in the bath saline from 200mM to 40mM, had a significant effect on the size of the generator potential produced in response to a 4 second pulse of light. This, along with reports of a loss of light response in the absence of sodium by

Figure VI.vi

The Effect of TEA [25 mM] on the Light Response of the Caudal Photoreceptor Recorded Intracellularly

Panel (A) shows the standard generator potential in normal saline and TTX.

Panel (B) shows the generator potential in the presence of TEA [25mM] approximately 24 minutes after the application of TEA.

Panel (C) shows the generator potential recovery following a wash with normal saline and TTX.

The dashed line underneath the traces represents the light stimulus.

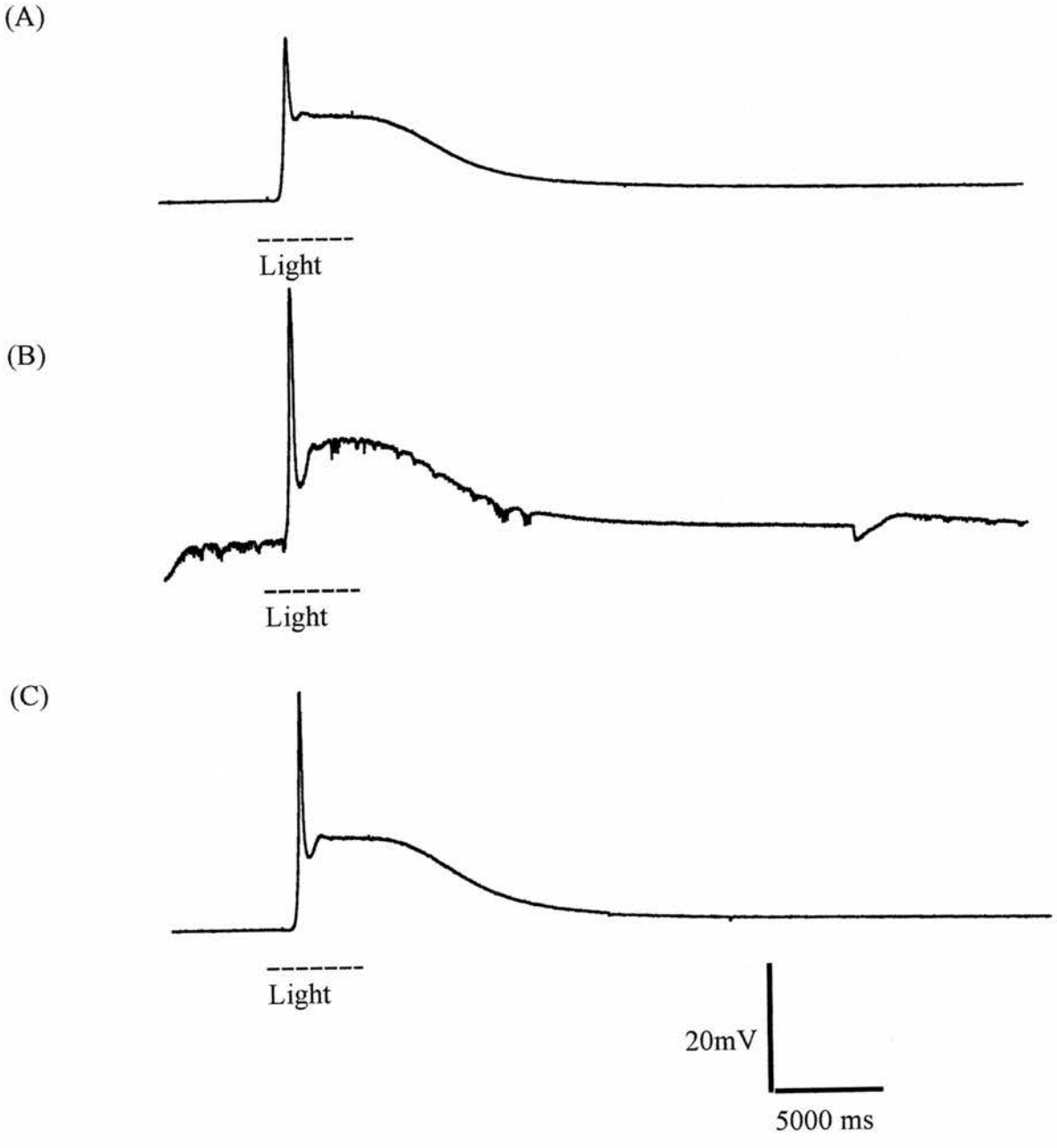
(A)
Light
(B)
Light
(C)
Light
20mV
5000 ms

Figure VI.vii

The Effect of TEA [25mM] on Features of the Generator Potential

Measurements are made from light responses stimulated every 3 minutes. The arrows indicate when TEA was applied and washed off with normal saline.

Panel (A) shows the effect of TEA [25mM] on the resting membrane potential measured in the first 5 seconds of the recording prior to the onset of light stimulus.

Panel (B) shows the effect of TEA [25mM] on the size of the transient peak calculated by subtracting the membrane potential at the peak from the resting membrane potential.

Panel (C) shows the effect of TEA [25mM] on the size of the plateau calculated by subtracting the membrane potential at the highest point of the plateau from the resting membrane potential.

Panel (D) shows the effect of TEA [25mM] on the area of the generator potential calculated from integral measurements under the curve of the graph.

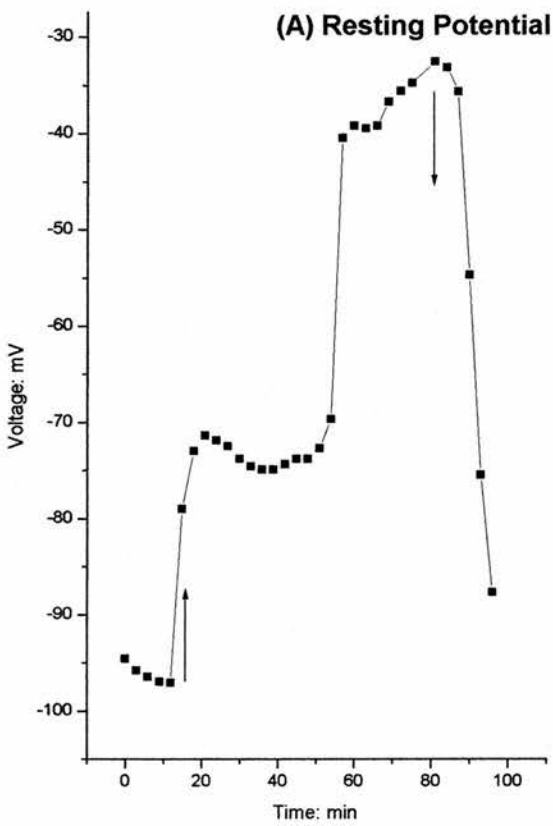
(A) Resting Potential
Voltage: mV
-30
-40
-50
-60
-70
-80
-90
-100
0
20
40
60
80
100
Time: min

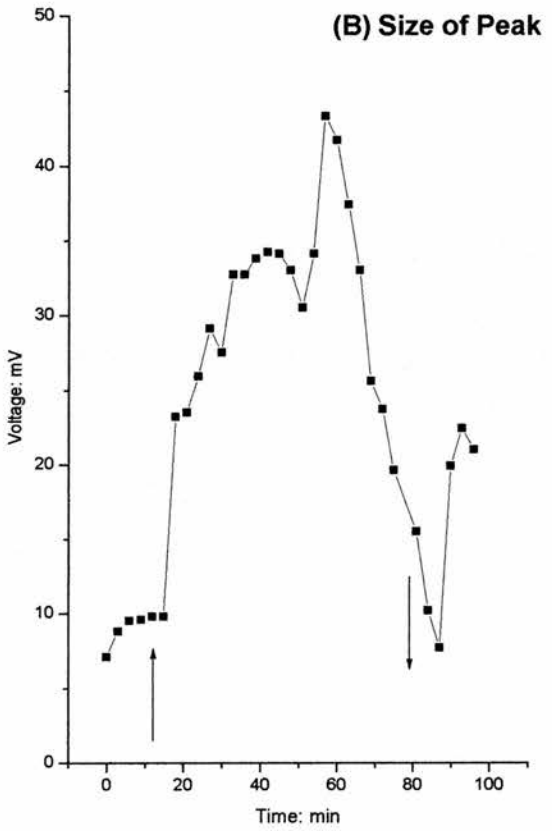
(B) Size of Peak
Voltage: mV
50
40
30
20
10
0
0
20
40
60
80
100
Time: min

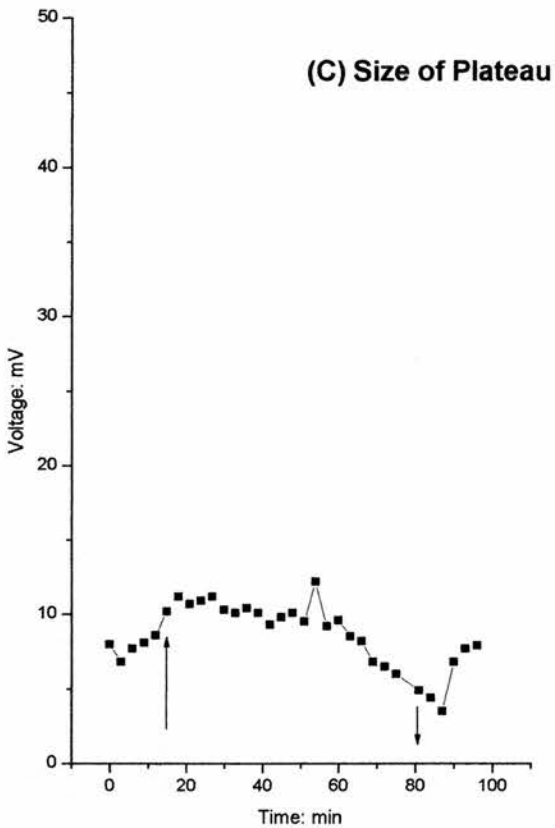
(C) Size of Plateau
Voltage: mV
50
40
30
20
10
0
0
20
40
60
80
100
Time: min

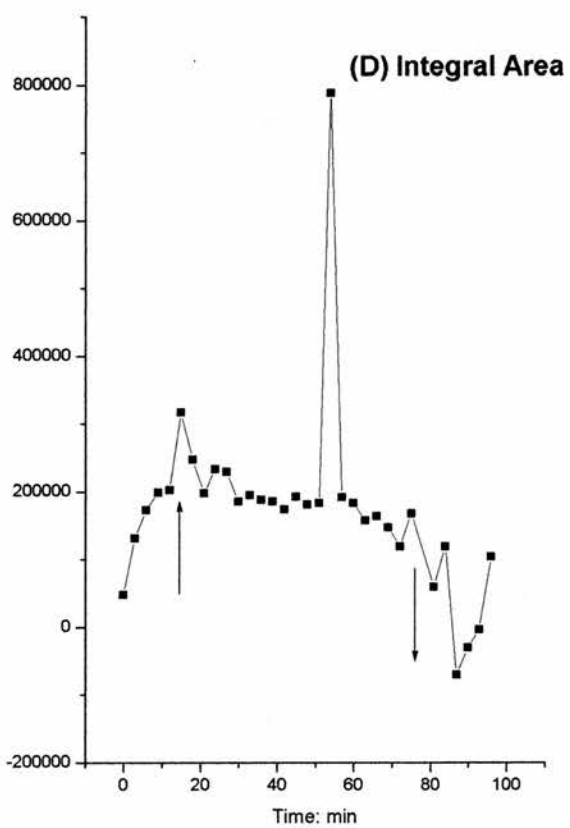
(D) Integral Area
800000
600000
400000
200000
0
-200000
0
20
40
60
80
100
Time: min

Kruszewska (1991) and Wilkens (1988), provides strong evidence that the light response of the crayfish CPR is in some way sodium dependent.

There are three ways in which sodium could be involved in the production of the generator potential of the CPR:

1. **Simple Nerst** – There could be an influx of sodium ions through light activated sodium channels in the membrane, in accordance with driving force of the Na^+ and the diffusion gradient. The increase in positive ions results in the cell having a more positive membrane potential and hence the depolarization.
2. **Indirect Nerst** – Sodium could be necessary for the opening of some other class of light activated ion channel leading to a depolarization of the membrane potential.
3. **Non-Nerstian** – There may be a sodium dependent electrogenic mechanism within the cell, which would then go on to open or close an ion channel.

Of these, the simplest explanation is that of the Simple Nerst theory, *i.e.*, that there is an influx of sodium ions in the presence of light.

One problem with this is that the peak and the plateau decline at different rates. The plateau phase reduces in amplitude before the peak does. It is hard to explain this in terms of a Simple Nerst mechanism. One possibility is that the two phases are generated in different parts of the neuron, and therefore experience the drop in Na^+ concentration at different times.

6.4.2 Evidence for a Change in Conductance During the Photic Response of the Caudal Photoreceptor

The conductance measurements made here from injecting pulses of current into the CPR failed to produce any convincing results. Some of the results indicated that there was a closing of ion channels, others that there was an opening, and others failed to show any change in conductance whatsoever. It is, therefore, impossible to draw any conclusions as to whether there is a conductance change from this set of experiments.

One explanation for the inconsistency in results could be that the recording site was not where any conduction changes were taking place. Given the position of the electrode one can be fairly certain that recordings are being made in the dendritic branching thought to be the site of photoreception rather than in the cell body or from the neurite that leads to it, both of which

Figure VI.viii

Control: The Effect of TEA [25mM] on the Size and Width of the Driven Action Potential of the Lateral Giant Fibre (LG)

The lateral giant fibre was penetrated on the left hand side of the 3rd abdominal ganglion, and the ventral nerve cord electrically stimulated between the last thoracic and 1st abdominal ganglion.

Black – the action potential of the lateral giant fibre (LG).

Red – the action potential of the LG in the presence of TEA [25mM].

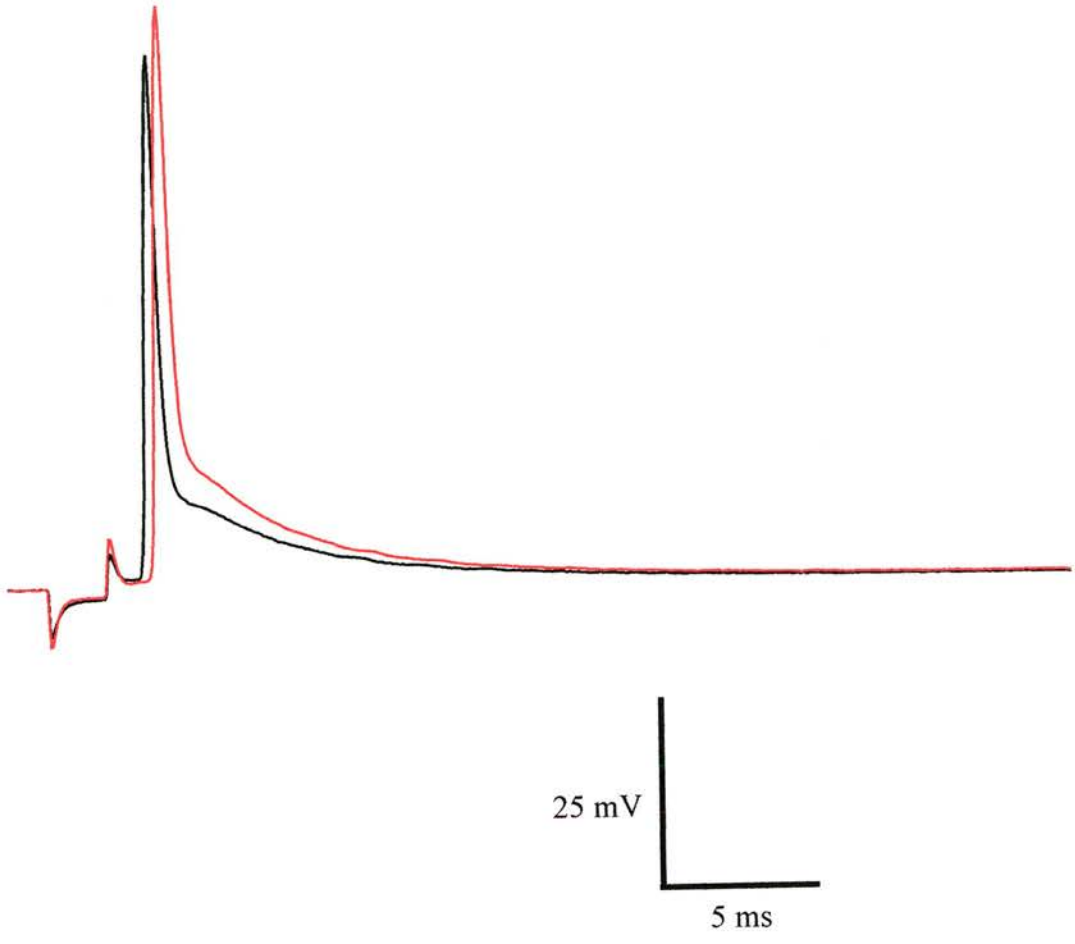
25 mV
5 ms

Figure VI.ix

Control: The Effect of TEA [25mM] on the Resting Membrane Potential of Non-CPR Neurons compared with the CPR

Panel (A) the resting membrane potential of the CPR during the application of TEA [25mM].

Panel (B) the resting membrane potential of the CPR during the application of TEA [25mM].

Panel (C) the resting membrane potential of a random non-CPR neuron in the terminal ganglion during the application of TEA [25mM].

Panel (D) the resting membrane potential of a random non-CPR neuron in the terminal ganglion during the application of TEA [25mM].

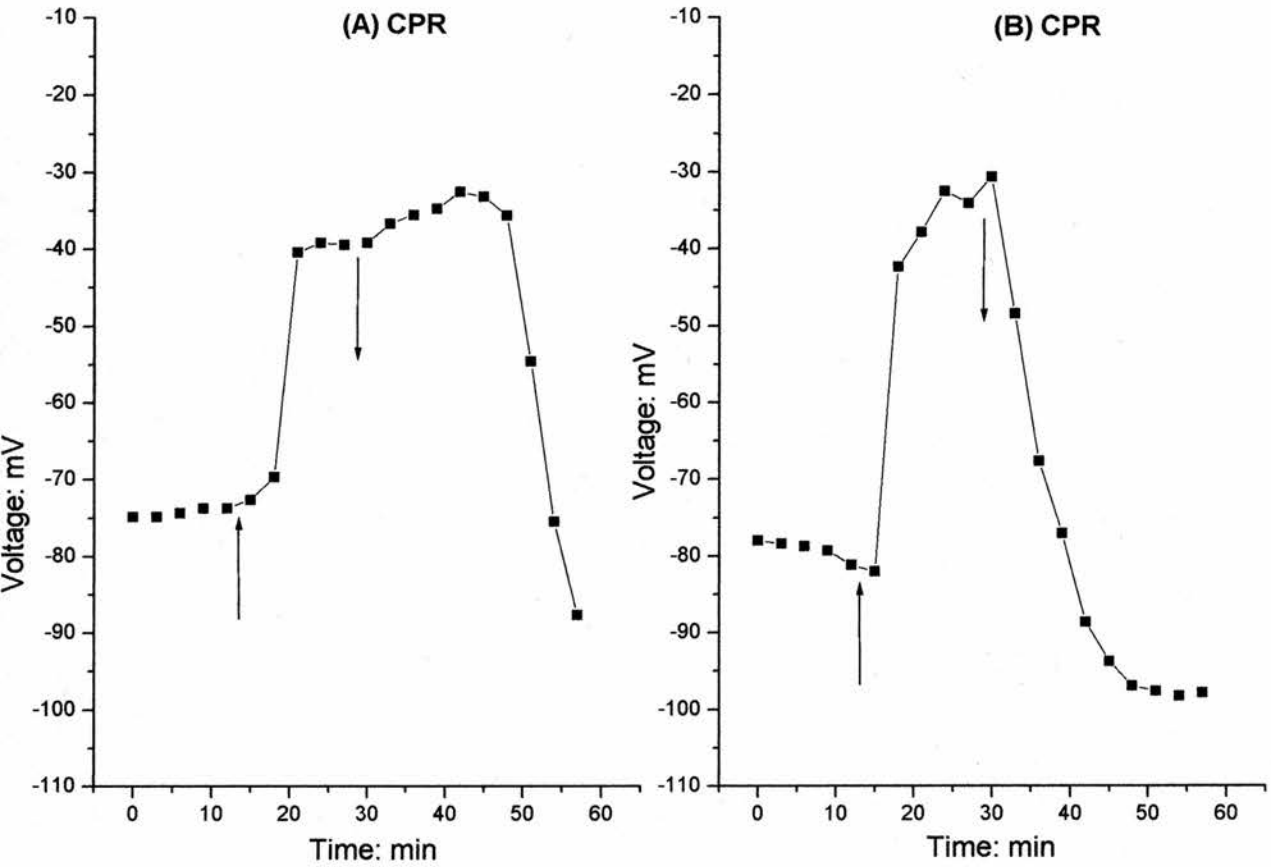
(A) CPR
Voltage: mV
Time: min
-10
-20
-30
-40
-50
-60
-70
-80
-90
-100
-110
0
10
20
30
40
50
60

(B) CPR
Voltage: mV
Time: min
-10
-20
-30
-40
-50
-60
-70
-80
-90
-100
-110
0
10
20
30
40
50
60

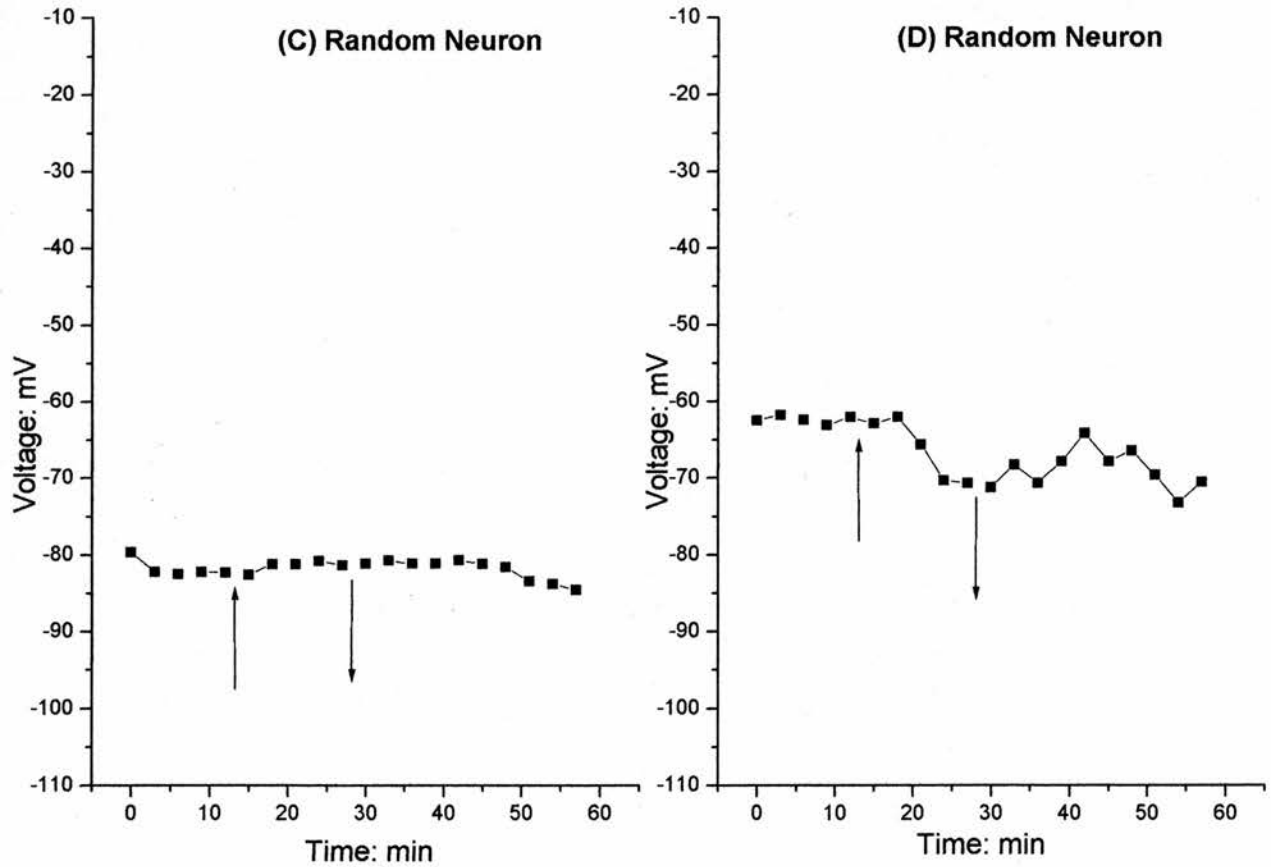
(C) Random Neuron
Voltage: mV
Time: min
-10
-20
-30
-40
-50
-60
-70
-80
-90
-100
-110
0
10
20
30
40
50
60

(D) Random Neuron
Voltage: mV
Time: min
-10
-20
-30
-40
-50
-60
-70
-80
-90
-100
-110
0
10
20
30
40
50
60

have been shown not to be the site of photoreception (Larimer, 1972). Given that it is possible to detect the generator potential from the recording site it would also seem likely that this is most likely to be the region of conductance change within the cell if such a conductance change were to be taking place. This then takes us back to looking for other reasons why the conductance results were inconsistent.

There is always the possibility that no change in membrane conductance exists and, therefore, there is nothing that could be detected. This seems unlikely given the precedent that all photoreceptive cells investigated to date have shown a change in conductance leading to either a depolarization or a hyperpolarization. And even if it were a closing of ion channels rather than an opening of sodium ion channels as proposed by this model, one would still expect to be able to detect a change in conductance. What if the proposed conductance change is just too small to be seen in relation to the membrane potential of the neuron? Using the Goldman equation the conductance change required to shift the membrane potential by the equivalent of the generator potential has been calculated using the standard parameters for the squid giant axon (Hodgkin and Katz, 1949):

$$P_{K^+} : P_{Na^+} : P_{Cl^-} = 1 : 0.04 : 0.45 = -55.97mV \text{ membrane potential}$$

Where P = permeability for any given ion.

If it is assumed that, on average, there is a 16mV depolarization during the generator potential of the CPR, and that this depolarization is produced by an increase in the number of sodium ion channels open in the membrane (or decrease in the resistance of the membrane) and therefore an increase in the net influx (or conductance) of sodium ions, there would only need to be a 4.5 fold increase in the number of Na^+ ion channels open from 0.04 to 0.18 to raise the membrane potential from -56mV to -40mV:

$$P_{K^+} : P_{Na^+} : P_{Cl^-} = 1 : 0.18 : 0.45 = -40.52mV$$

This 4.5 fold increase in the number of Na^+ channels open corresponds to a 9.4% increase in the sum of K^+, Na^+ and Cl^- channels open. Therefore, in order to produce a +16mV change in membrane potential there needs to be a conductance increase of less than 10%. In terms of the conductance measurements made in this study this means that the variability in voltage

deflections intended to be detected could be in the order of less than 10% and may not be detectable using the calculations that have been applied. Therefore, the only conclusive way to establish whether or not there is a conductance change would be to perform voltage clamp on the CPR during it photic response. This has been attempted but unsuccessfully. To produce the same +15mV depolarization from a reduction in potassium efflux there would need to be a hundred-fold decrease in P_K from 1 to 0.01.

6.4.3 The Effect of Tetraethyl Ammonium on the Generator Potential of the Caudal Photoreceptor

It has been discussed above that the generator potential is likely to be a result of an influx of sodium ions. However, in several photoreceptive systems a voltage sensitive potassium current has been detected which works in conjunction with this influx. In these cases there is a transducer induced sodium influx, which depolarizes the membrane potential, followed by a voltage induced potassium efflux, which hyperpolarizes the membrane potential. This potassium efflux in a sense limits the extent to which the neuron is being depolarized. This may well be what is happening in the CPR and would account for the photic response being brought down from the initial peak to a plateau phase that may be maintained providing there is on going photic stimulation.

The experiments in this study have clearly shown that potassium is involved in the maintenance of the membrane potential of the CPR far more so with other interneurons in that ganglion from the massive depolarization that occurs and the hyperpolatizing events which disturbs the typical smooth line of the generator potential.

The increase in the size of the transient peak when K^+ channels are blocked with TEA would suggest that potassium channels would normally be opening at this point and restricting the amplitude of the peak.

In the typical action potential the depolarization is mediated by an influx of Na^+ ions, when the membrane voltage reaches a given threshold, voltage sensitive K^+ channels are opened to allow for an efflux of K^+ ions to restore the cell's membrane to is resting potential. The after hyper-polarization seen following the action potential is caused by an over shot in efflux of potassium ions. On application of TEA the action potential of the LG widens. The

depolarization takes the same amount of time but the hyperpolarization from the efflux of potassium ions takes longer to reach the resting potential due to the blockage of potassium ions by TEA. The increased width of the electrically evoked action potential in the Lateral Giant fibre certainly confirms that the concentration of TEA (25mM) applied is adequate to block K^+ channels, therefore the effects seen are not likely to be an artefact of the salt used although both bromide and chloride forms were used to make sure.

The "flickering" of the generator potential between depolarized and hyperpolarized levels is one of the most dramatic effects of TEA and nothing similar was observed in any other control neurons. This strongly suggests that TEA is interfering with the phototransduction mechanism. However, it is not clear whether this interference is mediated by blocking voltage dependent K^+ channels or by some other unknown effect of TEA on the intracellular messenger cascade.

CHAPTER 7: OVERALL DISCUSSION

The crayfish CPR is unusual as a photoreceptor in that it produces both a shift in membrane potential, and action potentials in response to light. Its function as an extra-ocular photoreceptor is to provide the animal with photic information in addition to that which it receives from its compound eyes. It is necessary for the CPR to produce action potentials given that most of the cell, its cell body and its photoreceptive dendritic branching, are located in the terminal ganglion of the ventral nerve cord whilst its axon runs the length of the animal forming synapses in the cerebral ganglion.

Extracellular recordings from this axon in the connective are technically much easier to make than intracellular recording from the dendritic branching in the terminal ganglion; however the interpretation of data from such recordings is more complicated. This study begins with an examination of template recognition analysis, verifying it against threshold recognition of intracellular recordings. From these analytical tools frequency curves can be compiled which show that there is an initial high frequency peak on exposure to light that plateaus out to a lower frequency on prolonged exposure to light. When the light stimulus is removed the frequency tails off to nothing.

Application of TTX to the extracellular milieu removes action potentials by blocking voltage-gated Na^+ channels, thus revealing the shape of the underlying generator potential, which does, for the most part, resemble frequency curves generated when the action potentials are present. Therefore, this study lends credence to the theory that the shape of the generator potential determines the frequency of action potentials elicited. In this way the CPR is able to produce a graded response, allowing the animal to recognize how much light it has been exposed to and whether it is being newly exposed to light or whether it is moving out of the light.

This study found that there is an increase in activity in the CPR when serotonin is introduced into the extracellular milieu: in particular the photoreceptor shows spontaneous firing in the dark, which does not normally occur in this species. The evidence suggests that serotonin is either having an effect on the excitability of the CPR or the neurons that synapses onto it, rather than by affecting its photic properties. The CPR acts as a mechano-sensory integrating interneuron and as such it receives many excitatory and inhibitory inputs onto it from sensory

neurons in the tail fan. It is known that serotonin can affect the strength of synapses on to the LG and it is likely that it is having the same effect here with synapses onto the CPR.

The CPR is not only unusual as a photoreceptor in the photic response it produces but also in the way it produces that response. This is understandable given that this is a mechano-sensory integrating interneuron which is thought to have evolved photoreceptive properties as a secondary function. The visual photoreceptors of both vertebrate and invertebrates have very different intracellular transduction cascades, both of which end in a permeability change to Na^+ and a shift in the membrane potential. Krueswka (1991) and Krueswka and Larimer (1993) proposed a model for the crayfish CPR transduction cascade which is loosely based on that of the invertebrate visual photoreceptors (see Figure VII.i). In the present study staurosporine, lithium and caffeine were applied to the CPR during photic stimulation in order to elucidate further the transduction cascade of the CPR. Lithium had an inhibitory effect on the CPR confirming that IP_3 is involved in the photic response, while caffeine had an excitatory effect on the CPR suggesting that an increased release of calcium can enhance the photic response. Staurosporine had no effect, which suggests that there is no phosphorylation step involved in this transduction cascade. However, the possibility that Staurosporine did not penetrate through the tissue to the CPR cannot be discounted. Thus, for the most part this study has lent support for the model proposed by Krueswka (1991).

At the end of the transduction cascade proposed by Krueswka (1991) there is thought to be a permeability change although it is unknown whether the release of calcium from intracellular stores is directly affecting ion channels in the membrane or whether there are further steps down stream of calcium release that trigger a change in membrane conductance.

In most photoreceptors in the animal kingdom the membrane shift in response to light, whether it be a hyperpolarization, as seen in the vertebrate rod, or depolarization, as seen in the invertebrate compound eye, has been shown to be due to a change in the permeability of the membrane to Na^+.

This study has for the first time shown conclusively that the generator potential is sodium dependent. No clear evidence for a conductance change has been established that would confirm that the generator potential is Nerstian, although this is the most likely mechanism. The failure to detect a conductance change may be due to the fact that only a small relative

Figure VII.i

Summary: The response of the crayfish caudal photoreceptor to light.

Panel (A) A schematic diagram of the photic response of the CPR

Panel (B) Transduction cascade of the CPR

(A)

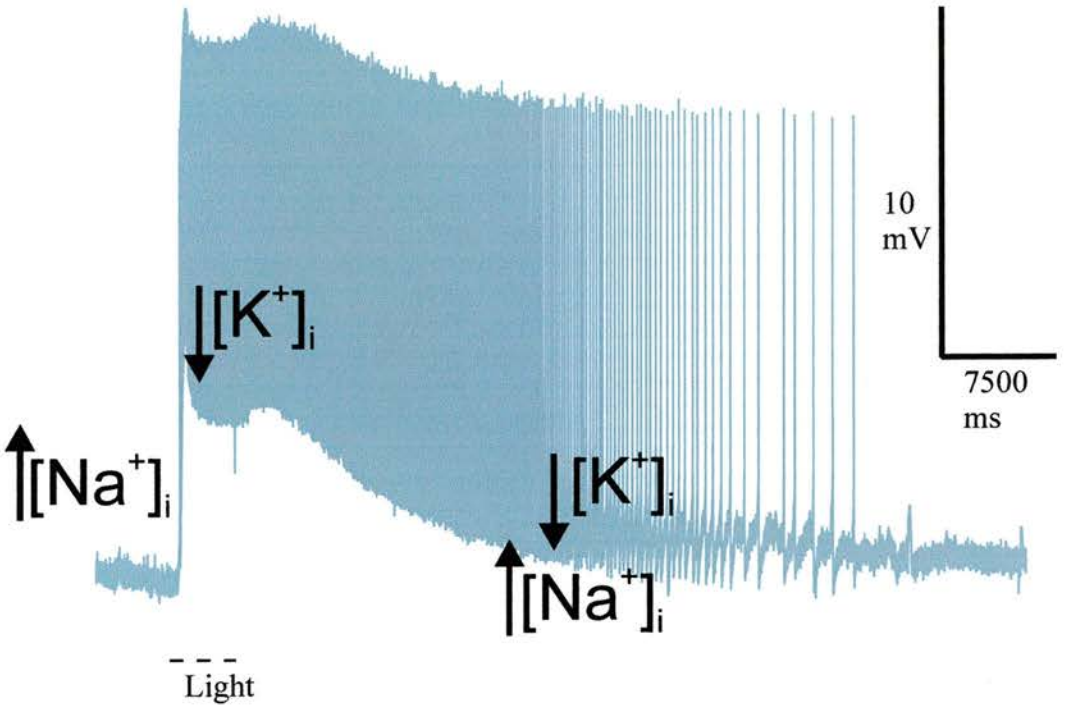
10
mV
7500
ms
[K+]i
[Na+]i
[K+]i
[Na+]i
Light

(B)

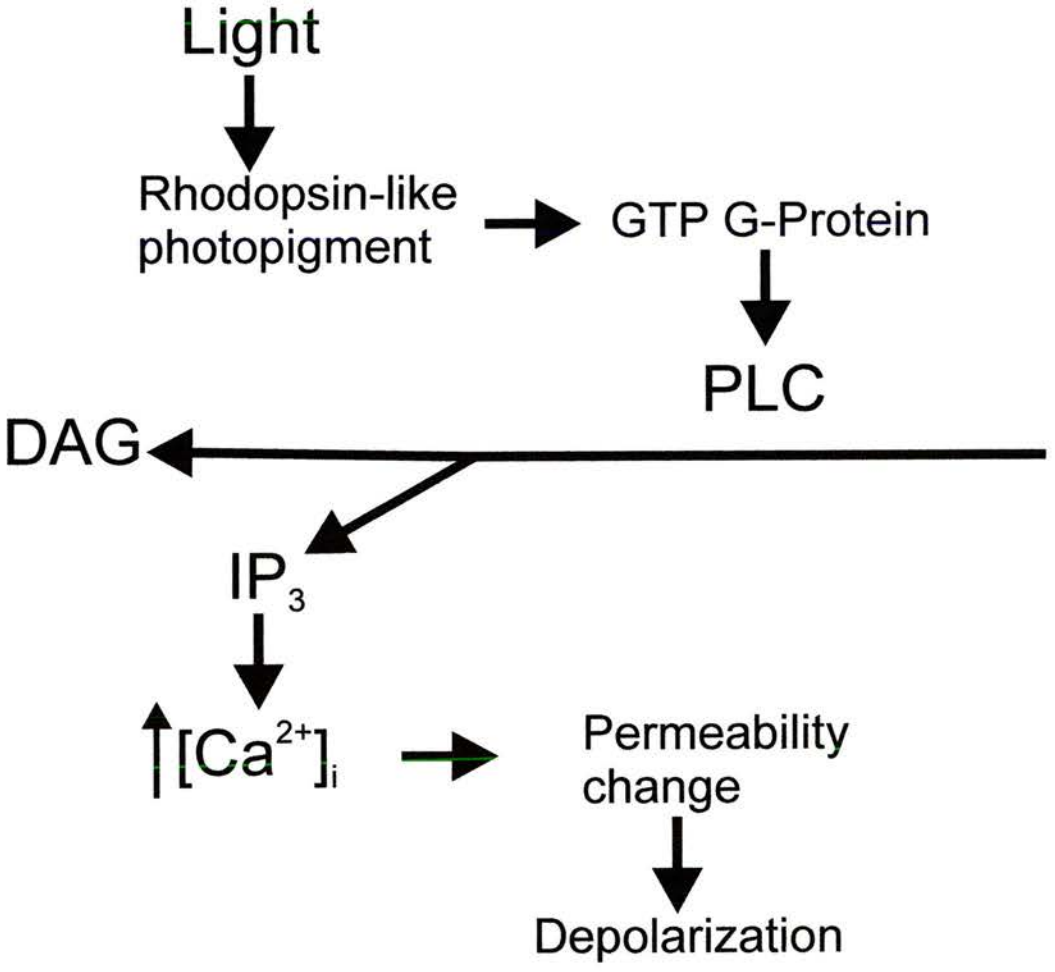
Light
Rhodopsin-like
photopigment
GTP G-Protein
PLC
DAG
IP3
[Ca2+]i
Permeability
change
Depolarization

change in conductance would be necessary to produce a change in membrane potential of the same magnitude as the generator potential. The application of TEA (a voltage-gated K^+ channel blocker) increases the amplitude of both the initial peak and plateau of generator potential, suggesting that the opening of voltage-gated K^+ channels are important in limiting and sculpting the extent of the depolarization of the photic response. Therefore it is thought that the generator potential waveform is the result of a transducer-induced opening of TTX-insensitive Na^+ channels (and an influx of Na^+) followed by a voltage-induced opening of K^+ channels (and an efflux of K^+) when the CPR is exposed to light (Figure VII.i). In the presence of a persistent light stimulus this balance of channels will hold the membrane at its relatively depolarized state.

REFERENCES

Amir S, Robinson B, Ratovitski T, Rea M A, Stewart J, Simaritov R (1988) A role for serotonin in circadian system revealed by the distribution of serotonin transporter and light-induced *Fos* immunoreactivity in the suprachiasmatic nucleus and intergeniculate leaflet. Neuroscience **84(4)**: 1059-1073

Arikawa K, Uchiumi K and Eguchi E (1981) Extraocular photoreceptors in the last abdominal ganglion of a swallowtail butterfly, Papilio xuthus. Naturwissenschaften **78**: 82-84

Armstrong C M and Binstock L (1965) Anomalous rectification in the squid giant axon injected with tetraethylammonium chloride. J. Gen. Physiol., **48:** 859-872

Armstrong C M and Hille B (1972) The inner quaternary ammonium ion receptor in potassium channels of the Node of Ranvier. J. Gen. Physiol., **59:** 388-400

Arvanitaki A and Chalazonitis N (1961) Excitatory and inhibitory processes initiated by light and infra-red radiations in single identifiable nerve cells (Giant ganglion cells of *Aplysia*). Pergamon Press, Oxford 194-231

Belanger J H (1988) Temperature acclimation of the caudal photoreceptor response in the crayfish *Orconectes rusticus* (Girard). Can. J. Zool., **66**: 1168-1171

Beltz B S and Kravitz E A (1986) Aminergic and peptidergic neuromodulation in crustacea. J. Exp. Biol. 124: 115-141

Beltz B S and Kravitz E A (1987) Physiological identification, morphological analysis, and development of identified serotonin-proctolin containing neurons in the lobster ventral nerve cord. J. Neurosci., 7: 533-546

Berridge M J (1989) The Albert Lasker Medical Awards. Inositol trisphosphate, calcium, lithium, and cell signalling. JAMA, **262:** 1834-1841

Block G D, Hudson D J and Lickey M E (1974) Extraocular photoreceptors can entrain the circadian oscillator in the eye of *Aplysia*. J. Comp. Physiol., **89**: 237-249

Briggs M H (1961) Visual pigment of *Grapsoid* crabs. Nature, **190**: 784-786

Brown J E, Faddis M and Combs A (1992) Light does not induce an increase in cyclic-GMP content of squid or *Limulus* photorecepors. Exp. Eye Res., **54**: 403-410

Bruno M S and Kennedy D (1962) Spectral sensitivity of photoreceptor neurons in the sixth ganglion of the crayfish. Comp. Biochem. Physiol., **6**: 41-46

Butt S J (2001) Aminergic modulation of acetylcholine responses recorded from an identified insect (*Periplaneta america*) motorneurone. PhD thesis, St. Andrews University, Scotland, UK

Chappel W D, (1960) Light and movement of crayfish. Masters' Thesis, Syracuse University. Cited in Kennedy (1963c)

Cuttle M F, Hevers W, Laughlin S B and Hardie R C (1995) Diurnal modulation of photoreceptor potassium conductance in the locust. J. Comp. Physiol. A, **176**: 307-316

Dawkins R (1996) In "Climbing Mount Improbable", pub. Viking, pp126-179

Delaney K, Tank D W and Zucker R S (1991) Presynaptic calcium and serotonin-mediated enhancement of transmitter release at crayfish neuromuscular junction. J. Neurosci., **11**: 2631-2643

Dodt E (1963) Photosensitivity of the pineal organ in the teleost, *Salmo irideus* (Gibbons). Experimentia, **19**: 642-643

Eakin R M and Westfall J A (1960) Further observations on the fine structure of the parietal eye of lizards. J. Biophys. Biochem. Cytol. **8**: 438-499

Edwards D H (1984) Crayfish extraretinal photoreception I. Behavioural and motoreneuronal responses to abdominal illumination. J. Exp. Biol., **109**: 291-306

Edwards D H and Kravitz E A (1997) Serotonin, social status and aggression. Curr. Opin. Neurobiol., **7**: 812-819

Eldred W D and Nolte J (1978) Pineal photoreceptors: Evidence for a vertebrate visual pigment with two physiologically active states. Vision Res., **18**: 29-32

Flood P M and Wilkens L A (1978) Directional sensitivity in a mechanoreceptive interneurone: analysis by root ablation. J. Exp. Biol., **77**: 89-106

Foster R G and Soni B G (1998) Extraretinal photoreceptors and their regulation of temporal physiology. Rev. Reproduct., **3**: 145-150

Freedman M S, Lucas R J, Soni B, von Schantz M, Muñox M, David-Gray Z and Foster R (1999) Regulation of mammalian circadian behavior by non-rod, non-cone, ocular photoreceptors. Science, **284**: 502-504

Fuentes-Pardo B and Inclan-Rubio V (1987) Caudal photoreceptors synchronize the circadian rhythms in crayfish - I Synchronization of ERG and locomotor circadian rhythms. Comp. Biochem. Physiol., **86A**: 523-527

Galeano C (1976) The caudal photoreceptor of crayfish. A review. Acta Physiol. Lat. Am., **26**: 169-185

Galeano C and Beliveau S (1973) Mechanoreceptor and photoreceptor tonic integration in the crayfish. Can. J. Physiol. Pharmacol., **51**: 949-958

Galeano C and Chow K.L (1971) Response of caudal photoreceptor of crayfish to continuous and intermittent photic stimulation. Can. J. Physiol. Pharmacol., **49**: 699-706

Gill M D and Skorupski P (1996) Modulation of spontaneous and reflex activity of crayfish leg motor neurons by octopamine and serotonin. J. Neurophysiol., **76**: 3535-3549

Glanzman D L and Krasne F B (1983) Serotonin and octopamine have opposite modulatory effects on the crayfish's lateral giant escape reaction. J. Neurosci., **3**: 2263-2269

Glanzman D L and Krasne F B (1986) 5, 7-Dihydroxtryptamine lesions of crayfish serotonin-containing neurons: effects on the lateral giant escape reaction. J. Neurosci. **6**: 1560-1569

Godchaux W III and Zimmerman W F (1979) Membrane-dependent guanine nucleotide binding and GTPase activities of soluble proteins from bovine rod outer segments. J. Bio. Chem., **254**: 7874-7884

Gotow T (1989) Photoresponses of an extraocular photoreceptor associated with a decrease in membreane conductance in an opsisthobranch mollusc. Brain Res., **479**: 120-129

Gras H and Weber W. (1983) Spectral light sensitivity of isolated chromatophores of the sea urchin, *Centrostephanus Longispinus*. Comp. Biochem. Physiol., **76A**, 279-281

Gwilliam G F (1969) Electrical responses to photic stimulation in the eyes and nervous system of *Nereid polychaetes*. Biol. Bull., **136**: 385-397

Halder G, Callaerts P and Gehring W J (1995) Induction of ectopic eyes by targeted expression of the eyeless gene in *Drosophilia*. Science, **267**: 1788-1792

Hama K (1961) A photoreceptor-like structure in the ventral nerve cord of the crayfish, *Cambarus virilus*. Anat. Rec., **140**: 329-336

Hamasaki D I and Streck P (1971) Properties of the epipysis cerebri of the small-spotted dogfish shark, *Scyliorhinus canicula*. I. Vision Res. **11**: 189-198

Harris-Warrick R M (1985) Amine modulation of extension command element-evoked motor activity in the lobster abdomen. J. Comp. Physiol. A, **156**: 875-884

Harris-Warrick R M and Kravitz E A (1984) Cellular mechanisms for modulation of posture by octopamine and serotonin in the lobster. J. Neurosci. **4**: 1976-1993

Harth M S and Heaton M B (1973) Nonvisual photic responsiveness in newly hatched pigeons (*Columba livia*) Science, **180**: 753-755

Hartwig H-G and Bauman C (1974) Letter to the editors: Evidence for photosensitive pigments in the pineal complex of the frog. Vision Res., **14**: 597-598

Hill-Venning C and Cottrell G A (1992) Modulation of voltage-dependent calcium current in *Helix Aspersa* buccal neurones by serotonin and protein kinase C activators. Exp. Physiol., **77**: 891-901

Hisano N, Cardinali D P, Rosner J M, Nagle C A and Tramezzani J H (1972) Pineal role in the duck extraretinal photoreception. Endocrinology, **91**: 1318-1322

Hodgkin A L and Katz B (1949) The effect of sodium ions on the electrical activity of a giant axon of the squid. **108**: 37-77

Hofbauer A and Buchner E (1989) Does *Drosophila* have seven eyes? Naturwissenschaften, **76**: 335-336

Huber R, Smith K, Delago A, Isaksson K and Kravitz E A (1997) Serotonin and aggressive motivation in crustaceans: Altering the decision to retreat. Proc. Natl. Acad. Sci. USA., **94**: 5939-5942

Hurley J B (1987) Molecular properties of the cGMP cascade of vertebrate photoreceptors. Ann. Rev. Physiol., **49**: 793-812

Inclan-Rubio V. and Fuentes-Pardo B. (1987) Caudal photoreceptors synchronize the circadian rhythms in crayfish - II Functional relationships between caudal and visual photoreceptors. Comp. Biochem. Physiol., **86A**: 529-536

Kandel E R, Schwartz J H and Jessell T M (1991) In "Principles of Neural Science, 3rd edition., pub. Elsevier Science Publishing Co. Inc., New York

Kennedy D (1958a) Responses from the crayfish caudal photoreceptor. Am. J. Opthalmol., **46**: 19-26

Kennedy D (1958b) Electrical activity of a "primative" photoreceptor. Ann. N. Y. Acad. Sci., **74**: 329-336

Kennedy D (1960) Neural photoreception in a lamellibranch mollusc. J. Gen. Physiol., **44**: 277-299

Kennedy D (1963a) Inhibition in visual systems. Scientific American, **209**: 123-130

Kennedy D (1963b) Physiology of photoreceptor neurons in the abdominal nerve cord of the crayfish. J. Gen. Physiol., **46**: 5-30

Kennedy D (1963c) Physiology of photoreceptor neurons in the abdominal nerve cord of the crayfish. J. Gen. Physiol., **46**: 551-572

Kennedy D and Bruno M S (1961) The spectral sensitivity of crayfish and lobster vision. J. Gen. Physiol., **44**:1089-1102

Kennedy D and Preston J B (1960) Activity patterns of interneurons in the caudal ganglion of the crayfish. J. Gen. Physiol., **43**: 655-670

Kivivuori L. (1982) Temperature acclimation of the caudal photoreceptor response in the crayfish *Astacus astacus* L. Comp. Biochem. Physiol., **72A**: 17-21

Kovac M (1974a) Abdominal movements during backward walking in crayfish. I: Properties of the motor program. J. Comp. Physiol., **95**: 61-78

Kovac M (1974b) Abdominal movements during backward walking in crayfish. II: The neuronal basis. J. Comp. Physiol., **95**: 79-94

Kravitz E A (2000) Serotonin and aggression: insights gained from a lobster model system and speculations on the role of amine neurons in a complex behavior. J. Comp. Physiol. A, **186**: 221-238

Kruszewska B (1991) Ultrastructure and transduction in a CNS photoreceptor. PhD thesis, University of Texas, Austin, Texas, USA

Kruszewska B and Larimer J L (1993) Specific second messengers activate the caudal photoreceptor of crayfish. Brain Res., **618**: 32-40

Land M F (1980) Compound eyes: old and new optical mechanisms. Nature, **287**: 681-686

Land M F and Fernald R D (1992) The evolution of eyes. Ann. Rev. Neurosci., 15: 1-29

Land M F and Nilsson D-E (2002) "Animal Eyes", pub. Oxford Animal Biology Series.

Larimer J L (1966) A functional caudal photoreceptor in blind cavernicolous crayfish. Nature, **210**: 204-205

Larimer J L (1967) The effects of temperature of the activity of the caudal photoreceptor. Comp. Biochem. Physiol., **22**: 683-700

Larimer J L and Kennedy D (1969) The central nervous control of complex movements in the uropods of crayfish. J. Exp. Biol., **51**: 135-150

Larimer J L, Trevino D L and Ashby E A (1966) A comparison of spectral sensitivities of caudal photoreceptors of epigeal and cavernicolous crayfish. Comp. Biochem. Physiol., **19**: 409-415

Laurienti P J and Blankenship J E (1997) Serotonergic modulation of a voltage-gated calcium current in parapodial swim muscle from *Aplysia brasiliana*. J. Neurophysiol., **77**: 1496-1502

Lent C M and Dickinson M H (1988) The neurobiology of feeding in leeches. Scientific American, **258**: 78-83

Liebmnan P A and Pugh E N, Jr. (1982) Gain, speed and sensitivity of GTP binding vs. PDE activation in visual excitation. Vision Res., **22**: 1475-1480

Livingstone M S, Harris-Warrick R M and Kravitz E A (1980) Serotonin and octopamine produce opposite postures in lobsters. Science, **208**: 76-79

Livingstone M S, Schaeffer S F and Kravitz E A (1981) Biochemistry and ultrastructure of serotonergic nerve endings in the lobster: Serotonin and octopamine are contained in different nerve endings. J. Neurobiol., **12**: 27-54

Lucas R J, Freedman M S, Muñoz M, Garcia-Fernández J-M and Foster R G (1999) Regulation of the mammalian pineal by non-rod, non-cone, ocular photoreceptors. Science, **284**: 505-507

Lundqvist C T, Baines R A and Bacon J P (1996) Evidence that histamine is a neurotransmitter in an insect extraocular photoreceptor pathway. J. Exp. Biol., **199**: 1973-1982

Lythgoe J N, Shand J and Foster R G (1984) Visual pigment in fish iridocytes. Nature, **308**: 83-84

McPhee M J and Wilkens J L (1989) Serotonin, but not dopamine or octopimine modifies locomotor and phototaxic behaviour in the crab, *Carcinus maenas*. Can. J. Zool., **67**: 391-393

McPherson D R and Blankenship J E (1991) Neural control of swimming in *Aplysia brasiliana*. III. Serotonergic modulatory neurons. J. Neurophysiol., **66**: 1366-1379

Marks P S (1976) Nervous control of light responses in the sea anemone, *Calamactis praelongus*. J. Exp. Biol., **65**: 85-96

Meyer J R (1977) Head capsule transmission of long-wavelength light in the curculionidae. Science, **196**: 524-525

Miller W H (1957) Morphology of the ommatidium of the compound eye of *Limulus*. J. Biophys. Biochem. Cytol., **3**: 421

Millott N (1968) The dermal light sense. Symp. Zool. Soc. Lond., **23**: 1-36

Moore D and Larimer J L (1987) Neural control of a cyclic postural behavior in the crayfish, *Procambarus clarkii*: the pattern-initiating interneurons. J. Comp. Physiol. A, **160**: 169-179

Mpitsos G J (1973) Physiology of vision in the mollusc *Lima scabra*. J. Neurophysiol. **36**: 371-383

Nilsson D-E (1989) Optics and evolution of the compound eye. In "*Facets of Vision*", eds. D G Staveng and R C Hardie, pub. Springer-Verlag, Berlin, pp 30-71

North W J (1957) Sensitivity to light in the sea anemone *Metriduim senile* (L). II. Studies on reaction time variability and effects of change in light intensity and temperature. J. Gen. Physiol., **40**: 715-733

Oniszk M and Barbacka-Surowiak (2003) Participation of serotonergic systems in function of mammalian circadian clock. Advances Cell Biol. **30**: 219-228

Page and Larimer (1976) Extra-retinal photoreception in entrainment of crustacean circadian rhythms. Photocem. Photobiol **23**:245-251

Pasztor V M and Golas L (1993) The modulatory effects of serotonin, neuropeptide F1 and proctolin on the receptor muscles of the lobster abdominal stretch receptor and their exoskeletal muscle homologues. J. Exp. Biol., **174**: 363-374

Pepose J S and Lisman J E (1978) Voltage-sensitive potassium channels in *Limulus* ventral photoreceptors. J. Gen. Physiol., **71:** 101-120

Philip A R, Bellingham J, Garcia-Fernandez J-M and Foster R G (2000) A novel rod-like opsin isolated from the extra-retinal photoreceptors of teleost fish. FEBS Letters, **468:** 181-188

Prieto-Sagredo J and Fanjul-Moles M J (2001) Spontaneous and light-evoked discharge of the isolated abdominal nerve cord of crayfish in vitro reveals circadian oscillations. Chronobiol. Int. **18(5)**: 759-765

Prosser C L (1934) Action potentials in the nervous system of the crayfish. II. Responses to illumination of the eye and the caudal ganglion. J. Cell. Comp. Physiol., **4**: 363-377

Provencio I, Rollag M D and Castrucci A M (2002) Photoreceptive net in the mammalian retina. Nature, **415**: 493

Sandeman D C, Sandeman R E and de Couet H G (1990) Extraretinal photoreceptors in the brain of the crayfish *Cherax destructor*. J. Neurobiol., **21**: 619-629

Satterlie R A (1995) **Serotonergic modulation of swimming speed in the pteropod mollusc *Clione limacine*. J. Exp. Biol.,** 198**: 905-916**

Simon T W and Edwards D H (1990) Light-evoked walking in crayfish: Behavioural and neuronal responses triggered by the caudal photoreceptor. J. Comp. Physiol. A., **166**: 745-755

Taylor D H (1972) Extra-optic photoreception and compass orientation in larval and adult salamanders (*Ambystoma Tigrinum).* Anim. Behav., **20**: 233-236

Terakita A, Hariyama T, Tsukahara Y, Katsukura Y and Tashiro H (1993) Interaction of GTP-binding protein Gq with photoactivated rhodopsin in the photoreceptor membranes of crayfish. FEBS Letters, **330**: 197-200

Tierney A J and Mangiamele L A (2001) Effects of serotonin and serotonin analogs on posture and agonistic behavior in crayfish. J. Comp. Physiol. A, **187**: 757-767

Truman J W (1974) Physiology of insect rhythms. IV. Role of the brain in regulation of the flight rhythm of the giant silkmoths. J. Comp. Physiol., **95**: 281-296

Uchizono K (1962) The structure of possible photoreceptive elements in the sixth abdominal ganglion of the crayfish. J. Cell. Biol., **15**: 151-154

Underwood H and Menaker M (1970) Extraretinal light perception: Entrainment of the biological clock controlling lizard locomotor activity. Science, **170**: 190-193

Van Veen T, Hartwig H G and Muller K (1976) Light-dependent motor activity and photonegative behaviour in the eel (*Anguilla anguilla* L.). Evidence for extraretinal and extrapineal photoreception. J. Comp. Physiol., **111**: 209-219

Vogt K (1980) Die Spiegeloptik des Flusskresbsauges. The optical system of the crayfish eye. J. Comp. Physiol. A, **135**: 1-19

Wald G and Hubbard R (1957) Visual Pigment of a decapod crustacean: The lobster. Nature, **180**: 278-280

Weiss K R, Cohen J L and Kupfermann I (1978) Modulatory control of buccal musculature by a serotonergic neuron (metacerebral cell) in Aplysia. J Neurophysiol., **41**: 181-203

Welsh J N (1934) The caudal photoreceptor and the response of the crayfish to light. J. Cell. Comp. Physiol., **4:** 379-388

Wetterberg L, Geller E and Yuwiler A (1970) Haderian Gland: An extraretinal photoreceptor influencing the pineal gland in neonatal rats? Science, **167**: 884-885

Wilden U, Hall S S and Kuhn H (1986) Phosphodiesterase activation by photoexcited rhodopsin is quenched when rhodopsin is phosphorylated and binds the intrinsic 48 kD protein of rod outer segments. Proc. Natl. Acad. Sci. USA., **83**: 1174-1178

Wilkens L A (1988) The crayfish caudal photoreceptor: Advances and questions after the first half century. Comp. Biochem. Physiol., **91C**: 61-68

Wilkens L A and Larimer J L (1972) The CNS photoreceptor of crayfish: Morphology and synaptic activity. J. Comp. Physiol., **80**: 389-407

Wilkens L A and Larimer J L (1976) Photosensitivity in the sixth abdominal ganglion of decapod crustaceans: A comparative study. J. Comp. Physiol., **106**: 69-75

Wilkens L A and Marzelli G A (1979) Central inhibition of an identified mechanosensory interneuron in the crayfish. J. Neurobiol., **X**: 247-254

Wilkens J L, Mercier A J and Evans J (1985) Cardiac and ventilatory responses to stress and to neurohormonal modulators by the shore crab *Carcinus maenas*. Comp. Biochem. Physiol., **82C 2**: 337-343

Willard A L (1981) Effects of serotonin on the generation of the motor program for swimming by the medicinal leech. J. Neurosci. **1**: 936-944

Wolken J J and Mogus M A (1979) Yearly review: Extra-ocular photosensitivity. Photochem. Photobiol., **29**: 189-196

Wolken J J, Capano J and Turano A (1957) Photoreceptor structures. III. *Drosophilia melanogaster*. J. Biophys. Biochem. Cytol., **3**: 441

Wurtman R J, Axelrod J, and Kelly D E (1968) "The Pineal", pub. Academic Press.

Yarfitz S and Hurley J B (1994) Minireview: Transduction mechanisms of vertebrate and invertebrate photoreceptors. J. Biol. Chem., **269**: 14329-14332

Yasuyama K and Meinertzhagen I A (1999) Extraretinal photoreceptors at the compound eye's posterior margin in *Drosophila melanogaster*. J. Comp. Neurol., **412**: 193-202

Yeh S-R, Fricke R A and Edwards D H (1996) The effect of social experience on serotonergic modulation of the escape circuit of crayfish. Science, **271**: 366-369

Yeh S-R, Musolf B E and Edwards D H (1997) Neuronal adaptations to changes in the social dominance status of crayfish. J Neurosci., **17**: 697-708

Yoshida M and Kobayashi M (1995) Modulation of the buccal muscle contraction by identified serotonergic and peptidergic neurons in the snail *Achatina fulica*. J. Exp. Biol., **198**: 729-738

Yu B, Gamkrelidze G N, Laurienti P J and Blankenship J E (2001) Serotonin directly increases a calcium current in swim motoneurons of *Aplysia brasiliana*. Amer. Zool., **41**: 1009-1025

Zoran M J, Haydon P G and Matthews P J (1989) Aminergic and peptidergic modulation of motor function at an identified neuromuscular junction in *Helisoma*. J. Exp. Biol., **142**: 225-243